



---

CMS-SMP-23-006  
TOTEM 2024-002

 CERN-EP-2024-273  
2024/12/02

# Proton reconstruction with the TOTEM Roman pot detectors for high- $\beta^*$ LHC data

The CMS and TOTEM Collaborations\*

## Abstract

The TOTEM Roman pot detectors are used to reconstruct the transverse momentum of scattered protons and to estimate the transverse location of the primary interaction. This paper presents new methods of track reconstruction, measurements of strip-level detection efficiencies, cross-checks of the LHC beam optics, and detector alignment techniques, along with their application in the selection of signal collision events. The track reconstruction is performed by exploiting hit cluster information through a novel method using a common polygonal area in the intercept-slope plane. The technique is applied in the relative alignment of detector layers with  $\mu\text{m}$  precision. A tag-and-probe method is used to extract strip-level detection efficiencies. The alignment of the Roman pot system is performed through time-dependent adjustments, resulting in a position accuracy of  $3 \mu\text{m}$  in the horizontal and  $60 \mu\text{m}$  in the vertical directions. The goal is to provide an optimal reconstruction tool for central exclusive physics analyses based on the high- $\beta^*$  data-taking period at  $\sqrt{s} = 13 \text{ TeV}$  in 2018.

*Submitted to the Journal of Instrumentation*



## 1 Introduction

Elastic and diffractive interactions of high-energy protons at the CERN LHC are characterised by scattered protons emerging at small angles (microradians) with respect to the beam direction. These protons can be measured with detectors that are inserted into the beam pipe called “Roman pots” (RPs), which are movable near-beam devices that allow the detectors to be brought very close (down to a few mm) to the beam without affecting the vacuum, beam stability, or other aspects of accelerator operations.

This paper describes methods for the reconstruction of the scattered proton trajectories in such near-beam detectors. These reconstruction techniques have been developed by the CMS and TOTEM Collaborations for the studies of central exclusive hadron production [1–3], where in addition to the two scattered protons, a central system of particles is created. This paper is based on data jointly taken by the CMS and TOTEM detectors in a special, low instantaneous luminosity run in July 2018, at the proton-proton (pp) centre-of-mass energy of 13 TeV, with an integrated luminosity of  $4.7 \text{ pb}^{-1}$  [4].

The acceptance of the RP detector system for elastically or diffractively scattered protons is determined by the beam optics configuration. With the so-called high- $\beta^*$  setting, the beam divergence is small, and the forward, near-beam detectors are thus able to measure the scattered protons at low angles and small transverse momenta. Here  $\beta^*$  denotes the value of the amplitude function at the interaction point (IP) [5]. The acceptance as a function of the squared four-momentum transfer of the protons ( $t$ ) starts at  $-0.03 \text{ GeV}^2$ . The proton kinematic properties are determined from the proton scattering angle, independently of the momentum loss if the latter is small. Protons with fractional momentum loss up to 20% can be observed, with wide acceptance for the invariant mass of the created central hadron system [1, 2].

The present paper covers subjects ranging from signal clustering in the silicon microstrip detectors used in the RPs, to the reconstruction of proton tracks, the cross-check of the beam optics, and the alignment with respect to the beam line. The aim is to measure the scattered proton momentum and the location of the primary interaction for central exclusive physics events [6]. Improvements relative to earlier methods are presented for the selection and analysis of signal events, specifically for the precise momentum balance of forward protons with centrally produced particles. Several of the discussed techniques are relevant to other beam optics settings as well.

The paper is organised as follows. An overview of the LHC beam parameters and the RP detectors is given in Section 2, along with some considerations on the scattered proton trajectory, and details of the data set used. The reconstruction of the proton hit locations within the RPs is discussed in Section 3, including pattern recognition and matching, relative alignment of the detector layers, extraction of the strip hit efficiencies, and determination of the correction factors. The reconstruction of the full proton trajectory is detailed next (Section 4), together with a discussion of the cross-checks of the beam optics, the distributions of the interaction point locations and scattering angles, and the absolute alignment of the RPs. Results on momentum resolution and applications for event classification and selection for physics analyses are also shown. The paper ends with a summary in Section 5.

## 2 The CMS and TOTEM detectors

We use a right-handed coordinate system, with the origin at the nominal collision point, the  $x$  axis pointing to the centre of the LHC ring, the  $y$  axis pointing up (perpendicular to the LHC

plane), and the  $z$  axis along the anti-clockwise beam direction.

## 2.1 The LHC beam parameters

In this low instantaneous luminosity data-taking period, the  $\beta^*$  values in the horizontal and vertical directions are  $\beta_x^* = 45\text{ m}$  and  $\beta_y^* = 90\text{ m}$ , respectively. The initial nominal emittance is in the range  $\varepsilon_n = 1.2\text{--}1.6\text{ }\mu\text{m}$  [7]. The half-crossing angle in the horizontal plane is  $60\text{ }\mu\text{rad}$ . At the nominal IP, the transverse size of the beam is  $\sigma = \sqrt{\varepsilon\beta^*}$  and the angular beam size (beam divergence) is  $\sigma' = \sqrt{\varepsilon/\beta^*}$ , where the emittance  $\varepsilon$  is related to the nominal emittance as  $\varepsilon_n = \varepsilon\beta\gamma$ . Here  $\beta$  is the ratio of the velocity of the beam particles to the speed of light, and  $\gamma$  is the Lorentz factor. Given the beam energy of  $p_{\text{beam}} = 6500\text{ GeV}$ , we have  $\beta\gamma \approx 6930$  and the expected value of the emittance is  $\varepsilon \approx 0.2\text{ nm}$ . The transverse momentum spread is  $\sigma_{p_{x/y}} = p_{\text{beam}}\sigma'_{x/y}$ . Table 1 summarises the relevant beam parameters.

The transverse size of the beam spot (BS) can be calculated from the beam width as  $\sigma^{\text{BS}} = \sigma/\sqrt{2}$ . The size of the beam spot is measured by using reconstructed interaction vertices with tracks in the central silicon tracker of the CMS detector [8]. It slowly increases within an LHC fill from  $70$  to  $110\text{ }\mu\text{m}$  in  $x$ , and from  $90$  to  $110\text{ }\mu\text{m}$  in the  $y$  direction. With an assumed average initial nominal emittance  $\varepsilon_n \approx 1.4\text{ }\mu\text{m}$  we expect in the horizontal direction  $\sigma_x^{\text{BS}} \approx 65\text{ }\mu\text{m}$ ,  $\sigma'_x \approx 2.1\text{ }\mu\text{rad}$ ,  $\sigma_{p_x} \approx 14\text{ MeV}$ , and in the vertical direction  $\sigma_y^{\text{BS}} \approx 95\text{ }\mu\text{m}$ ,  $\sigma'_y \approx 1.5\text{ }\mu\text{rad}$ ,  $\sigma_{p_y} \approx 10\text{ MeV}$ . Both the measured horizontal and vertical initial beam spot width values are close to their expectations ( $70$  and  $90\text{ }\mu\text{m}$ ).

Table 1: The beam parameters and related quantities at the CMS interaction point for the  $\beta^* = 90\text{ m}$  run at  $\sqrt{s} = 13\text{ TeV}$  in 2018.

Beam parameter	Value
Horizontal amplitude function at IP, $\beta_x^*$	45 m
Vertical amplitude function at IP, $\beta_y^*$	90 m
Nominal emittance (expected), $\varepsilon_n$	$1.2\text{--}1.6\text{ }\mu\text{m}$
Horizontal beam spot width (measured), $\sigma_x^{\text{BS}}$	$70\text{--}110\text{ }\mu\text{m}$
Vertical beam spot width (measured), $\sigma_y^{\text{BS}}$	$90\text{--}110\text{ }\mu\text{m}$
Half of horizontal crossing angle	$60\text{ }\mu\text{rad}$

## 2.2 Roman pot detectors

The intersection points of the LHC are numbered from 1 to 8. The CMS detector operates at interaction point 5, and the adjacent LHC sectors are referred to as “45” and “56”. The proton spectrometer of the TOTEM experiment consists of two telescope arms, referred to as “Arm 1” (in sector 45) and “Arm 2” (in sector 56) for positive and negative pseudorapidities, respectively [9, 10]. In each arm there are two stations located at about  $\pm 213\text{ m}$  (near) and  $\pm 220\text{ m}$  (far) relative to the nominal IP. Each station consists of two units. Only the units with vertical pots are considered in this paper. Each unit has two RPs, one located above (“top” or T), and one below (“bottom” or B) the LHC beam. The names of the RP detector layer groups are given in Table 2 and Fig. 1 (left panel). The term “parallel” refers to cases where both RP detectors above or below the beamline (top-top or TT, bottom-bottom or BB) have signals above predefined thresholds, whereas the “diagonal” configuration refers to the other two cases (top-bottom or TB, bottom-top or BT).

An RP contains ten layers of silicon strip detectors, placed alternately in two orthogonal orientations (u and v) with five layers in each. The strips are directed at  $45^\circ$  with respect to the

Table 2: The naming of the various RP layer groups.

Arm	Location	Vertical position	Proj.	Name	Arm	Location	Vertical position	Proj.	Name
1	near	top	$u$	1nTu	2	near	top	$u$	2nTu
1	near	top	$v$	1nTv	2	near	top	$v$	2nTv
1	near	bottom	$u$	1nBu	2	near	bottom	$u$	2nBu
1	near	bottom	$v$	1nBv	2	near	bottom	$v$	2nBv
1	far	top	$u$	1fTu	2	far	top	$u$	2fTu
1	far	top	$v$	1fTv	2	far	top	$v$	2fTv
1	far	bottom	$u$	1fBu	2	far	bottom	$u$	2fBu
1	far	bottom	$v$	1fBv	2	far	bottom	$v$	2fBv

vertical ( $y$ ) axis for the far pots (Fig. 1, right), and at  $37^\circ$  or  $53^\circ$  for the near pots. The layers can approach the beam at a distance of a few millimetres without affecting the LHC operation (they are retracted before each beam injection and inserted again afterwards).

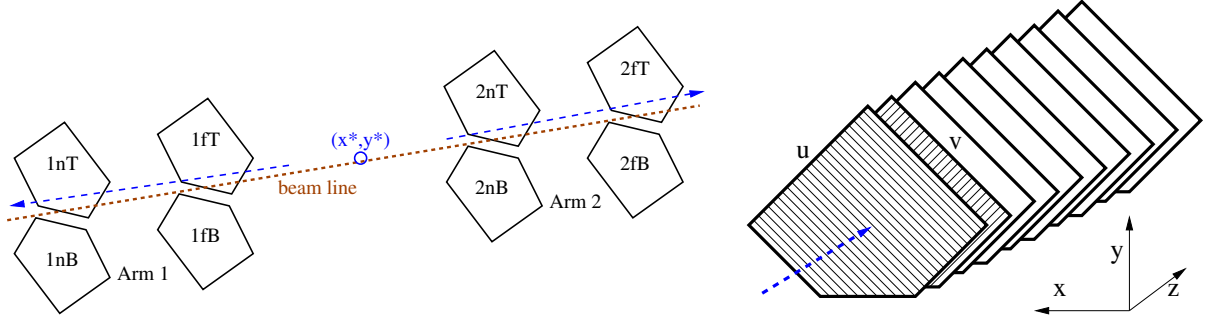


Figure 1: Left: The eight RP units in Arm 1 and Arm 2 with the beam line, along with the location  $(x^*, y^*)$  of the primary interaction and two proton trajectories (dashed blue arrows), not to scale. Right: An RP unit comprising 10 layers with strips oriented alternately in the  $u$  and  $v$  directions. The blue dashed arrow represents an incoming proton. The axes of the local coordinate system are indicated with black solid arrows.

Schematic displays of some events with hits and projections of reconstructed local straight tracks, called “tracklets”, in RPs are displayed in Fig. 2. Normally, the scattered protons are detected by both the near and far pots, yielding a total of four tracklets. Events with more than four tracklets, pointing to energetic secondaries or multiple simultaneous primary pp collisions, are excluded from the analysis. The RPs share a common readout with the CMS detector.

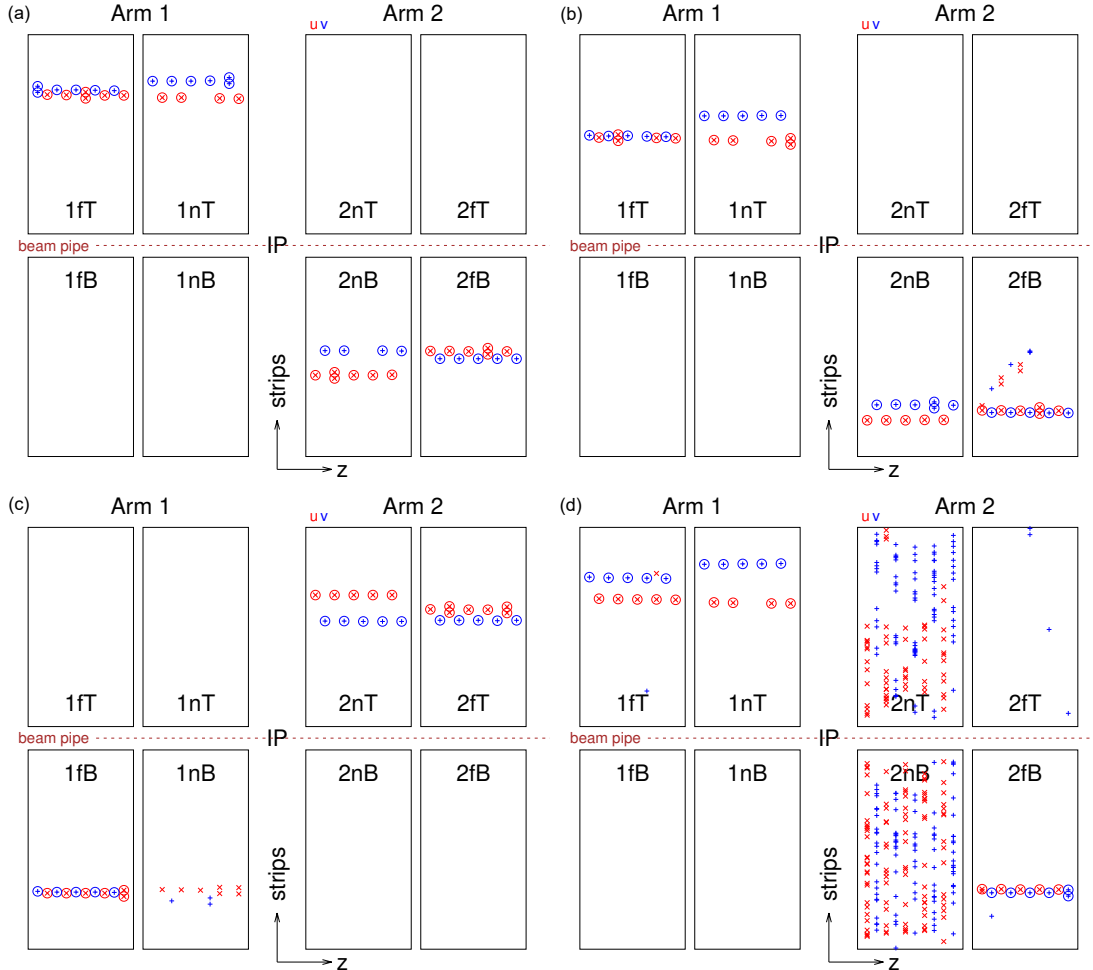


Figure 2: Schematic displays of four events with hits and projections of reconstructed local tracks (tracklets) in RPs, with outlines of Arm 1 and 2, near and far, upper and lower plots (not to scale). Strips of reconstructed clusters in  $u$  and  $v$  layers are plotted with red  $x$  and blue  $+$  markers, respectively. Two vertically adjacent symbols represent a two-strip cluster. Reconstructed clusters on a found tracklet are marked with circles. From left to right and from top to bottom: (a) normal event, (b) normal event with additional secondary particles; (c) not reconstructed event (less than three hits in the  $v$  orientation of 1n); (d) not reconstructed event (hadronic interaction in some beam element before 2n).

### 2.3 Proton trajectory

Once the scattered protons leave the interaction region, they traverse the magnetic fields created by the CMS solenoid and the LHC beam magnets until they reach the first and then the second RP stations. During their flight they do not traverse the beam pipe. The RP stations have their own secondary vacuum, separated by a  $300\ \mu\text{m}$  thin steel window from the primary LHC vacuum, and they are in a region where the magnetic field is zero. Of course, to determine the scattered proton kinematics the inhomogeneous magnetic fields due to the sequence of several quadrupole and dipole magnets need to be modelled.

The effects of multiple scattering and nuclear collisions in the detector material and in the stainless steel window that separates the LHC primary vacuum from the RP secondary vacuum, need to be considered. The sensitive detector elements are silicon layers with a thickness  $d = 300\ \mu\text{m}$ . Silicon (steel) has a radiation length  $X_0 = 9.370\ (1.757)\ \text{cm}$ , and a nuclear collision length  $\lambda = 30.16\ (10.37)\ \text{cm}$ . For multiple scattering within one layer, the standard deviation of the scattering angle, in a Gaussian approximation [11], is given by  $\theta_0 \approx 13.6\ \text{MeV}/(\beta cp) \times z\sqrt{d/X_0}$ , where  $z$  is the charge number of the incident particle, and we have neglected the logarithmic correction. With the proton momentum  $p = 6500\ \text{GeV}$ , we get  $\theta_0 \approx 0.12\ (0.27)\ \mu\text{rad}$  for the silicon (steel) layer. Within an RP, assuming 9 detector planes, after a distance of 36 mm between the first and the last layer, the average resulting shift is 15 nm, and is neglected. After 10 scattering planes and a distance of 7 m between two pots, the shift is  $3\ \mu\text{m}$ , which again is neglected. The probability of a nuclear collision within a silicon (steel) layer is  $d/\lambda \approx 10^{-3}\ (3 \times 10^{-3})$ . In the case of an RP with two thin windows and 10 layers, it adds up to 1.6%. The nuclear collisions thus contribute to the tails of the hit location distributions.

### 2.4 The data set

In the high- $\beta^*$  data-taking period considered here, the average number of pp collisions per bunch crossing is small (0.1–0.3), and for the same reason the collected integrated luminosity is limited. For this data set, the Level 1 (hardware) trigger requires detected protons in the far RPs in each arm, in parallel or diagonal configurations (Section 2.2). Triggering is based on “trigger roads”, groups of 32 consecutive silicon strips. The trigger bit is set if trigger roads at the same location have signals above a predefined threshold in several detector layers. The elastic pp cross section is much larger than that of central exclusive production events, and therefore the available bandwidth of the data acquisition system would be saturated. Suitable combinations of the trigger bits from the RPs are used to reject elastic events. The high-level trigger has multiple components [12]; the pixel and track activity filters of the CMS silicon tracker system require hits or tracks from centrally produced charged particles.

For these studies two data sets are used. One data set with no centrally reconstructed charged particles (“0-track” data set with some unrelated hits in the pixel detector) contains 39 million events of which 29 million have all four tracklets reconstructed. The other data set has two oppositely-charged centrally reconstructed particles (“2-track” data set) contains 119 million events of which 88 million have all four tracklets reconstructed.

## 3 Tracklet reconstruction

In various exclusive physics analyses, the classification of signal events is based on the conservation of momentum between the incoming and outgoing particles. To maximise the selection efficiency, an optimisation of the standard local tracklet reconstruction [9, 10] was performed, which led to improvements of resolution and uncertainty estimations.

Every RP detector layer contains 512 strips, each with a width (pitch) of  $66\text{ }\mu\text{m}$ . A hit cluster is a group of adjacent strips, each with a collected charge above a certain threshold. Most of the clusters are one-strip wide, with the hit in the central area of the strip. The less frequent two-strip clusters arise through drifting and diffusing electrons from hits in the region between two strips. The fraction of two-strip clusters for each detector layer is shown in Fig. 3, in groups of similarly oriented layers (layer groups). The result of a Gaussian fit is also indicated, with a mean  $f_2 = 10.5\%$ . The outliers, mostly at smaller values, belong to layers with low strip-level efficiencies. Two-strip clusters carry important information and provide better spatial resolution than one-strip clusters (Section 3.1). Clusters with three or more strips are rare, with a rate below half a percent, demonstrating that the effect of capacitive coupling between neighbouring strips is negligible.

Lacking an analog strip readout, the location of a cluster cannot be computed using a charge-weighted cluster mean. Hence the location of a one-strip cluster can be associated to an integer number  $s_i$ , whereas the location of two-strip cluster is the average of their integer numbers (half-integer).

### 3.1 Pattern recognition

Track finding usually starts with local hit reconstruction that, in case of segmented detectors, also includes cluster finding. Based on the hits found, track seeds, i.e., compatible hit multiplets, are built. These are used as starting points for a global track finding by extending them towards other detector layers and picking up free, unused hits (through a Kalman filtering method [13, 14]). Finally, the track candidates are scanned for split or multiply reconstructed trajectories, their momentum vectors are determined, and they are used to fit a common global event vertex. The calibration of a tracking detector includes its alignment by means of cosmic ray muons or particles originating from particle collisions, but sometimes also implies a gain calibration. The performance of a tracking system is usually characterised by its position and momentum resolutions [15].

In the case of RP layers, local hit reconstruction is performed by searching for groups of contiguous strips, mostly one-strip and two-strip clusters, resulting in integer and half-integer cluster coordinates. The strips do not provide pulse height information, but only binary information based on signal discrimination. Since a cluster is a series of adjacent strips with a given width, the trajectory-hit residuals follow rectangular distributions. For this reason, instead of performing least-square fits, a different approach is chosen with the aim to use as much information as possible.

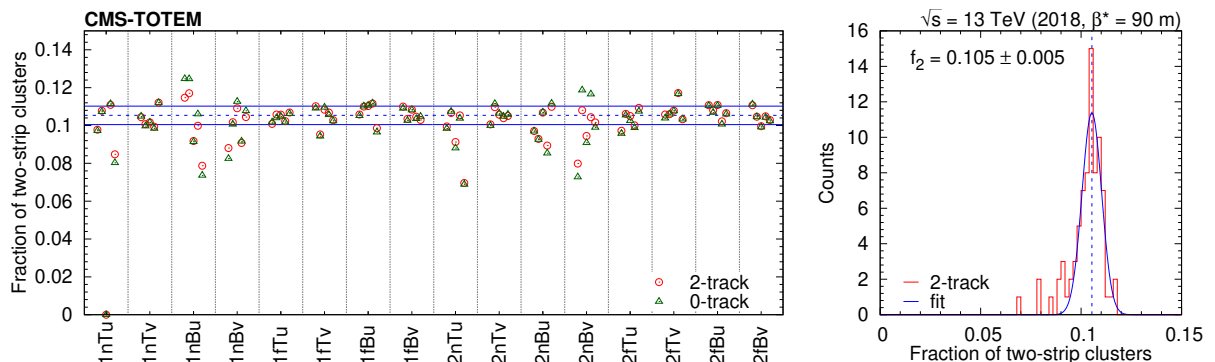


Figure 3: Left: Fraction of two-strip clusters for each detector layer, in groups of similarly oriented layers. Right: Distribution of the fraction of two-strip clusters with the result of a Gaussian fit.

In each RP, the orientations  $u$  and  $v$  are handled separately, since the strips in the two orientations are orthogonal. The tracklet model is a straight line with local hit coordinate  $u_i$  (or  $v_i$ ) in the  $i$ th layer:

$$u_i = az_i + b + \delta_i, \quad (1)$$

where  $a$  is the slope and  $z_i$  is the coordinate of the location of the detector layer along the beam direction. The centre of the RP is at  $z = 0$  where the tracklet has the coordinate  $b$  (intercept). The misalignment of the detector layers is quantified by relative shifts  $\delta_i$  (Section 3.2). Common translation (all  $\delta_i$  values are equal) and shear (linear relation  $\delta_i = \tau_{\text{shear}} z_i$ ) are weak modes and are difficult to detect, and therefore the alignment is carried out with the outermost (first and fifth) layers fixed,  $\delta_1 = 0$  and  $\delta_5 = 0$ . The  $z$ -locations of the layers for Arm 1 are 20.3, 11.3, 2.3,  $-6.7$ ,  $-15.7$  mm ( $u$  orientation) and 15.7, 6.7,  $-2.3$ ,  $-11.3$ ,  $-20.3$  mm ( $v$  orientation); the same values hold for Arm 2, but with opposite sign.

An ideal track traverses two pots (near and far), i.e., in total four layer groups, and each layer group can have up to five hits. Using all events in the 0-track and 2-track data sets, a database of hit location patterns is built. This database is essential for pattern matching, in connection with a tag-and-probe method [16], for precise relative alignment (Section 3.2) and for the determination of individual strip hit efficiencies (Section 3.3). Such a procedure employs an unbiased sample of probe objects that is used to measure the efficiency of a specific set of selection criteria. Here tracklets with at least four hits are tagged, and in each layer a hit at the expected location is searched for. In the case of layer group 1nTu, at least three hits are required since one of its layers is inefficient.

To greatly reduce the number of hit location patterns, common translation (of the first layer,  $s_1$ ) and average shear are removed. Since we want to distinguish between one-strip and two-strip clusters, only integer displacements  $-[s_1]$  are applied. This way, the relative location in the first layer will be either 0 (one-strip) or 0.5 (two-strip). If the first layer is empty, the next layer with valid hit is taken as reference. The average integer shear is also removed by subtracting the value  $i\langle s_i - [s_1] \rangle$  for layer  $i$ , where  $\langle s_i - [s_1] \rangle$  is deduced from  $\sum i(s_i - [s_1]) / \sum i$  by rounding down to an integer, where  $s_i$  is the strip number on layer  $i$ . Some examples for the final patterns are  $(0, 0.5, 1, 1, 2)$ ,  $(0, 0, -1, -3, -2)$ , or  $(0.5, 1, 1, 2.5, 2)$ . Our data sets provide a database of relative hit location patterns with about 15 thousand entries for each layer group (there are altogether 16 layer groups).

If the relative shifts  $\delta_i$  are known, the predicted hit location on the  $i$ th layer is  $u_i^{\text{pred}} = az_i + b + \delta_i$  in strip-width units. The hit distribution of the incoming protons is locally uniform. The incidence angles of the protons are very small, and the protons enter the silicon planes perpendicularly to the planes. If the proton hit is closer than  $w$  to the boundary line between two adjacent strips, it deposits enough energy, such that both strips collect charge above threshold: we get a two-strip cluster. Here  $w$  is measured in pitch units. If the hit is farther than that, the proton deposits a sizeable amount of charge only in one central strip, leading to a one-strip cluster. Because of the local uniformity of the incoming proton distribution, the occurrence of two- and one-strip clusters is directly proportional to the width of the areas described above. For two-strip clusters  $f_2 = 2w$ , hence  $w \approx 0.0525$ . For one-strip clusters the cluster centre  $u^{\text{meas}}$  is expected to lie closer than  $1/2 - w = 0.4475$  to the hit, whereas for two-strip clusters the distance should be below  $w$ . This way, two-strip clusters provide better spatial resolution by a factor of  $(1 - f_2)/f_2 \approx 8.5$  with respect to one-strip clusters. The above requirements can be written down as

$$|u^{\text{meas}} - u^{\text{pred}}| < w \quad \text{or} \quad u_i^{\text{meas}} - az_i - \delta_i - w < b < u_i^{\text{meas}} - az_i - \delta_i + w. \quad (2)$$

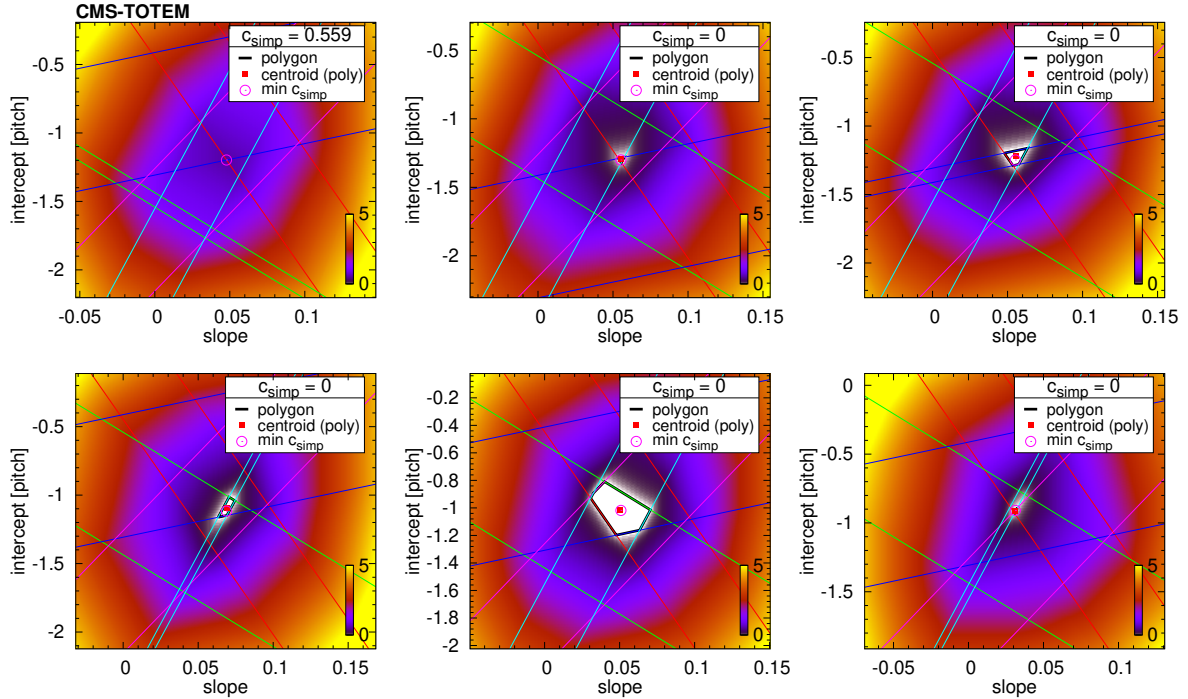


Figure 4: Examples of tracklet fits. The colour represents the value of the tracklet penalty function  $c$  in the intercept-slope ( $b-a$ ) plane. Bands corresponding to individual detector layers are shown with differently coloured parallel straight lines. The intersection of these bands, if it exists, is shown as a white polygonal area ( $c = 0$ ) framed with thick black lines, and its centroid is marked with a red filled square. In each plot, the result of the simplex minimisation  $c_{\text{simp}}$  is given, and the location of the minimum indicated with a purple open circle.

These two inequalities define a band in the intercept-slope ( $b-a$ ) plane (Fig. 4).

Since each detector layer provides such a constraint, we look for the intersection of five bands, i.e., a polygonal area. The determination of this common area is carried out iteratively. First, the intersection of the first two bands, i.e., a parallelogram, is determined. Next, the third band is taken, and intersections of its boundary lines with the sides of the parallelogram are looked for. If such points are found, they are added to the polygon as new vertices, and the vertices that became unnecessary are removed. The process is continued until all bands are dealt with, and we end up with a polygon  $(a_j, b_j)$  of  $j = 1, \dots, n$  vertices. All points within this final polygon are equally probable and valid. The best value and variance of the intercept are represented through the centroid and the moment of inertia of the polygon [17]. Some examples for the common polygons are shown in Fig. 4.

In some cases such a common polygon does not exist. This can happen if there are one or more layers where the cluster centre is farther than the expected distance  $w$  from the location of the predicted hit. In such cases the above polygon method does not work: one needs to define a suitable goodness-of-fit measure. It is accomplished by means of a penalty function  $c$ : if the distance  $d$  of the predicted hit and the cluster is larger than  $w$ , we collect and sum terms  $|d - w|$ . Such a choice, instead of the squared difference, favours the suppression of outlier (noise or background) clusters. The minimisation of the  $c$  value in the  $b-a$  plane is accomplished by using the downhill simplex method of Nelder–Mead [18]. The minimisation usually converges in 3–5 steps, but always finds the minimum in less than 50 steps. Some examples can be seen in Fig. 4. In these cases the standard deviation of the measurement in the  $b$  direction is taken to be 0.3 units. This choice ensures a smooth and monotonic relation between the measured and the

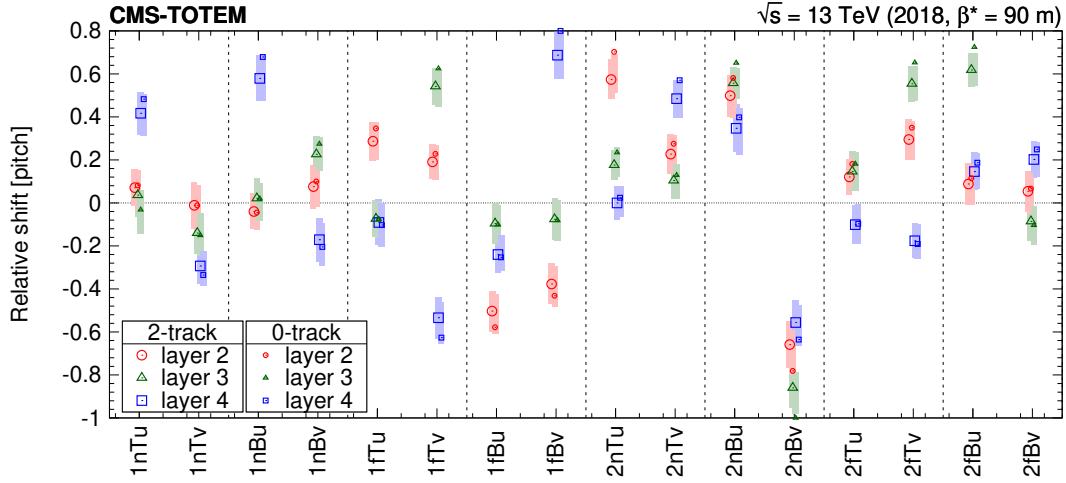


Figure 5: Deded alignment parameters for inner layers ( $\delta_2$  – red circle,  $\delta_3$  – green triangle,  $\delta_4$  – blue square) in layer groups, in units of strip-width. Larger open symbols represent the 2-track data set, and the smaller ones are based on the 0-track data set. Shaded bars indicate the estimated systematic uncertainties (Section 3.2).

predicted variances of the proton momentum sum ( $\sum p_x$ ) distributions (Section 4.4, Fig. 21).

### 3.2 Relative alignment of the detector layers

Tracklet fits can be converted into a tool to determine the relative alignment of the detector layers. The parameters of this three-dimensional problem are the relative shifts of the inner layers ( $\delta_2, \delta_3, \delta_4$ ). The goal is to minimise the joint goodness-of-fit measure, i.e., the sum of  $c$  values for a large set of the tracklets. The employed minimisation method is again the downhill simplex method of Nelder–Mead [18]. The best  $\delta_i$  values for the 16 layer groups, corresponding to the lowest sum, are displayed in Fig. 5. The indicated systematic uncertainties represent the region where the sum of the  $c$  values (tracklet penalty) would increase by one percent, a well-visible change. The values from the 2-track and 0-track data sets are compatible with each other. The standard deviation of the relative shifts is about 0.35, in units of strip-width. The deduced relative shifts are cross-checked with an alternative method by counting the number of tracklets with  $c = 0$ , giving compatible results. One-dimensional line scans around the minima are shown in Fig. 6.

The distribution of the joint  $c$  values for tracklets is plotted in the upper panel of Fig. 7. Most tracklets (89%) have  $c = 0$ . The distribution of the standard deviation  $\sigma_u$  of fitted hit location in strip-width units for the polygon method, and for the cases where the simplex minimisation was necessary, is shown in the lower panel of Fig. 7. The average spatial resolution is 0.10 units, i.e., about  $6\text{--}7 \mu\text{m}$ . This is to be compared with the naive expectation from averaging three box distributions,  $66 \mu\text{m}/\sqrt{12 \times 3} \approx 11 \mu\text{m}$ , which worsens once the contribution from the standard deviation of the relative shifts ( $66 \mu\text{m} \times 0.35/\sqrt{3} \approx 13 \mu\text{m}$ ) is also included.

To control and cross-check the deduced calibrations and to extract the tracklet efficiencies, a simple, strip-level simulation containing one million events was set up. Hit creation at the strip level is performed including individual shifts and efficiencies. Conditions for triggering and for tracklet reconstruction are properly included. A reasonable agreement between the simulated and measured tracklet joint penalty and  $\sigma_u$  distributions (Fig. 7, right column) is achieved.

In summary, the advanced treatment just described results in better spatial and transverse mo-

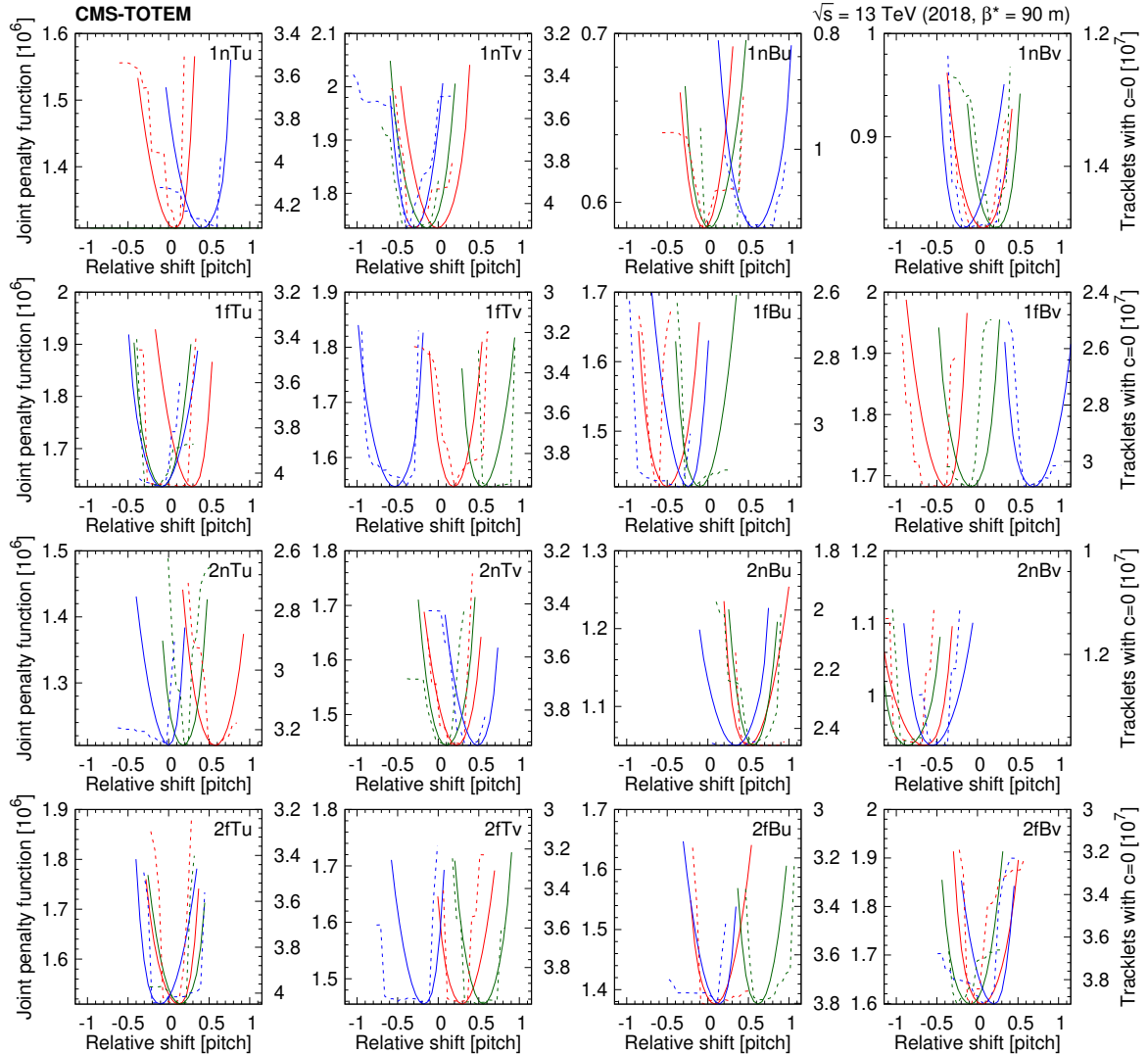


Figure 6: One-dimensional line scans of the relative shifts ( $\delta_2$  – red,  $\delta_3$  – green,  $\delta_4$  – blue) for the 16 layer groups around the best values found. The joint  $c$  value is plotted as a function of the relative shifts of the inner layers around the found minima (solid curves, left vertical scale). Goodness-of-fit from an alternative method, counting tracks with  $c = 0$ , is also indicated (dashed lines, right vertical scale, number of such tracks with inverted axis). In the 1nTu panel (upper left corner) the curve corresponding to the third layer is missing since that layer is inefficient.

mentum resolutions.

### 3.3 Strip hit efficiencies

The tracklet measurement is redundant since in each RP there are five layers in each orientation ( $u$  and  $v$ ), but three hits are enough for triggering (using the far RPs) and for reconstruction (using all RPs). A reduced efficiency in all detector layers in an RP, as is the case in the near bottom RPs in both arms discussed below, results in tracklet detection inefficiency and a reduced proton reconstruction efficiency. In these detector layers, the inefficiency is a function of the sequential strip number in each layer and is probably caused by two factors: the instantaneous luminosity and the radiation damage accumulated during the lifetime of the detectors.

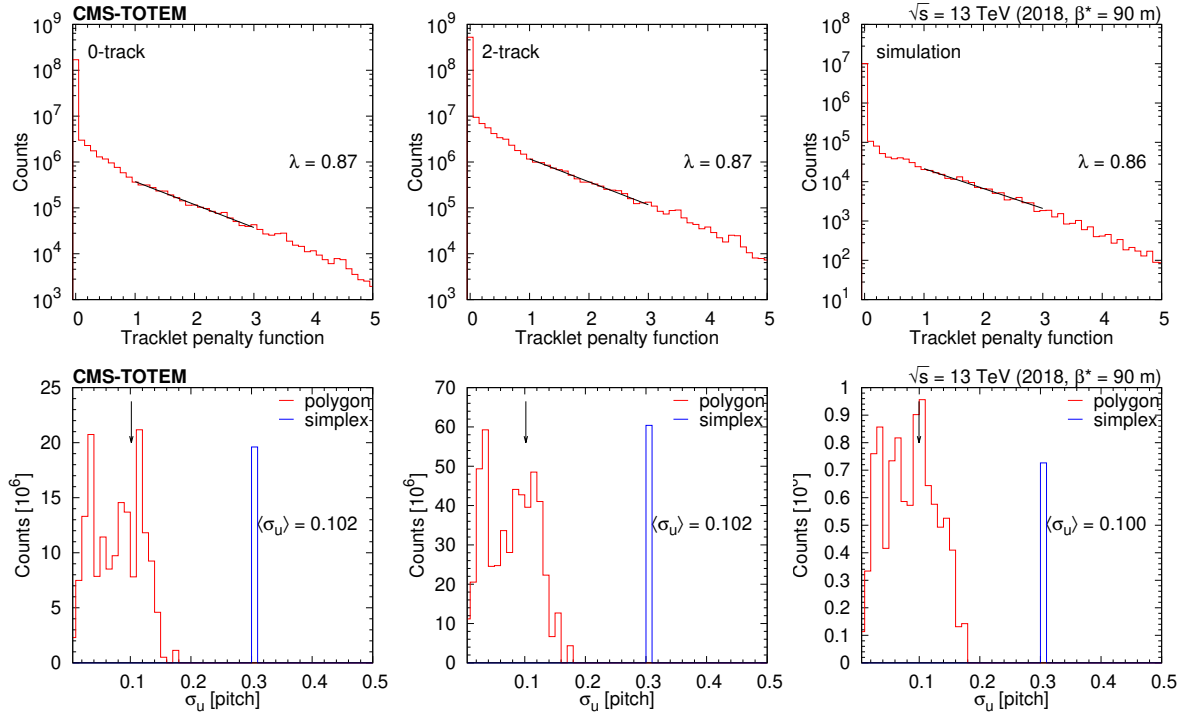


Figure 7: Upper: Distribution of the tracklet penalty function with the slope  $\lambda$  of an exponential fit (black line) in the range 1–3. Lower: Distribution of the standard deviation of the fitted hit location in strip-width units for the polygon method (red), and for those cases where the simplex minimisation was necessary (blue, at 0.3). The three columns correspond to the 0-track (left), 2-track (centre), and the simulated (right) data sets. The vertical arrow indicates the location of the average value.

Strip-level efficiencies are extracted from the data by using the dominant hit location patterns defined below. Using the library of patterns, we count the occurrence of similar patterns where the hit position in the given layer differs by either -2, -1.5, -1, -0.5, 0, 0.5, 1, 1.5, or 2 strip units. If the most common pattern has a frequency of more than 90% among the variants, and possesses a one-strip hit in the given layer, this pattern is called dominant.

For a tracklet with no missing hit, layers are selected one by one. If the pattern for a layer is dominant, the strip must have a hit, and the efficacy counter ( $n_1$ ) for this strip is increased. For a tracklet with exactly one missing hit, the location of that hit can be predicted through the dominant pattern, and the inefficacy counter ( $n_0$ ) for that strip is increased. The strip efficiency and its uncertainty are estimated using these counters.

Strip hit efficiencies extracted from the data are shown for a given layer in the 1nTv and 2nBu layer groups, and for a representative run, in Fig. 8. Values based on the 2-track data set and those from the 0-track data are plotted. They are compatible with each other, and the effect of their uncertainty in the proton reconstruction efficiency is about 3%. There are regions where the efficiency is rather low—especially the layer groups 1nBu, 1nBv, 2nBu, and 2nBv. These are the near bottom RPs on both sides of the IP. Strip hit efficiencies as a function of run number, for strip #350, as an example, in layers 1–5 in various layer groups are shown in Fig. 9. The efficiencies are mostly constant, but for some planes they change with the run number by up to 20%.

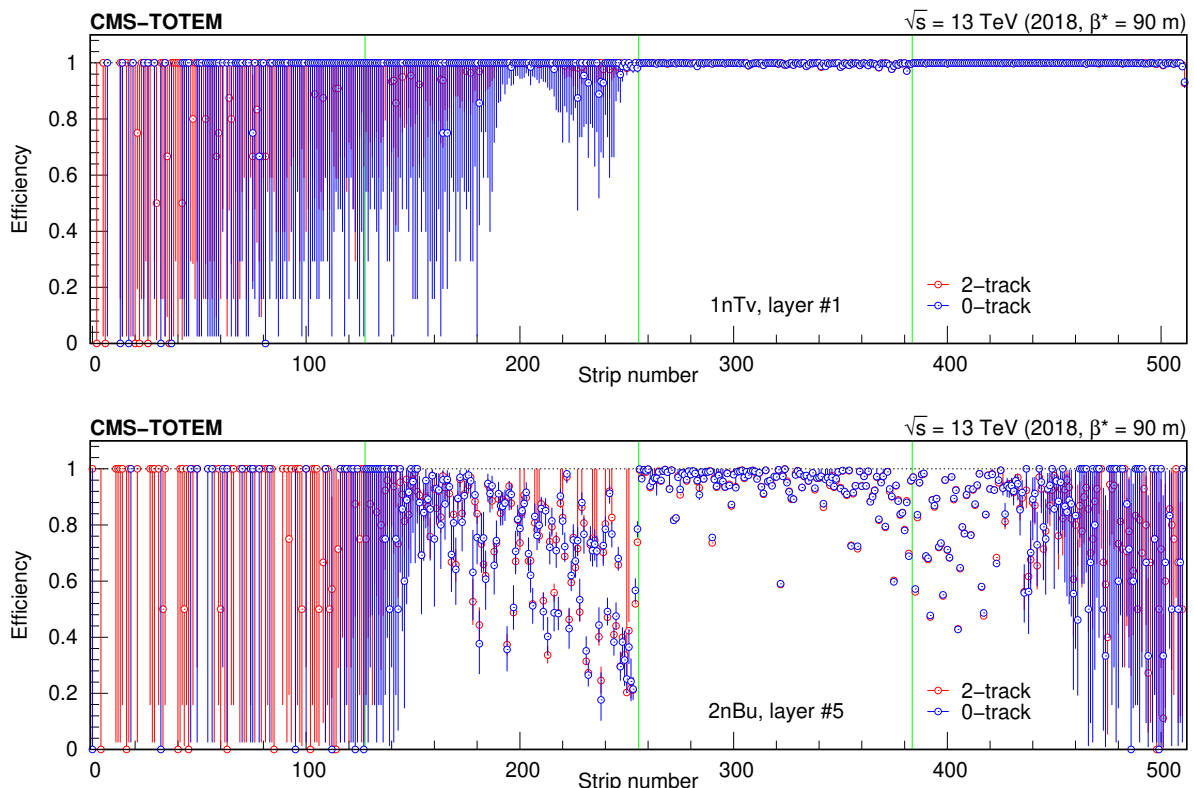


Figure 8: Strip hit efficiency from data, determined with a tag-and-probe method. Shown here are layer 5 in layer group 1nTv (top) and 2nBu (bottom) for a specific run. Values and statistical uncertainties based on the 2-track data set (red symbols) and those from 0-track data (blue symbols) are plotted. The borders of the front-end chips are indicated with (green) vertical lines. The uncertainties are large at the left and right edges, because those regions are rarely hit.

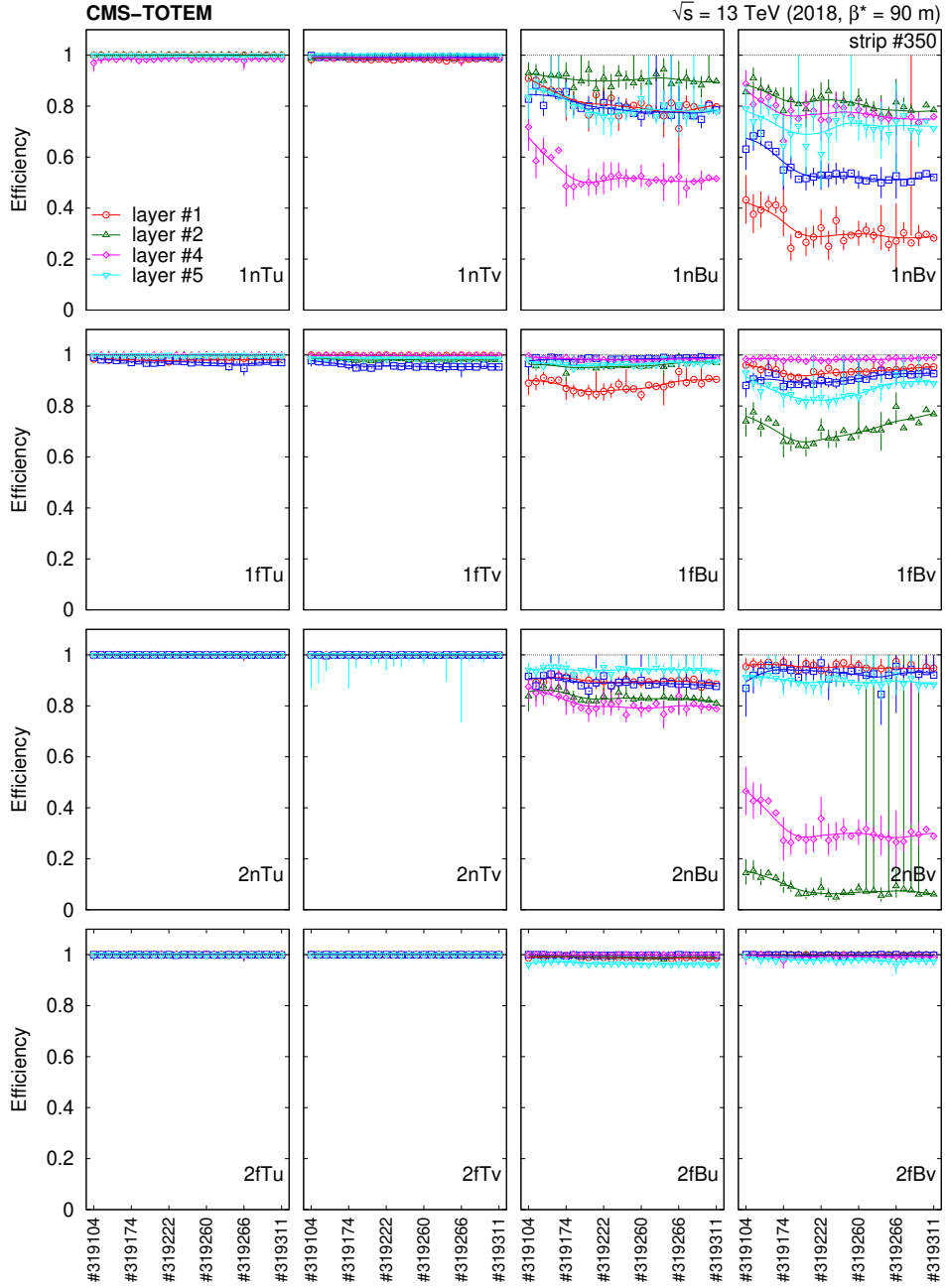


Figure 9: Strip hit efficiencies as functions of the run number for strip #350 in layers 1–5 (coloured points) in various layer groups (labels in the lower right corner). Statistical uncertainties are indicated with vertical bars. Lines are spline interpolations to guide the eye.

### 3.4 Tracklet efficiencies and joint weights

The tracklet reconstruction efficiencies are determined by means of a simulation based on the strip hit detection efficiencies. Efficiency as a function of the tracklet location at the centre of the RP (the track intercept) and of the track slope is shown for each layer group separately in Fig. 10, for a representative run. Substantial losses are present at specific tracklet locations and slopes. The periodic efficiency loss seen at every 32nd strip for the far RPs is due to the RP trigger that uses roads of 32 strips to define a track candidate. If the tracklet is in the border region between trigger roads, there is an increased chance that it is lost. This kind of pattern is not observed in the near RPs that were not used in the trigger.

In a normal event, where both scattered protons are detected by both near and far pots, we have four tracklets, each with  $u$  and  $v$  projections. The product of their corresponding tracklet efficiencies (obtained from a table, Fig. 10) gives the probability of detecting such an event. The reciprocal of this joint probability is the joint tracklet weight that is applied in physics analyses. As expected from the low strip hit efficiencies in the bottom RPs, events with trigger configuration BB suffer the most, while the detection of TT events is fully efficient.

Once the tracklet coordinates in  $u$  and  $v$  directions are fitted, the hit transverse location ( $x, y$ ) in the global coordinate system, at the centre of the RP (on the “reference surface”), is calculated through a rotation (Section 2.2).

The efficiency-corrected distribution of proton hit locations in the  $x$ - $y$  plane at the reference surfaces of the eight RPs, are shown in Fig. 11 for different trigger configurations. The wavy pattern seen in the plots of the events with the diagonal trigger (TB and BT) is a direct consequence of the trigger rejecting a large fraction of elastic events. This is performed by vetoing events where hits in the two arms have similar coordinates but with opposite sign. The halo seen in the 0-track sample for the parallel trigger configurations (TT and BB) shows that those are not elastic events, but overlapping inelastic events where the momentum loss of the scattered protons is significant.

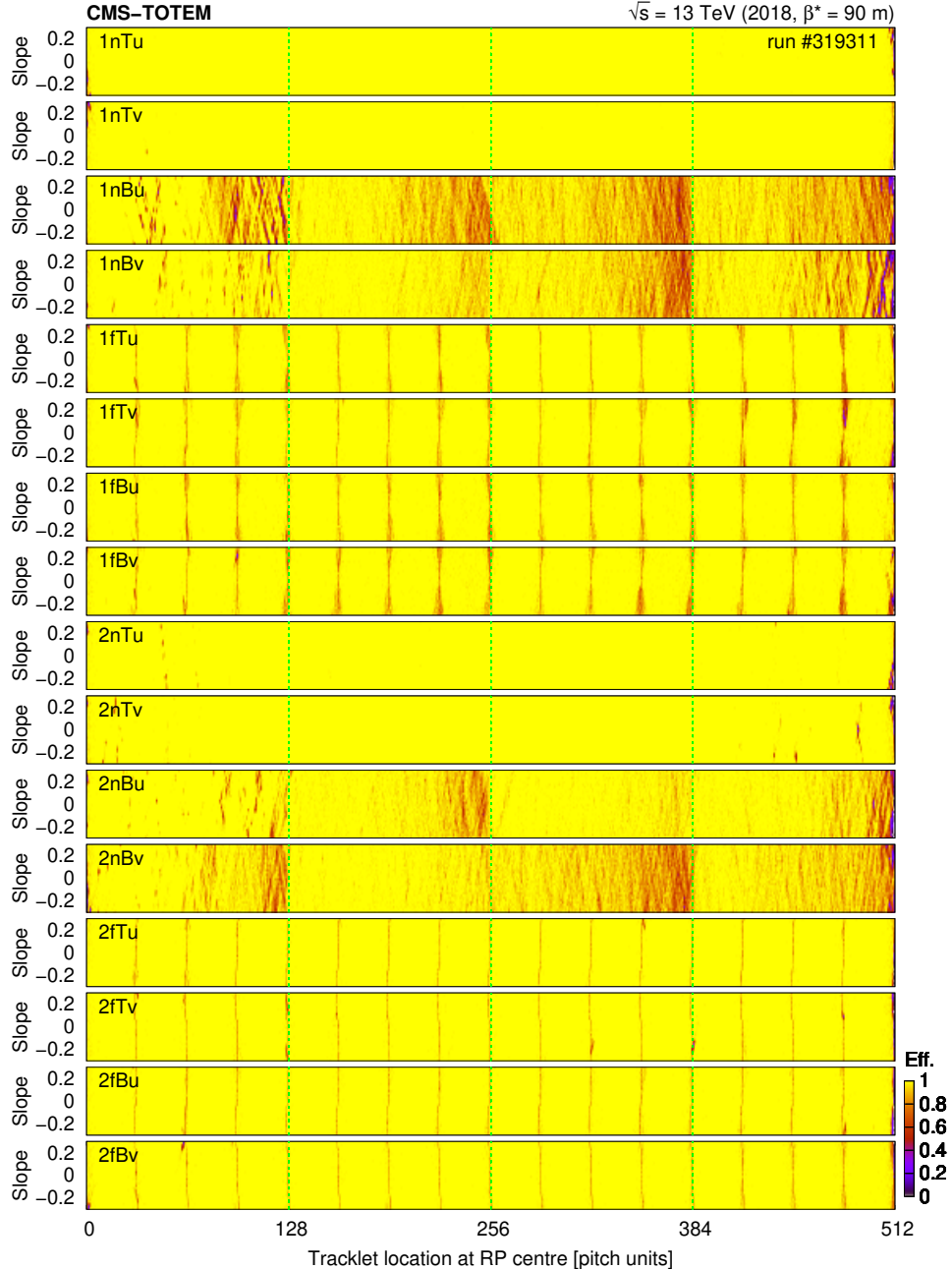


Figure 10: Tracklet reconstruction efficiency (colour scale) as a function of tracklet location at the centre of the RP (intercept) and the track slope, for a representative run, shown for each layer group separately. Yellow regions correspond to fully efficient tracklet reconstruction, whereas the red regions exhibit substantial losses with efficiencies in the range 0.4–0.6. Vertical green lines denote boundaries of the front-end chips.

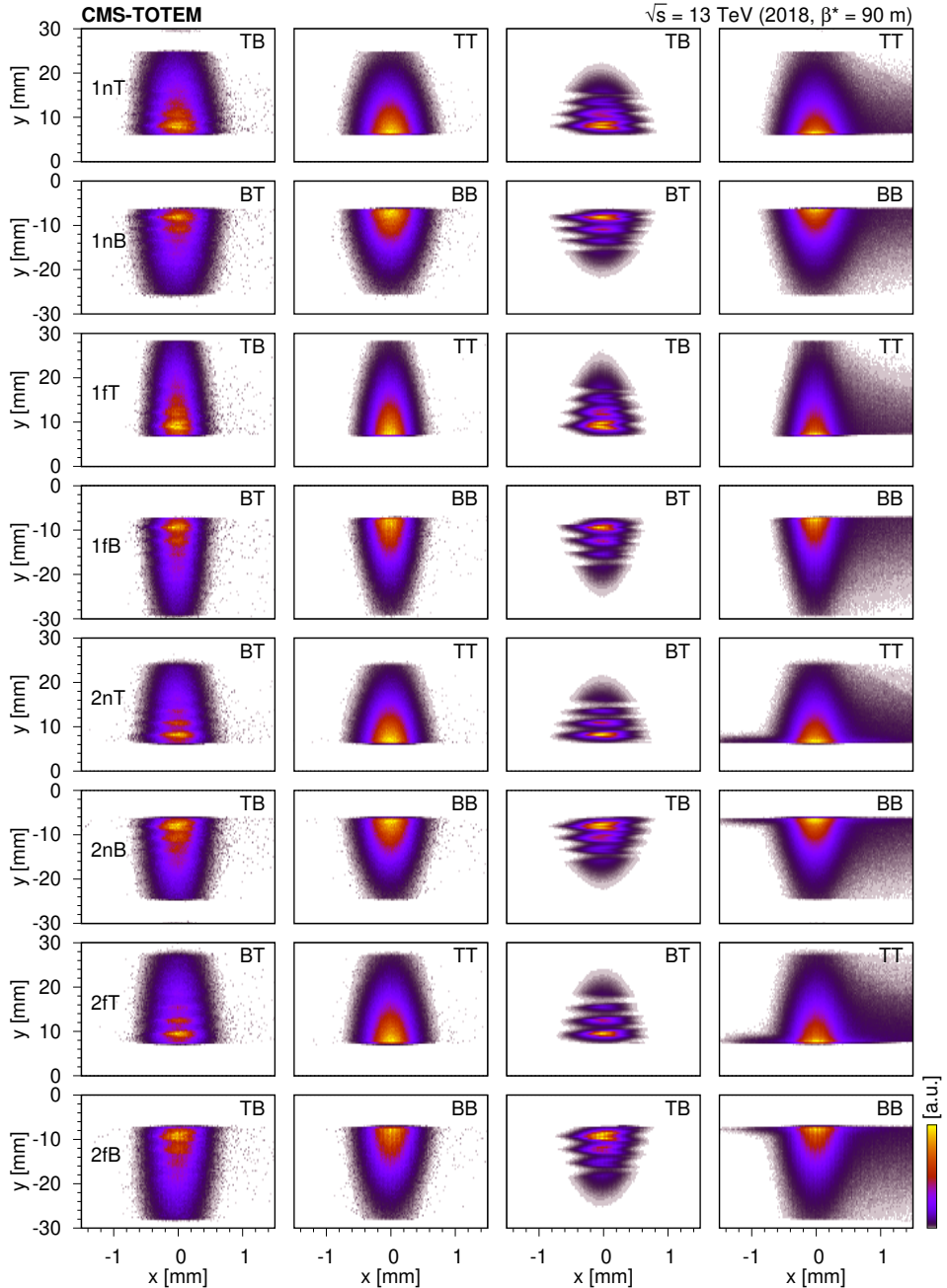


Figure 11: Efficiency-corrected distribution of proton hit locations in the  $x$ - $y$  plane at the references surfaces of the eight RPs (rows), for different trigger configurations (labels at the upper right corner). The two columns on the left side refer to the 2-track data set, whereas the two on the right side display distributions based on the 0-track data set. The wavy pattern and the halo seen in the 0-track data set is explained in the text.

## 4 Proton reconstruction

Our goal is to reconstruct the  $(p_x, p_y)$  transverse momentum vectors, or the emission angles  $(\theta_x^*, \theta_y^*)$ , and the locations  $(x^*, y^*)$  of the scattered protons in the transverse plane at the nominal IP. This is accomplished by using only the fitted hit locations  $(x, y)$  of the proton tracklets at the reference surfaces of the RPs. The deduced local slopes  $(dx/dz$  and  $dy/dz)$  are not used since those have poor resolution. A detailed cross-check of the beam optics based on the measured hit position covariances, and a precise run-by-run alignment are also described in the following.

### 4.1 Beam optics

The nominal optics determination and alignment procedure for RPs uses elastic events [19, 20] and MAD-X [21], which is a general purpose accelerator design program. The method exploits kinematical distributions of elastically scattered protons observed in the RPs. It varies the rotation angles and currents of the six quadrupoles between the IP and the RPs for both beams, as well as the beam energy of both beams, each within its uncertainty. Theoretical predictions, as well as Monte Carlo studies, show that the residual uncertainty in the deduced optical parameters is smaller than 0.25%.

The transverse coordinate  $x$  of a particle (proton) at position  $s$  along the beamline can be described as [22]

$$x(s) = \sqrt{\beta_x(s)\varepsilon} \cos [\phi_0 + \Delta\mu(s)] + D_x(s)\Delta p/p, \quad (3)$$

where  $\beta$  is the betatron amplitude,  $\varepsilon$  is the emittance,  $\phi_0$  is the phase offset,  $\Delta\mu$  is the phase advance,  $D$  is the dispersion function, and  $\Delta p/p$  is the relative momentum loss of the scattered proton. The quantities characterising the LHC optics are the horizontal and vertical betatron amplitude  $\beta(s)$ , the magnification  $v(s) = \sqrt{\beta(s)/\beta^*} \cos \Delta\mu(s)$ , and the effective length  $L(s) = \sqrt{\beta(s)\beta^*} \sin \Delta\mu(s)$ . The phase advance  $\Delta\mu(s)$  is calculated as  $\Delta\mu(s) = \int_0^s ds'/\beta(s')$ , in other words  $d\Delta\mu/ds = 1/\beta(s)$ . At the nominal IP ( $s = 0$ ), the location of the particle is  $x^* = x(0)$ ,  $y^* = y(0)$ , and  $\beta^* = \beta(0)$ ,  $\Delta\mu(0) = 0$ . The dependences of  $x$  on  $x^*$ ,  $\theta^*$ , and  $\Delta p/p$  around a given location can be linearised, and in an arm for the two RP stations (subscript  $n$  for near, and  $f$  for far) we have:

$$x_n = v_{x,n}x^* + L_{x,n}\theta_x^* + D_{x,n}\Delta p/p, \quad (4)$$

$$x_f = v_{x,f}x^* + L_{x,f}\theta_x^* + D_{x,f}\Delta p/p, \quad (5)$$

where the path-dependent dispersion function  $D_x(s)$  is needed for the description of particles with momentum spread or momentum loss ( $\Delta p$ ). For  $\beta^* = 90$  m, the expected values are approximately  $L_x \approx 0$ ,  $L_y \approx 262$  m,  $v_x \approx -1.9$ ,  $v_y \approx 0.0$ ,  $D_x \approx -0.041$  m, and  $D_y \approx 0$ , based on Table 6.1 in Ref. [23]. The actual values are a bit different, asymmetric, and are shown in Table 3 (truncated to four or five significant digits), based on MAD-X calculations and subsequent matching with data [19, 20]. The optics is such that the  $x$  and the  $y$  directions decouple. In the  $y$  direction the magnification and dispersion are close to zero; therefore, only the emission angle can be determined with good precision, through a simple proportionality relation  $\theta_y^* = y_n/L_{y,n}$  or  $y_f/L_{y,f}$ .

For elastic and central exclusive collisions ( $|\Delta p/p| \ll 1$ ), the above Eqs. (4)-(5) can be solved as

$$x^* = (L_{x,f}x_n - L_{x,n}x_f)/d, \quad (6)$$

$$\theta_x^* = (v_{x,n}x_f - v_{x,f}x_n)/d, \quad (7)$$

where the determinant is  $d \equiv v_{x,n}L_{x,f} - v_{x,f}L_{x,n}$ . It can be shown that  $d$  equals the distance between the two RP stations, more precisely the distance between their reference surfaces in the beam direction (in our case,  $d = 7000$  mm).

Cross-checks of beam optics were performed with data, based on the measured variances and covariance of the proton hit positions in  $x$ . Once these quantities are measured, the variance  $\text{var}(x^*)$  is obtained as

$$\text{var}(x^*) = \frac{\text{var}(x_n)\text{var}(x_f) - \text{cov}(x_n, x_f)^2}{\text{var}(x_f)v_{x,n}^2 - 2\text{cov}(x_n, x_f)v_{x,n}v_{x,f} + \text{var}(x_n)v_{x,f}^2}, \quad (8)$$

which does not depend on the actual values of the effective lengths, but only on the given magnifications  $v_{x,n}$  and  $v_{x,f}$ , and the measured hit position variances and covariances. The ratio of far and near effective lengths is

$$\frac{L_{x,f}}{L_{x,n}} = \sqrt{\frac{\text{var}(x_f) - \text{var}(x^*)v_{x,f}^2}{\text{var}(x_n) - \text{var}(x^*)v_{x,n}^2}}. \quad (9)$$

The variance of the emission angle is

$$\text{var}(\theta_x^*) = \frac{\text{var}(v_{x,f}x_n - v_{x,n}x_f)}{|d|^2}. \quad (10)$$

With that, the effective lengths are

$$L_{x,n} = \sqrt{\frac{\text{var}(x_n) - \text{var}(x^*)v_{x,n}^2}{\text{var}(\theta_x^*)}}, \quad L_{x,f} = \sqrt{\frac{\text{var}(x_f) - \text{var}(x^*)v_{x,f}^2}{\text{var}(\theta_x^*)}}. \quad (11)$$

The estimated size of the beam spot in the  $x$  direction is  $\sigma_{x^*} \approx 100 \mu\text{m}$ , consistent with measurements using charged particles reconstructed in the central CMS silicon tracker. The emission angle is  $\sigma_{\theta_x^*} \approx 28 \mu\text{rad}$  for 0-track and  $42 \mu\text{rad}$  for 2-track events. These values are substantially larger than the beam divergence ( $2.1 \mu\text{rad}$ , Section 2.1), since the characteristic width of the proton emission angle is dominated by the much larger scale of the various physics processes. The ratio of effective lengths for Arm 1 is  $L_{x,f}/L_{x,n} \approx -0.3$ , and for Arm 2  $L_{x,f}/L_{x,n} \approx -4$ . These are to be compared with the nominal values  $-0.17$  and  $-15$ , yielding only a poor agreement. This first look is refined, and shows a much better agreement, once the precise run-by-run RP alignment is put in place (Section 4.3).

## 4.2 Effects of the IP transverse location and proton emission angle

The correlation of the proton hit locations in the  $x$  and  $y$  directions reflects various physics effects, such as momentum loss, width of the beam at the nominal IP, and the influence of effective length ratios.

Table 3: Nominal values of beam optics variables (magnifications  $v$ , effective lengths  $L$ ) [19, 20], truncated to four or five significant digits.

Arm	Station	$v_x$	$L_x$ [m]	$v_y$	$L_y$ [m]
1	near	-2.204	3.1042	0.032395	238.2
1	far	-1.884	-0.5225	0.007509	271.3
2	near	-2.245	0.1943	0.018513	238.3
2	far	-1.923	-2.9508	-0.008295	271.3

For elastic collisions, the momentum loss of the protons is very small, its spread is  $|\Delta p/p| \lesssim 10^{-4}$ , reflecting the momentum variance of the beam. This corresponds to about  $5\text{ }\mu\text{m}$  hit position spreading, which is hardly detectable. The acceptance of the central tracker limits the detectable 2-track central exclusive events to  $|\Delta p/p| \lesssim 10^{-3}$  through momentum conservation, corresponding to a  $50\text{ }\mu\text{m}$  shift in hit position (comparable to the strip width of  $66\text{ }\mu\text{m}$ ). Here “shift” refers to the difference between the true hit position and the predicted track impact point position assuming the nominal beam momentum. For diffractive and highly inelastic collisions, where the momentum loss of the incoming protons is sizeable, a well-detectable displacement is visible: a 10% momentum loss corresponds to a 5 mm shift. The events show a linear correlation between  $x_{\text{f}}$  and  $x_{\text{n}}$  (Fig. 12) with a slope  $D_{x,f}/D_{x,n} \approx 0.68$  for Arm 1, and  $\approx 0.64$  for Arm 2, as expected.

The effect of the beam width at the nominal IP,  $\sigma_{x,y}^* \sim \mathcal{O}(100\text{ }\mu\text{m})$ , can be propagated to the RPs ( $v_x x^*$ ) and results in a spread of about  $200\text{ }\mu\text{m}$ . Such an event-by-event shift is correlated between the two arms (the protons come from the same actual IP) and is well detectable. For a transverse momentum  $p_x = 200\text{ MeV}$  we have  $\theta_x^* \approx 10^{-4}$ , which results in a shift of  $20\text{--}300\text{ }\mu\text{m}$ . The higher values are already detectable and in the case of elastic collisions there should be a clear correlation between the two arms.

In the case of small  $x$  values (Fig. 13), the distribution consists mostly of elastic and central exclusive events with  $\Delta p/p \approx 0$ . For the diagonal configuration, the 0-track data set (mostly elastic events) shows a slope of 0.79 for Arm 1, and 0.92 for Arm 2. For the parallel configuration (in part central exclusive events), the slope is 0.70–0.73 for Arm 1, and 0.95–0.99 for Arm 2. The slopes for elastic and central exclusive events differ because the variance of the proton emission angle  $\text{var}(\theta_x^*)$  in the two cases is different. The quantities shown in Fig. 13 are used for estimating  $\text{var}(x^*)$  using Eq. (8).

In the  $y$  direction, the measured data match our expectations with the slope  $L_{y,f}/L_{y,n} = 271.3/238.2 \approx 1.14$  (Fig. 14).

### 4.3 Absolute run-by-run alignment

An inspection of collision events shows apparent deviations from momentum conservation. This is corrected by means of additional shifts of the RPs in the  $x$  and  $y$  directions. This absolute alignment is tested through symmetry and momentum conservation by studying the distributions of the deduced IP coordinates and of the momentum sum, and more specifically their means.

The alignment in both the  $x$  and  $y$  directions must be performed for each run separately, since sizeable apparent displacements from run to run are observed. The changes are mostly due to the drifting LHC proton orbit, since the RP movement system ensures a position reproducibility of about  $20\text{ }\mu\text{m}$ . However, instead of correcting the incoming proton direction, for the sake of simplicity, in the present analysis the RPs are artificially shifted. The goal is to determine the additional shifts  $\delta x$  and  $\delta y$  for the eight RPs, i.e., altogether 16 values.

The measured deviations  $\vec{\Delta}$  and the local shifts  $\vec{x}_0$  are connected through a linear transformation  $A\vec{x}_0 = \vec{\Delta}$ , where  $A$  is a matrix. The shifts  $\vec{\delta}x$  are such that  $A(\vec{x}_0 + \vec{\delta}x) = 0$ , and therefore they can be determined from solving  $A\vec{\delta}x = -\vec{\Delta}$ .

The alignment in the  $x$  direction is based on the nearly Gaussian hit location and momentum sum distributions, since they must be symmetric about zero:

- the location of the primary interaction  $x^* = (x_{\text{n}}L_{x,f} - x_{\text{f}}L_{x,n})/d$ . This quantity is

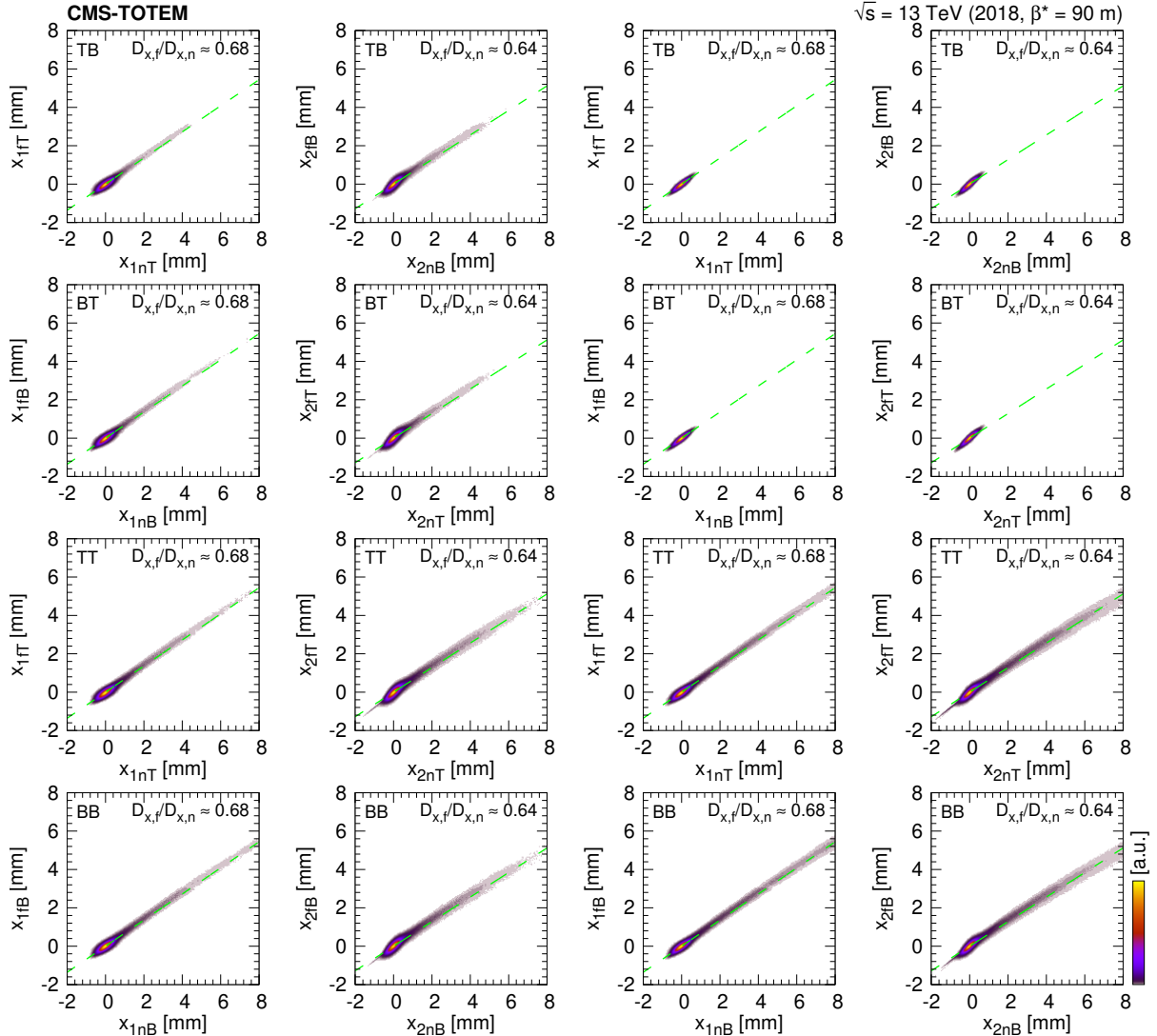


Figure 12: Correlation of proton hit locations in the  $x$  direction (two-dimensional occupancy histograms) in the far and near RPs, shown for various trigger configurations (TB, BT, TT, and BB, in rows). The two columns on the left side refer to the 2-track data set, and the two on the right side display distributions based on the 0-track data set. A straight line corresponding to the expectation  $x_f = x_n D_{x,f} / D_{x,n}$  is also plotted, where  $D_{x,f} / D_{x,n} \approx 0.68$  for Arm 1, and  $\approx 0.64$  for Arm 2. The plots are produced with the final detector alignment.

calculated in a single arm (1 or 2), using either the top or the bottom pots (T or B), hence the notations 1T, 1B, 2T, and 2B.

- the sum of particle momenta  $\sum p_x$  in elastic or exclusive events. For scattered protons in the RPs,  $p_x$  is calculated as  $p_x = p_{\text{beam}}(x_f v_{x,n} - x_n v_{x,f}) / d$ .

We can use the measured means of 16 distributions: the location of the IPs  $x^*$ , calculated from RP arm configurations 1T, 1B, 2T, and 2B (4 values); the sum of the proton transverse momenta  $\sum p_x$  for RP trigger configurations TB, BT, TT, and BB (4 values); the local hit positions  $x$  in each

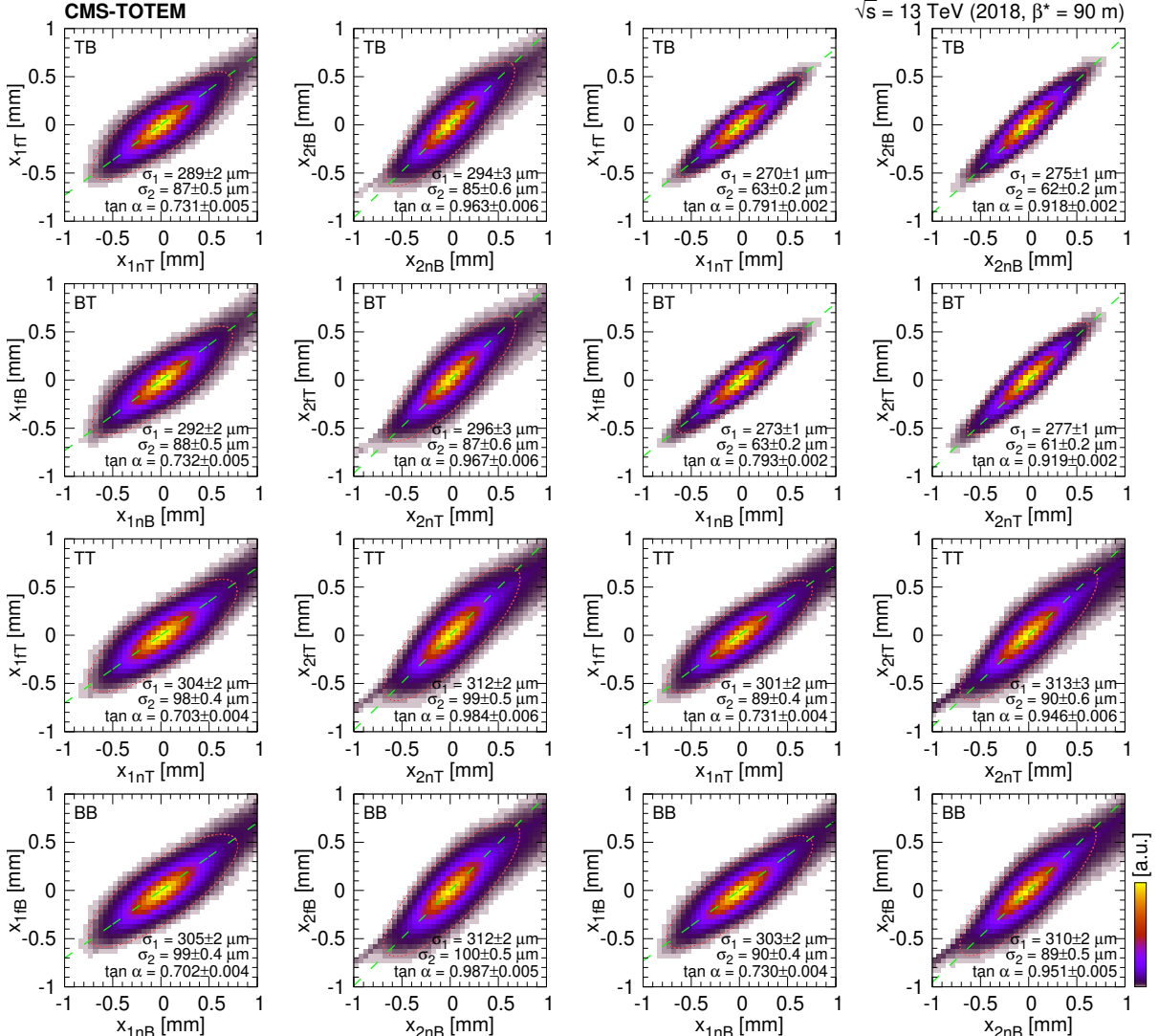


Figure 13: Correlation of proton hit locations in the  $x$  direction (two-dimensional occupancy histograms) in the far and near RPs, shown for various trigger configurations (TB, BT, TT, and BB, in rows), with a restricted scale. Parameters (standard deviations in major and minor axis directions  $\sigma_1$  and  $\sigma_2$ , and the rotation angle  $\alpha$ ) of the fitted tilted two-dimensional normal distributions are displayed in the plots. The corresponding ellipses cover 99% of the points; the dashed green lines indicate their major axes. The two columns on the left side refer to the 2-track data set, whereas the two on the right side display distributions based on the 0-track data set. The plots are produced with the final detector alignment.

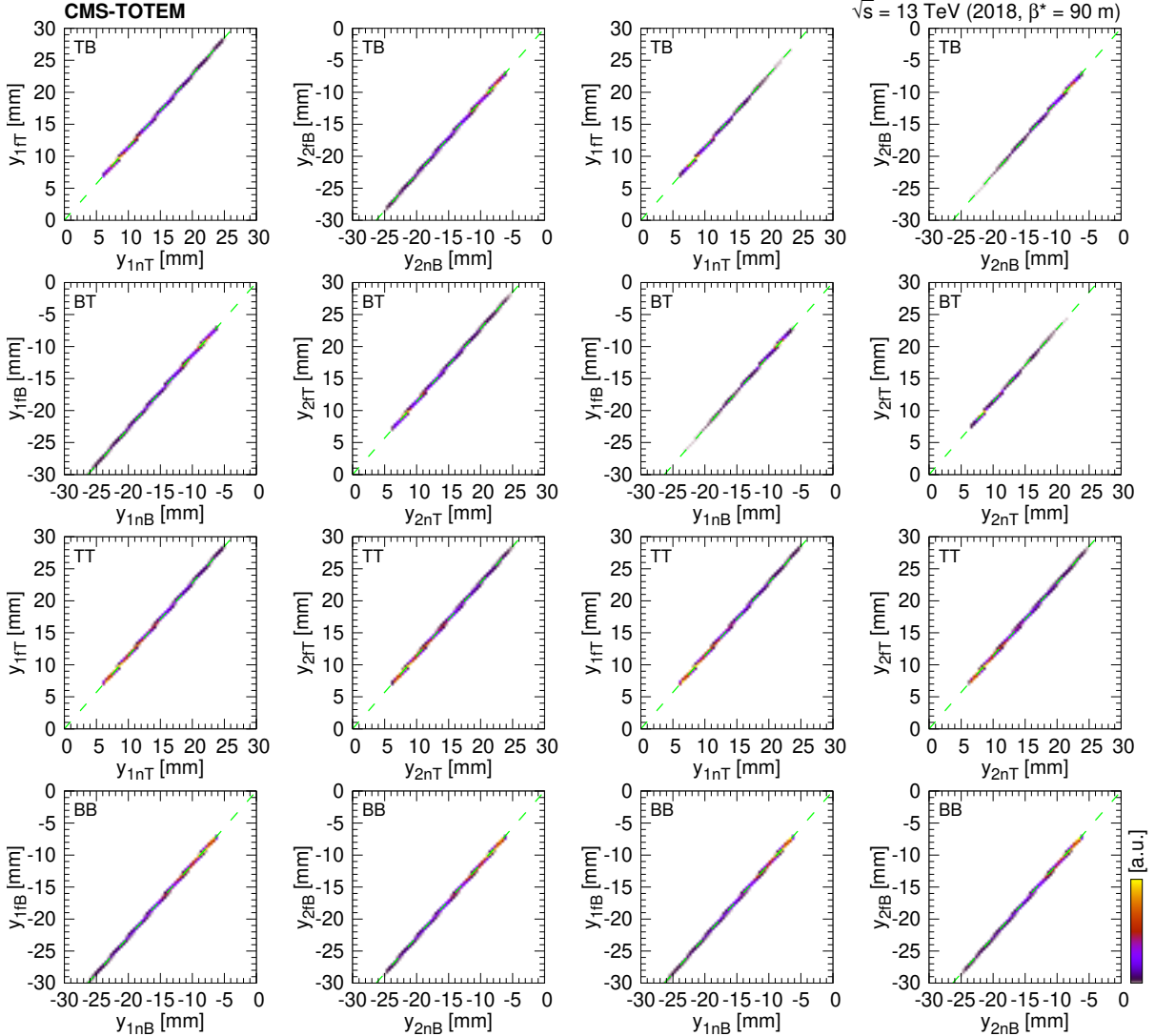


Figure 14: Correlation of proton hit locations in the  $y$  direction (two-dimensional occupancy histograms) in the far and near RPs, shown for various trigger configurations (TB, BT, TT, and BB, in rows). The two columns on the left side refer to the 2-track data set, whereas the two on the right side display distributions based on the 0-track data set. A straight line corresponding to the expectation  $y_f = y_n L_{y,f} / L_{y,n}$  is also plotted, where  $L_{y,f} / L_{y,n} \approx 1.14$ . The plots are produced with the final detector alignment. The apparent piecewise linear segments are simply the consequence of the binning.

RP (8 values). The transformation matrix is

$$A_x = \begin{pmatrix} L_{1f}/d & -L_{1n}/d & 0 & 0 & 0 & 0 & 0 & 0 \\ 0 & 0 & L_{1f}/d & -L_{1n}/d & 0 & 0 & 0 & 0 \\ 0 & 0 & 0 & 0 & L_{2f}/d & -L_{2n}/d & 0 & 0 \\ 0 & 0 & 0 & 0 & 0 & 0 & L_{2f}/d & -L_{2n}/d \\ -pv_{1f}/d & pv_{1n}/d & 0 & 0 & 0 & 0 & -pv_{2f}/d & pv_{2n}/d \\ 0 & 0 & -pv_{1f}/d & pv_{1n}/d & -pv_{2f}/d & pv_{2n}/d & 0 & 0 \\ -pv_{1f}/d & pv_{1n}/d & 0 & 0 & -pv_{2f}/d & pv_{2n}/d & 0 & 0 \\ 0 & 0 & -pv_{1f}/d & pv_{1n}/d & 0 & 0 & -pv_{2f}/d & pv_{2n}/d \end{pmatrix}, \quad (12)$$

where  $p = p_{\text{beam}}$ , and the transformation itself is

$$A_x \begin{pmatrix} \delta x_{1nT} \\ \delta x_{1fT} \\ \delta x_{1nB} \\ \delta x_{1fB} \\ \delta x_{2nT} \\ \delta x_{2fT} \\ \delta x_{2nB} \\ \delta x_{2fB} \end{pmatrix} = \begin{pmatrix} -\langle x_{1T}^* \rangle \\ -\langle x_{1B}^* \rangle \\ -\langle x_{2T}^* \rangle \\ -\langle x_{2B}^* \rangle \\ -\langle \sum p_{x,TB} \rangle \\ -\langle \sum p_{x,BT} \rangle \\ -\langle \sum p_{x,TT} \rangle \\ -\langle \sum p_{x,BB} \rangle \end{pmatrix}. \quad (13)$$

The top and bottom RPs are independently movable, and their hit location distribution in the  $y$  direction has a gap in the middle. In addition, because of the varying  $p_y$  acceptance of various pots, the normalisation of the distributions in the top and bottom parts is unrelated. Hence the alignment in the  $y$  direction cannot be based on the hit location distributions alone. There are two variables whose distributions must be symmetric about zero, and are not biased:

- the location of the primary interaction  $y^*$ . In an arm, using either the top or the bottom RPs, it is calculated as  $y^* = (y_n L_{y,f} - y_f L_{y,n})/d$ . There are four such independent equations (two arms, top or bottom RPs).
- the sum of particle momenta  $\sum p_y$  in elastic or exclusive events. For scattered protons in the RPs,  $p_y$  is calculated as  $p_y = p_{\text{beam}}[2(y_n/L_{y,n} + y_f/L_{y,f})]$ . There are four such independent equations, one for each configuration.

We have the measured means of twelve distributions: the location of the IPs  $y^*$ , calculated from RP pairs 1T, 1B, 2T, and 2B (4 values); the sum of proton transverse momenta  $\sum p_y$  for RP trigger configurations TB, BT, TT, and BB (4 values); the averaged local hit positions  $y$  in RP groups 1n, 1f, 2n, and 2f (4 values). The transformation matrix is

$$A_y = \begin{pmatrix} L_{1f}/d & -L_{1n}/d & 0 & 0 & 0 & 0 & 0 & 0 \\ 0 & 0 & L_{1f}/d & -L_{1n}/d & 0 & 0 & 0 & 0 \\ 0 & 0 & 0 & 0 & L_{2f}/d & -L_{2n}/d & 0 & 0 \\ 0 & 0 & 0 & 0 & 0 & 0 & L_{2f}/d & -L_{2n}/d \\ p/(2L_{1n}) & p/(2L_{1f}) & 0 & 0 & 0 & 0 & p/(2L_{2n}) & p/(2L_{2f}) \\ 0 & 0 & p/(2L_{1n}) & p/(2L_{1f}) & p/(2L_{2n}) & p/(2L_{2f}) & 0 & 0 \\ p/(2L_{1n}) & p/(2L_{1f}) & 0 & 0 & p/(2L_{2n}) & p/(2L_{2f}) & 0 & 0 \\ 0 & 0 & p/(2L_{1n}) & p/(2L_{1f}) & 0 & 0 & p/(2L_{2n}) & p/(2L_{2f}) \end{pmatrix}, \quad (14)$$

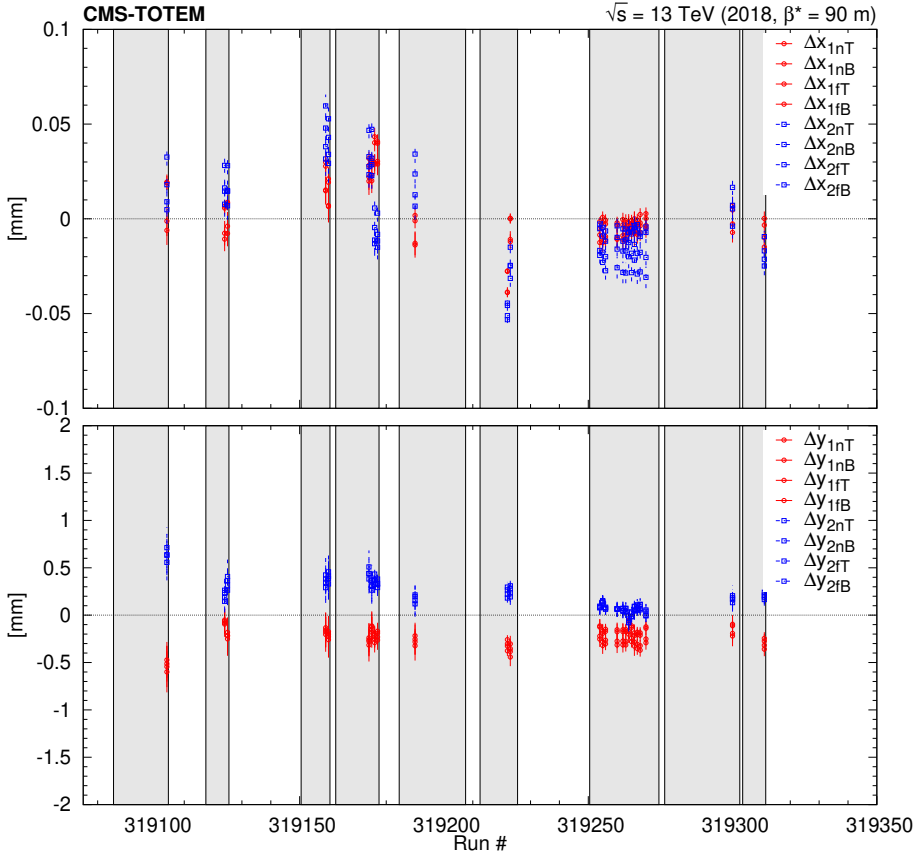


Figure 15: Deduced displacements of RPs in the  $x$  (top) and  $y$  (bottom) directions as a function of run number. Statistical uncertainties are shown with vertical bars. The LHC fills are indicated by grey areas.

and the transformation itself is

$$A_y \begin{pmatrix} \delta y_{1nT} \\ \delta y_{1fT} \\ \delta y_{1nB} \\ \delta y_{1fB} \\ \delta y_{2nT} \\ \delta y_{2fT} \\ \delta y_{2nB} \\ \delta y_{2fB} \end{pmatrix} = \begin{pmatrix} -\langle y_{1T}^* \rangle \\ -\langle y_{1B}^* \rangle \\ -\langle y_{2T}^* \rangle \\ -\langle y_{2B}^* \rangle \\ -\langle \sum p_{y,TB} \rangle \\ -\langle \sum p_{y,BT} \rangle \\ -\langle \sum p_{y,TT} \rangle \\ -\langle \sum p_{y,BB} \rangle \end{pmatrix}. \quad (15)$$

The optimisation of the additional shifts was performed through a joint least squares fit using the estimated variances of  $\langle x^* \rangle$  and  $\langle y^* \rangle$  values, and those of the momentum sums. The extracted values in the  $x$  and  $y$  directions as a function of run number are shown in Fig. 15. All RPs in an arm need to be artificially shifted in a coordinated manner, although the two arms appear to be independent. The necessary run-by-run adjustments are in the range  $\pm 50 \mu\text{m}$  in  $x$ , and  $\pm 0.5 \text{ mm}$  in  $y$ . The time dependence of the additional shifts was examined, but they show no obvious periodic behaviour. We conclude that the observed behaviour does not reflect an actual displacement of the RPs, but the drifting of the incoming proton beam orbits.

Details and cross-checks for a specific run (#319311) after full alignment are shown in Fig. 16, including the distribution of the IP coordinates  $(x^*, y^*)$  and that of the four-particle momentum

sum ( $\sum p_x, \sum p_y$ ) for each RP configuration, as well as the distribution of the local hit coordinates in the  $x$  (single Gaussian) and  $y$  directions (separate Gaussians). The measured residuals and those expected from the extracted displacements are shown in Fig. 17. Although not all the constraints can be satisfied at the same time, the relevant quantities used for event selection and physics analysis, i.e., the momentum sums  $\sum p_x$  and  $\sum p_y$ , are well optimised.

Estimates, based on measured data, of the effective lengths at the location of the near ( $L_{n,x}$ ) and far pots ( $L_{f,x}$ ) as functions of the run number are shown in Fig. 18. They were deduced from near-far hit covariances in RPs for arm configurations 1T, 1B, 2T, and 2B. Systematic uncertainties are obtained by varying the size of the selection ellipse (Fig. 13) by 50%, and by varying the values of magnification ( $v_{x,n}$  and  $v_{x,f}$ ) within their expected uncertainties (0.2%). Values of the nominal optics [19, 20] are also plotted for reference, with black lines. The comparison between the nominal and averaged estimates from collected events is given in Table 4 where any run-by-run variation of the estimated value is included in the uncertainty. They are in good agreement.

Table 4: Nominal values and estimates of the effective lengths  $L_x$ , truncated to two decimal places. For the estimates, the systematic uncertainties are indicated; the statistical ones are negligible.

Arm	Station	$L_x$ [m]	
		Nominal	Estimated
1	near	3.10	$3.05 \pm 0.11$
1	far	-0.52	$-0.57 \pm 0.12$
2	near	0.19	$0.39 \pm 0.16$
2	far	-2.95	$-2.78 \pm 0.12$

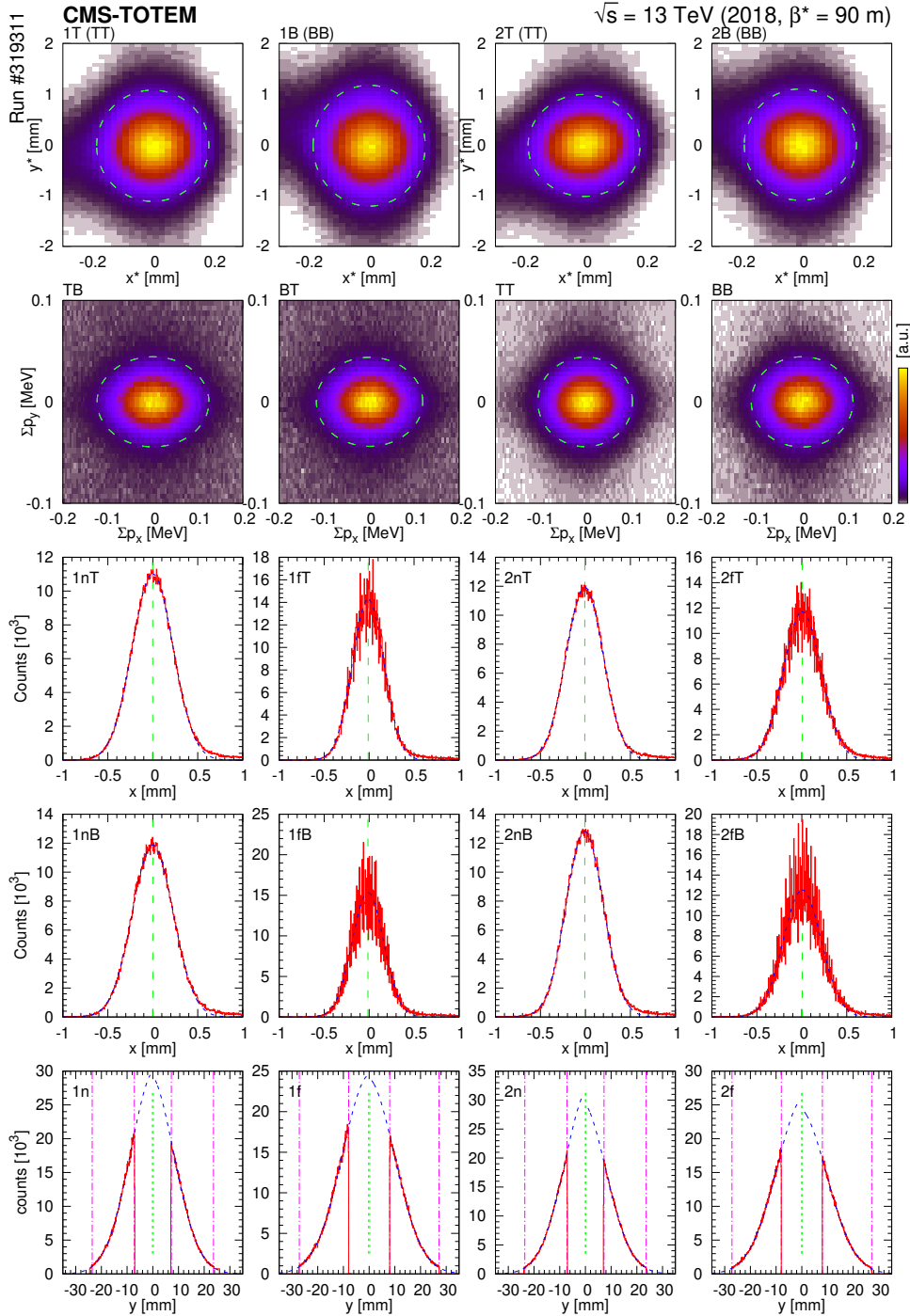


Figure 16: Cross-check of the full alignment, shown here for run #319311. From top to bottom: Distribution of the IP coordinates ( $x^*$ ,  $y^*$ ) for RP arm configurations 1T, 1B, 2T, and 2B. Distribution of the four-particle momentum sum ( $\sum p_x$ ,  $\sum p_y$ ) for the RP trigger configurations TB, BT, TT, and BB. In both cases the two-dimensional Gaussian fits are indicated (at  $2\sigma$ ) with green dotted ellipses. Distribution of local hits in the RPs in the  $x$  (single Gaussian) and  $y$  directions (separate Gaussians). Dashed blue curves represent the Gaussian fits, vertical green dashed lines indicate the deduced relative shifts, vertical magenta dash-dotted lines on  $y$  plots show fit ranges.

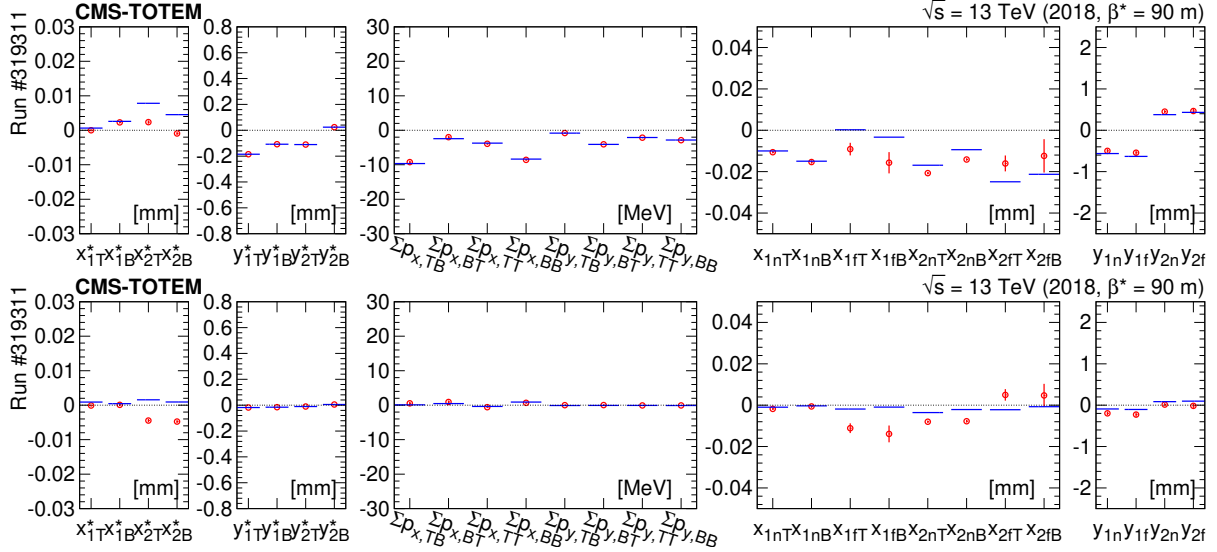


Figure 17: The measured residuals (red symbols) and those expected from the extracted displacements (horizontal blue lines) for run #319311, before (upper) and after (lower) the alignment.

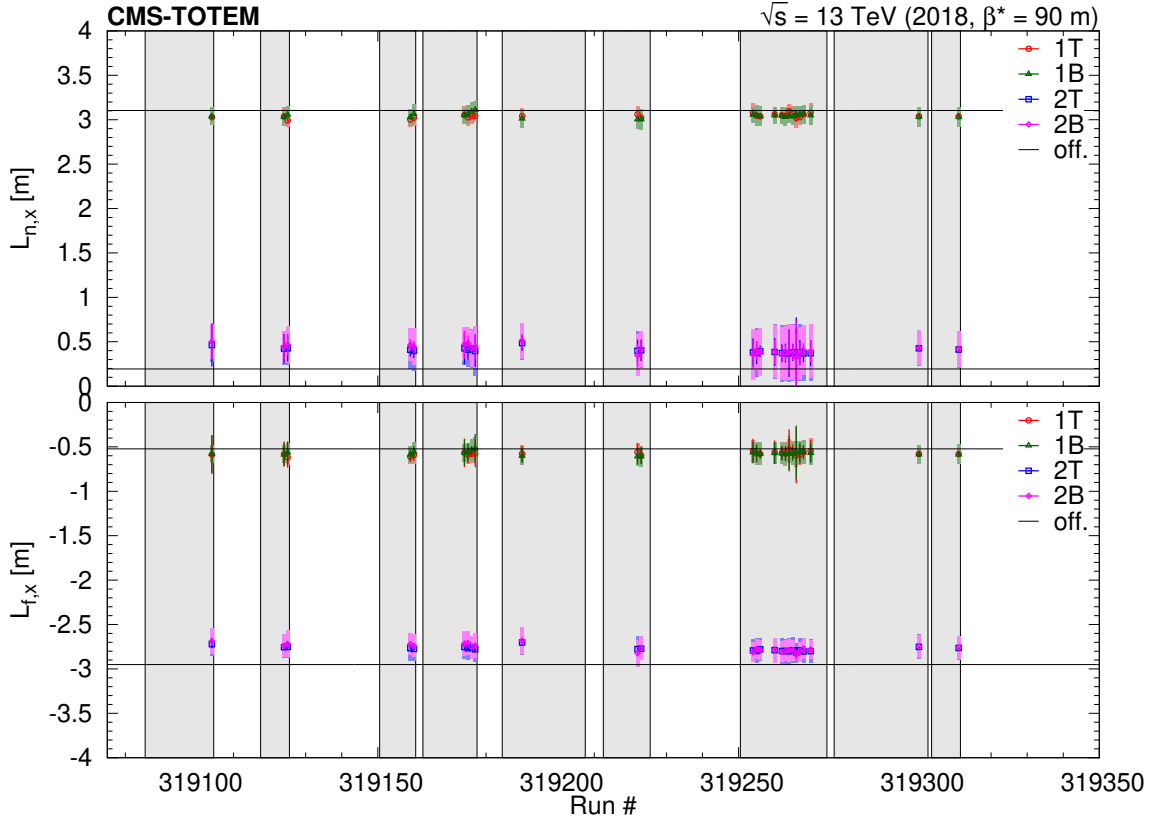


Figure 18: Effective lengths at the location of the near ( $L_{n,x}$ ) and far pots ( $L_{f,x}$ ) as functions of the run number, deduced from near-far hit covariances in RPs for RP arm configurations 1T, 1B, 2T, and 2B. Statistical uncertainties are indicated with error bars, systematic ones are plotted with shaded rectangles. Values of the nominal TOTEM optics parameters (Table 4) are also shown with horizontal black lines. LHC fills are indicated by grey areas.

#### 4.4 Results

The locations of the primary pp interactions in the  $x^*$ - $y^*$  plane at the IP using RPs in Arm 1 or in Arm 2 are shown for each trigger configuration in Fig. 19. All the distributions are well centred at  $(0, 0)$ . The elongated regions at negative  $x^*$  values correspond to protons with large momentum loss. The width of the distributions is the result of various factors: the beam spot size, the effect of multiple scattering of the protons within the RP material, and the local position resolution of the RPs. The joint distributions of  $x^*$  (or  $y^*$ ) coordinates deduced using RPs in Arm 1 and 2 are shown for each trigger configuration in Fig. 20. The  $x^*$  coordinates are determined with good precision, and they correlate well between Arm 1 and 2, with a beam spot size of  $135/\sqrt{2} \approx 95 \mu\text{m}$  and resolution  $10/\sqrt{2} \approx 6\text{--}7 \mu\text{m}$ . The  $y^*$  coordinates have much larger uncertainties, but their distributions are well centred around  $(0, 0)$ , with tails from non-exclusive events.

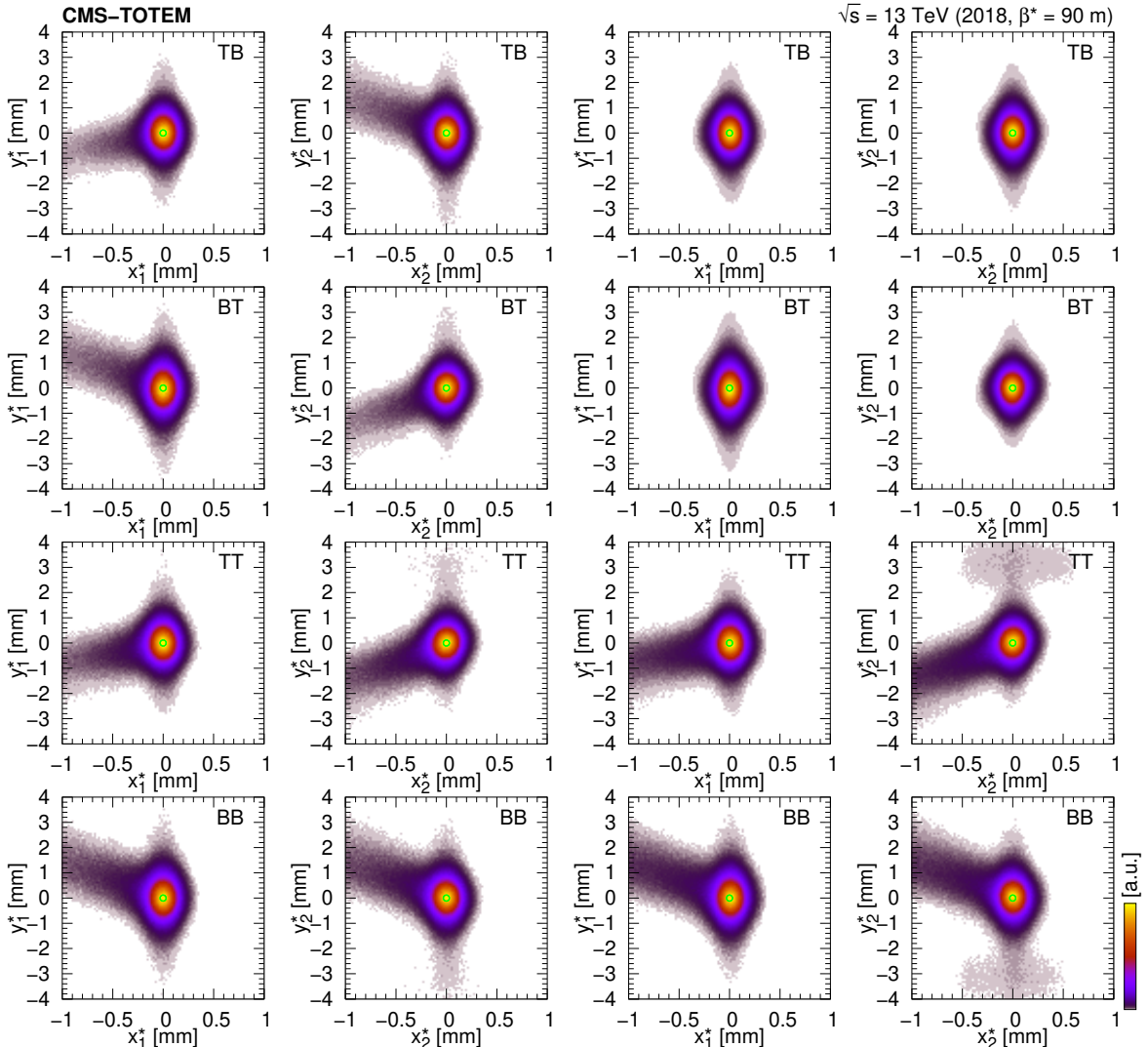


Figure 19: Location of the primary pp interaction in the  $x^*$ - $y^*$  plane at the IP using RPs in Arm 1 or 2 (subscripts 1 or 2), shown for various trigger configurations (TB, BT, TT, and BB, in rows). The two columns on the left side refer to the 2-track data set, whereas the two on the right side display distributions based on the 0-track data set. The elongated regions at negative  $x^*$  values correspond to events with large proton momentum loss. The green circles mark  $(0, 0)$ .

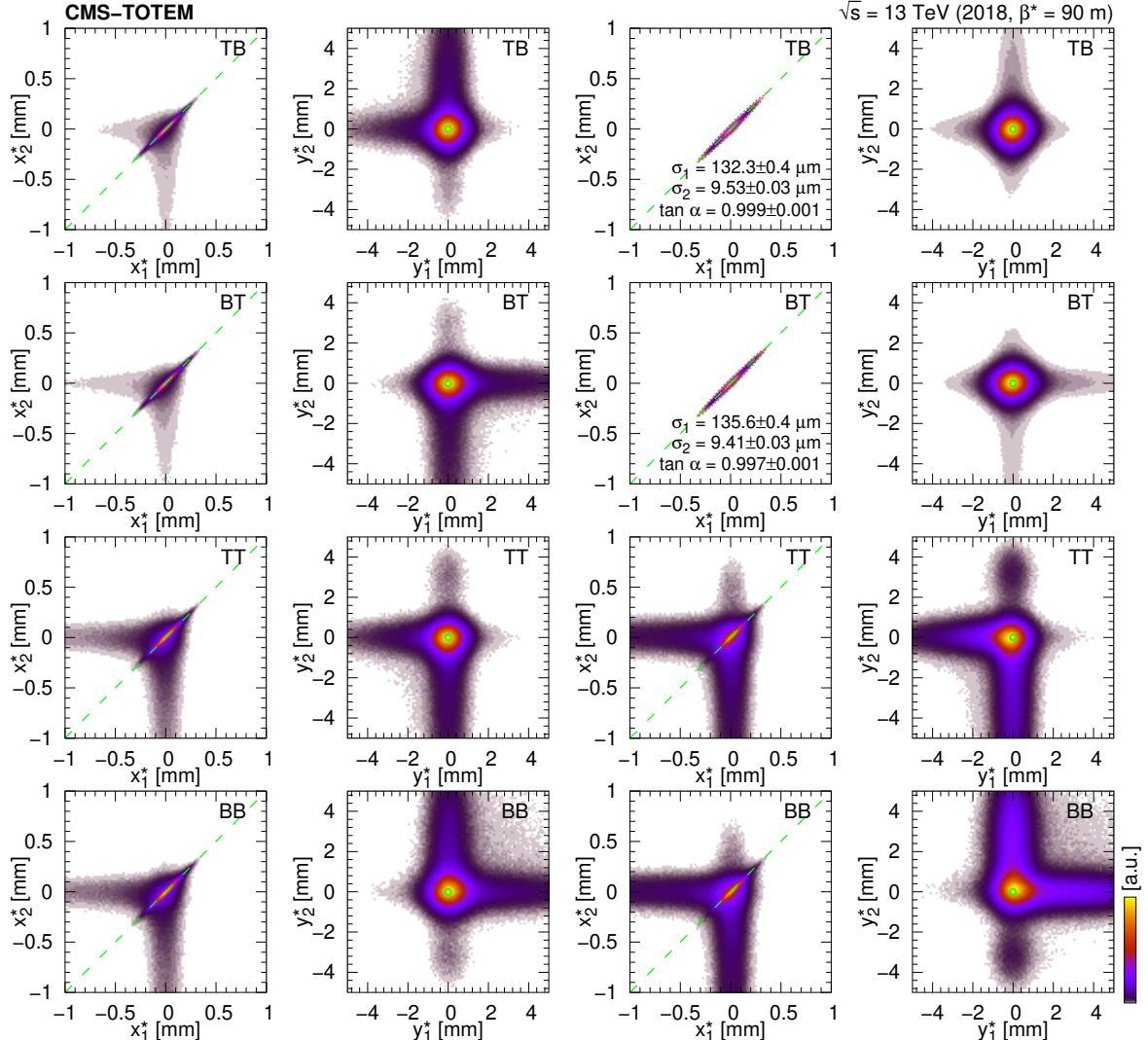


Figure 20: Joint distribution of  $x^*$  (or  $y^*$ ) coordinates deduced using RPs in Arm 1 and 2 (subscripts 1 and 2), shown for various trigger configurations (TB, BT, TT, and BB, in rows). The two columns on the left side refer to the 2-track data set, whereas the two on the right side display distributions based on the 0-track data set. In the case of the diagonally triggered (TB and BT) 0-track (in part elastic) events the parameters (standard deviations in major and minor axis directions  $\sigma_1$  and  $\sigma_2$ , and the rotation angle  $\alpha$ ) of the fitted ellipses are displayed in the plots. The green circles mark  $(0,0)$ , the dashed green lines are the identity lines.

The standard deviation of the momentum sum  $\sum p_x$  for the 0-track data as a function of the predicted standard deviation from the RP position resolution is shown in Fig. 21, where the result of a fit using the functional form  $(\sigma_0^2 + \sigma_{\sum p_x}^2)^{1/2}$  is indicated. The constant contribution of  $\sigma_0 \approx 39$  MeV is the result of several factors: the divergence of both incoming proton beams ( $\Delta\sigma_0 \approx 20$  MeV, Section 2.1), multiple scattering of the protons within the RP material, and most importantly the physics process itself. Here inelastic scattering contributes significantly to  $\sigma_0$  if undetected particles lead to an apparent momentum imbalance.

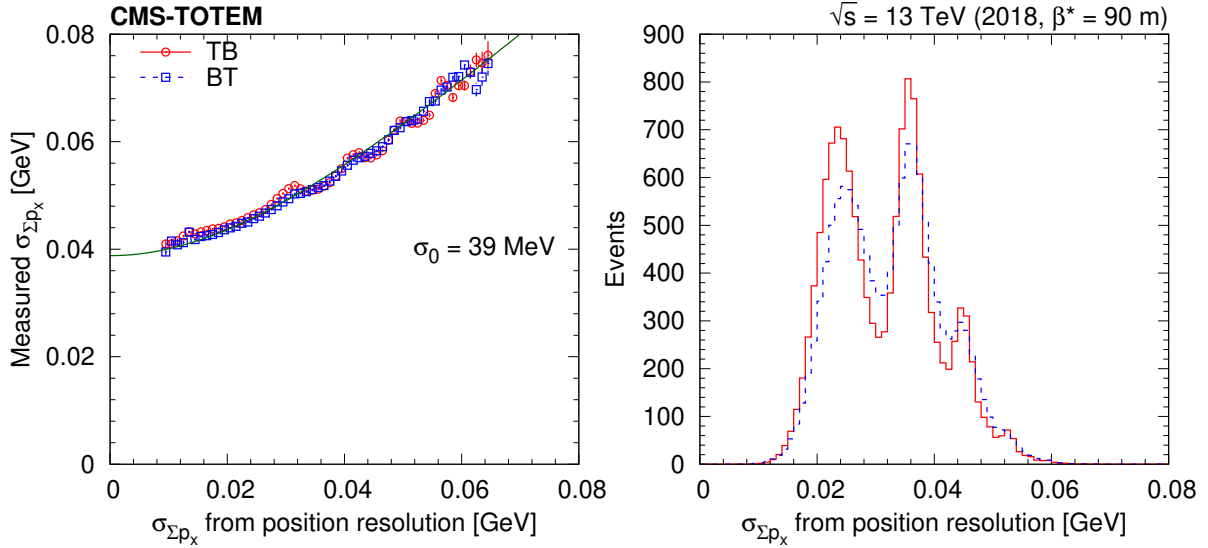


Figure 21: Left: Standard deviation of the momentum sum  $\sum p_x$  for the 0-track data (TB and BT configurations), as a function of the predicted standard deviation from the RP position resolution. Statistical uncertainties are shown with vertical bars. A fit using the functional form  $(\sigma_0^2 + \sigma_{\sum p_x}^2)^{1/2}$  is plotted with a green curve. Right: The occurrence of  $\sigma_{\sum p_x}$ . The peaks correspond to events with protons causing one or more two-strip clusters, and hence better resolution.

Distributions of the sum of the scattered proton momenta ( $\sum_2 p_x, \sum_2 p_y$ ), two particles, for diagonally triggered events are shown in Fig. 22, left. The measured distributions in the  $\sum_2 p_y$  direction are slightly distorted, a consequence of the elastic veto (Section 3.4). Distributions of the sum of scattered proton and central hadron momenta ( $\sum_4 p_x, \sum_4 p_y$ ), four particles, shown for each trigger configuration for 2-track events, are plotted in Fig. 22, right. Both distributions are well centred on (0,0).

The distribution of the sum of scattered proton and central hadron momenta and the sum of scattered proton momenta ( $\sum_4 p_x$  and  $\sum_2 p_x, \sum_4 p_y$  and  $\sum_2 p_y$ ) is shown for each trigger configuration for 2-track events in Fig. 23. The contributions of true elastic (only two scattered protons, vertical band) and true central exclusive (two scattered protons and two central charged hadrons, horizontal band) are well visible. In addition, a slanted area due to non-exclusive or inelastic background is present.

The procedures just described are used for the precise transverse momentum measurement of the scattered protons, for event classification and selection in the physics analysis of central exclusive production, where two oppositely charged hadrons are detected by the CMS silicon tracker [3].

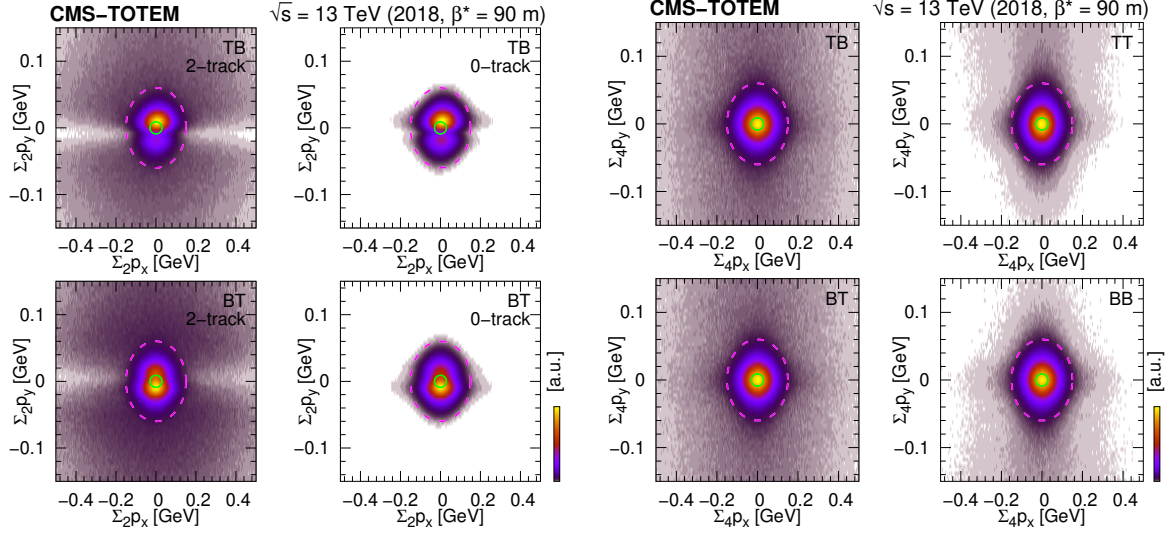


Figure 22: Left: Distribution of the sum of scattered proton momenta ( $\Sigma_2 p_x, \Sigma_2 p_y$ ) for diagonally triggered events (TB and BT). The left column refers to the 2-track data set, whereas the right one displays the distribution based on the 0-track data set. Right: Distribution of the sum of scattered proton and central hadron momenta ( $\Sigma_4 p_x, \Sigma_4 p_y$ ) shown for various trigger configurations (TB, BT, TT, and BB) for 2-track events. Ellipses with semi-minor axes of 150 MeV ( $x$ ) and 60 MeV ( $y$ ) are overlaid. The green circles mark  $(0, 0)$ .

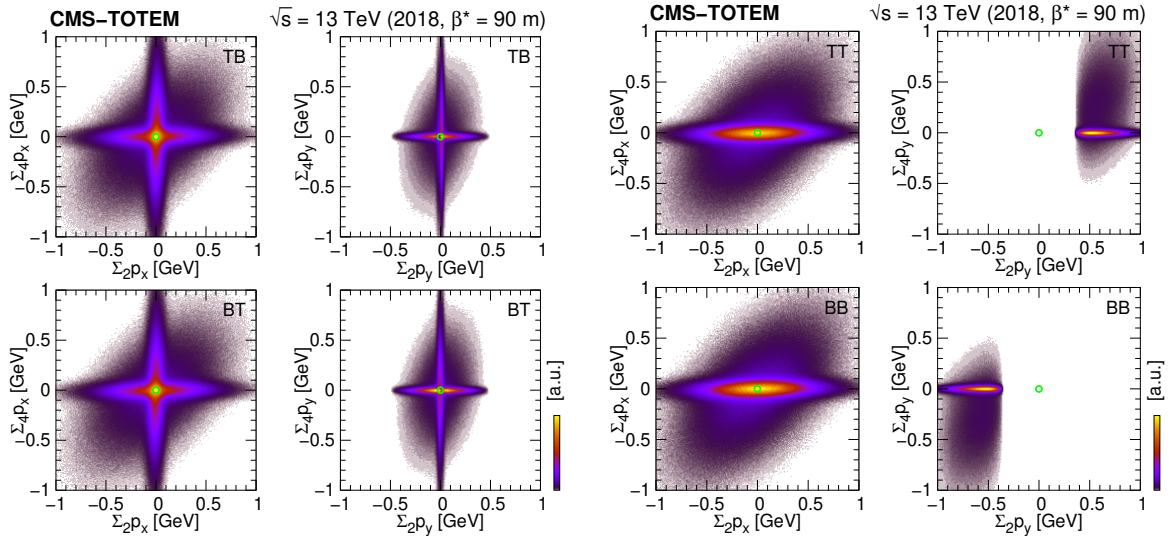


Figure 23: Distribution of the sum of scattered proton and central hadron momenta and the sum of scattered proton momenta only ( $\Sigma_4 p_x$  and  $\Sigma_2 p_x, \Sigma_4 p_y$  and  $\Sigma_2 p_y$ ) shown for various trigger configurations (TB, BT, TT, and BB) for 2-track events. The green circles mark  $(0, 0)$ .

## 5 Summary

The Roman pot detectors of the TOTEM experiment are used to reconstruct the transverse momentum of scattered protons and to estimate the transverse location of the primary interaction. In this study advanced methods for track reconstruction, measurements of strip-level detection efficiencies, cross-checks of beam optics, and the detector alignment procedure are presented, along with their application in the selection of signal events.

The track reconstruction is performed by finding a common polygonal area in the intercept-slope plane, thus exploiting all available cluster information. As a result, an ultimate spatial resolution of  $6\text{--}7 \mu\text{m}$  is achieved, which is an order of magnitude smaller than the strip width. The tool is applied to the relative alignment of detector layers with  $\mu\text{m}$  precision. A tag-and-probe method is used to extract strip-level detection efficiencies. They are mostly high and constant, but for some strips they change with time; there are up to 20% variations. The tracklet efficiencies are calculated using a probabilistic model, based on the temporal variation of the hit detection efficiencies. These are functions of the tracklet location and slope. There are up to 50% losses in specific but small areas, to be corrected in the physics analyses.

The alignment of the Roman pot system (8 numbers for each arm) is performed by means of 16 measured quantities in the horizontal, and 12 in the vertical direction, resulting in a position accuracy of  $3 \mu\text{m}$  in the horizontal and  $60 \mu\text{m}$  in the vertical directions. The deduced locations of the primary interaction, the distribution of the scattered proton momenta, and their correlations confirm the success of the detailed calibration process and provide a solid ground for exclusive physics analyses based on the high- $\beta^*$  data set. The developed methods have been successfully applied in the analysis of central exclusive production events [3].

## Acknowledgments

We congratulate our colleagues in the CERN accelerator departments for the excellent performance of the LHC and thank the technical and administrative staffs at CERN and at other CMS and TOTEM institutes for their contributions to the success of the common CMS-TOTEM effort. In addition, we gratefully acknowledge the computing centres and personnel of the Worldwide LHC Computing Grid and other centres for delivering so effectively the computing infrastructure essential to our analyses. Finally, we acknowledge the enduring support for the construction and operation of the LHC, the CMS and TOTEM detectors, and the supporting computing infrastructure provided by the following funding agencies: SC (Armenia), BMBWF and FWF (Austria); FNRS and FWO (Belgium); CNPq, CAPES, FAPERJ, FAPERGS, and FAPESP (Brazil); MES and BNSF (Bulgaria); CERN; CAS, MoST, and NSFC (China); MINCIENCIAS (Colombia); MSES and CSF (Croatia); RIF (Cyprus); SENESCYT (Ecuador); ERC PRG, RVTT3 and MoER TK202 (Estonia); Academy of Finland, Magnus Ehrnrooth Foundation, MEC, HIP, and Waldemar von Frenckell Foundation (Finland); CEA and CNRS/IN2P3 (France); SRNSF (Georgia); BMBF, DFG, and HGF (Germany); GSRI (Greece); NKFIH (Hungary); DAE and DST (India); IPM (Iran); SFI (Ireland); INFN (Italy); MSIP and NRF (Republic of Korea); MES (Latvia); LMTLT (Lithuania); MOE and UM (Malaysia); BUAP, CINVESTAV, CONACYT, LNS, SEP, and UASLP-FAI (Mexico); MOS (Montenegro); MBIE (New Zealand); PAEC (Pakistan); MES and NSC (Poland); FCT (Portugal); MESTD (Serbia); MCIN/AEI and PCTI (Spain); MOSTR (Sri Lanka); Swiss Funding Agencies (Switzerland); MST (Taipei); MHESTI and NSTDA (Thailand); TUBITAK and TENMAK (Turkey); NASU (Ukraine); STFC (United Kingdom); DOE and NSF (USA).

Individuals have received support from the Marie-Curie programme and the European Re-

search Council and Horizon 2020 Grant, contract Nos. 675440, 724704, 752730, 758316, 765710, 824093, 101115353, 101002207, and COST Action CA16108 (European Union); the Leventis Foundation; the Alfred P. Sloan Foundation; the Alexander von Humboldt Foundation; the Science Committee, project no. 22rl-037 (Armenia); the Belgian Federal Science Policy Office; the Fonds pour la Formation à la Recherche dans l'Industrie et dans l'Agriculture (FRIA-Belgium); the F.R.S.-FNRS and FWO (Belgium) under the “Excellence of Science – EOS” – be.h project n. 30820817; the Beijing Municipal Science & Technology Commission, No. Z191100007219010 and Fundamental Research Funds for the Central Universities (China); the Ministry of Education, Youth and Sports (MEYS) of the Czech Republic; the Shota Rustaveli National Science Foundation, grant FR-22-985 (Georgia); the Deutsche Forschungsgemeinschaft (DFG), among others, under Germany’s Excellence Strategy – EXC 2121 “Quantum Universe” – 390833306, and under project number 400140256 - GRK2497; the Hellenic Foundation for Research and Innovation (HFRI), Project Number 2288 (Greece); the Hungarian Academy of Sciences, the New National Excellence Program - ÚNKP, the NKFIH research grants K 131991, K 133046, K 138136, K 143460, K 143477, K 146913, K 146914, K 147048, 2020-2.2.1-ED-2021-00181, and TKP2021-NKTA-64 (Hungary); the Council of Science and Industrial Research, India; ICSC – National Research Centre for High Performance Computing, Big Data and Quantum Computing and FAIR – Future Artificial Intelligence Research, funded by the NextGenerationEU program (Italy); the Latvian Council of Science; the Ministry of Education and Science, project no. 2022/WK/14, and the National Science Centre, contracts Opus 2021/41/B/ST2/01369 and 2021/43/B/ST2/01552 (Poland); the Fundação para a Ciência e a Tecnologia, grant CEECIND/01334/2018 (Portugal); the National Priorities Research Program by Qatar National Research Fund; MCIN/AEI/10.13039/501100011033, ERDF “a way of making Europe”, and the Programa Estatal de Fomento de la Investigación Científica y Técnica de Excelencia María de Maeztu, grant MDM-2017-0765 and Programa Severo Ochoa del Principado de Asturias (Spain); the Chulalongkorn Academic into Its 2nd Century Project Advancement Project, and the National Science, Research and Innovation Fund via the Program Management Unit for Human Resources & Institutional Development, Research and Innovation, grant B39G670016 (Thailand); the Kavli Foundation; the Nvidia Corporation; the SuperMicro Corporation; the Welch Foundation, contract C-1845; and the Weston Havens Foundation (USA).

## References

- [1] TOTEM Collaboration, “Timing measurements in the vertical Roman pots of the TOTEM experiment”, 2014. CERN-LHCC-2014-020, TOTEM-TDR-002.  
<https://cds.cern.ch/record/1753189>.
- [2] K. Österberg on behalf of the TOTEM Collaboration, “Potential of central exclusive production studies in high  $\beta^*$  runs at the LHC with CMS-TOTEM”, *Int. J. Mod. Phys. A* **29** (2014) 1446019, doi:10.1142/S0217751X14460191.
- [3] CMS and TOTEM Collaborations, “Nonresonant central exclusive production of charged-hadron pairs in proton-proton collisions at  $\sqrt{s} = 13$  TeV”, *Phys. Rev. D* **109** (2024) 112013, doi:10.1103/PhysRevD.109.112013, arXiv:2401.14494.
- [4] CMS Collaboration, “CMS luminosity measurement for the 2018 data-taking period at  $\sqrt{s} = 13$  TeV”, CMS Physics Analysis Summary CMS-PAS-LUM-18-002, 2018.
- [5] H. Wiedemann, “Particle accelerator physics: basic principles and linear beam dynamics”. Springer Berlin Heidelberg, 2013. ISBN 9783662029039.

- [6] M. G. Albrow, T. D. Coughlin, and J. R. Forshaw, “Central exclusive particle production at high energy hadron colliders”, *Prog. Part. Nucl. Phys.* **65** (2010) 149, doi:10.1016/j.ppnp.2010.06.001, arXiv:1006.1289.
- [7] H. Burkhardt, “High-beta optics and running prospects”, *Instruments* **3** (2019) 22, doi:10.3390/instruments3010022.
- [8] CMS Collaboration, “The CMS experiment at the CERN LHC”, *JINST* **3** (2008) S08004, doi:10.1088/1748-0221/3/08/S08004.
- [9] TOTEM Collaboration, “The TOTEM experiment at the CERN Large Hadron Collider”, *JINST* **3** (2008) S08007, doi:10.1088/1748-0221/3/08/S08007.
- [10] TOTEM Collaboration, “Performance of the TOTEM Detectors at the LHC”, *Int. J. Mod. Phys. A* **28** (2013) 1330046, doi:10.1142/S0217751X13300469, arXiv:1310.2908.
- [11] Particle Data Group, S. Navas et al., “Review of particle physics”, *Phys. Rev. D* **110** (2024) 030001, doi:10.1103/PhysRevD.110.030001.
- [12] CMS Collaboration, “The CMS trigger system”, *JINST* **12** (2017) P01020, doi:10.1088/1748-0221/12/01/P01020, arXiv:1609.02366.
- [13] R. Frühwirth, “Application of Kalman filtering to track and vertex fitting”, *Nucl. Instrum. Meth. A* **262** (1987) 444, doi:10.1016/0168-9002(87)90887-4.
- [14] P. Billoir and S. Qian, “Simultaneous pattern recognition and track fitting by the Kalman filtering method”, *Nucl. Instrum. Meth. A* **294** (1990) 219, doi:10.1016/0168-9002(90)91835-Y.
- [15] R. Frühwirth and A. Strandlie, “Pattern recognition, tracking and vertex reconstruction in particle detectors”. Particle Acceleration and Detection. Springer, 2020. doi:10.1007/978-3-030-65771-0, ISBN 978-3-030-65770-3, 978-3-030-65771-0.
- [16] CMS Collaboration, “Measurements of inclusive W and Z cross sections in pp collisions at  $\sqrt{s} = 7$  TeV”, *JHEP* **01** (2011) 080, doi:10.1007/JHEP01(2011)080, arXiv:1012.2466.
- [17] C. Steger, “On the calculation of arbitrary moments of polygons”, Technical Report FGBV-96-05, Forschungsgruppe Bildverstehen (FG BV), Informatik IX, Technische Universität München, 1996.
- [18] J. A. Nelder and R. Mead, “A simplex method for function minimization”, *Comput. J.* **7** (1965) 308, doi:10.1093/comjnl/7.4.308.
- [19] TOTEM Collaboration, “LHC optics measurement with proton tracks detected by the Roman pots of the TOTEM experiment”, *New J. Phys.* **16** (2014) 103041, doi:10.1088/1367-2630/16/10/103041, arXiv:1406.0546.
- [20] F. J. Nemes, “Elastic scattering of protons at the TOTEM experiment at the LHC”. PhD thesis, Eötvös U., 2015. CERN-THESIS-2015-293.
- [21] W. Herr and F. Schmidt, “A MAD-X primer”, in *CERN Accelerator School and DESY Zeuthen: Accelerator Physics*, p. 505. 2004. CERN-AB-2004-027-ABP.
- [22] E. Wilson, “An introduction to particle accelerators”. Oxford Univ. Press, Oxford, 2001. doi:10.1093/acprof:oso/9780198508298.001.0001, ISBN 9780198508298.

- 
- [23] H. Niewiadomski, "Reconstruction of protons in the TOTEM Roman pot detectors at the LHC". PhD thesis, Manchester U., 2008. CERN-THESIS-2008-080.



## A The CMS Collaboration

### **Yerevan Physics Institute, Yerevan, Armenia**

A. Hayrapetyan, A. Tumasyan<sup>1</sup> 

### **Institut für Hochenergiephysik, Vienna, Austria**

W. Adam , J.W. Andrejkovic, L. Benato , T. Bergauer , S. Chatterjee , K. Damanakis , M. Dragicevic , P.S. Hussain , M. Jeitler<sup>2</sup> , N. Krammer , A. Li , D. Liko , I. Mikulec , J. Schieck<sup>2</sup> , R. Schöfbeck<sup>2</sup> , D. Schwarz , M. Sonawane , W. Waltenberger , C.-E. Wulz<sup>2</sup> 

### **Universiteit Antwerpen, Antwerpen, Belgium**

T. Janssen , T. Van Laer, P. Van Mechelen 

### **Vrije Universiteit Brussel, Brussel, Belgium**

N. Breugelmans, J. D'Hondt , S. Dansana , A. De Moor , M. Delcourt , F. Heyen, S. Lowette , I. Makarenko , D. Müller , S. Tavernier , M. Tytgat<sup>3</sup> , G.P. Van Onsem , S. Van Putte , D. Vannerom 

### **Université Libre de Bruxelles, Bruxelles, Belgium**

B. Bilin , B. Clerbaux , A.K. Das, I. De Bruyn , G. De Lentdecker , H. Evard , L. Favart , P. Gianneios , J. Jaramillo , A. Khalilzadeh, F.A. Khan , K. Lee , A. Malara , S. Paredes , M.A. Shahzad, L. Thomas , M. Vanden Bemden , C. Vander Velde , P. Vanlaer 

### **Ghent University, Ghent, Belgium**

M. De Coen , D. Dobur , G. Gokbulut , Y. Hong , J. Knolle , L. Lambrecht , D. Marckx , K. Mota Amarilo , K. Skovpen , N. Van Den Bossche , J. van der Linden , L. Wezenbeek 

### **Université Catholique de Louvain, Louvain-la-Neuve, Belgium**

A. Benecke , A. Bethani , G. Bruno , C. Caputo , J. De Favereau De Jeneret , C. Delaere , I.S. Donertas , A. Giammanco , A.O. Guzel , Sa. Jain , V. Lemaitre, J. Lidrych , P. Mastrapasqua , T.T. Tran 

### **Centro Brasileiro de Pesquisas Fisicas, Rio de Janeiro, Brazil**

G.A. Alves , E. Coelho , G. Correia Silva , C. Hensel , T. Menezes De Oliveira , C. Mora Herrera<sup>4</sup> , P. Rebello Teles , M. Soeiro, A. Vilela Pereira<sup>4</sup> 

### **Universidade do Estado do Rio de Janeiro, Rio de Janeiro, Brazil**

W.L. Aldá Júnior , M. Barroso Ferreira Filho , H. Brandao Malbouisson , W. Carvalho , J. Chinellato<sup>5</sup>, E.M. Da Costa , G.G. Da Silveira<sup>6</sup> , D. De Jesus Damiao , S. Fonseca De Souza , R. Gomes De Souza, T. Laux Kuhn<sup>6</sup>, M. Macedo , J. Martins , L. Mundim , H. Nogima , J.P. Pinheiro , A. Santoro , A. Sznajder , M. Thiel 

### **Universidade Estadual Paulista, Universidade Federal do ABC, São Paulo, Brazil**

C.A. Bernardes<sup>6</sup> , L. Calligaris , T.R. Fernandez Perez Tomei , E.M. Gregores , I. Maietto Silverio , P.G. Mercadante , S.F. Novaes , B. Orzari , Sandra S. Padula 

### **Institute for Nuclear Research and Nuclear Energy, Bulgarian Academy of Sciences, Sofia, Bulgaria**

A. Aleksandrov , R. Hadjiiska , P. Iaydjiev , M. Misheva , M. Shopova , G. Sultanov 

### **University of Sofia, Sofia, Bulgaria**

A. Dimitrov , L. Litov , B. Pavlov , P. Petkov , A. Petrov , E. Shumka 

**Instituto De Alta Investigación, Universidad de Tarapacá, Casilla 7 D, Arica, Chile**  
S. Keshri , D. Laroze , S. Thakur 

**Beihang University, Beijing, China**  
T. Cheng , T. Javaid , L. Yuan 

**Department of Physics, Tsinghua University, Beijing, China**  
Z. Hu , Z. Liang, J. Liu

**Institute of High Energy Physics, Beijing, China**

G.M. Chen<sup>7</sup> , H.S. Chen<sup>7</sup> , M. Chen<sup>7</sup> , F. Iemmi , C.H. Jiang, A. Kapoor<sup>8</sup> , H. Liao , Z.-A. Liu<sup>9</sup> , R. Sharma<sup>10</sup> , J.N. Song<sup>9</sup>, J. Tao , C. Wang<sup>7</sup>, J. Wang , Z. Wang<sup>7</sup>, H. Zhang , J. Zhao 

**State Key Laboratory of Nuclear Physics and Technology, Peking University, Beijing, China**  
A. Agapitos , Y. Ban , S. Deng , B. Guo, C. Jiang , A. Levin , C. Li , Q. Li , Y. Mao, S. Qian, S.J. Qian , X. Qin, X. Sun , D. Wang , H. Yang, L. Zhang , Y. Zhao, C. Zhou 

**Guangdong Provincial Key Laboratory of Nuclear Science and Guangdong-Hong Kong Joint Laboratory of Quantum Matter, South China Normal University, Guangzhou, China**  
S. Yang 

**Sun Yat-Sen University, Guangzhou, China**  
Z. You 

**University of Science and Technology of China, Hefei, China**  
K. Jaffel , N. Lu 

**Nanjing Normal University, Nanjing, China**  
G. Bauer<sup>11</sup>, B. Li<sup>12</sup>, K. Yi<sup>13</sup> , J. Zhang 

**Institute of Modern Physics and Key Laboratory of Nuclear Physics and Ion-beam Application (MOE) - Fudan University, Shanghai, China**  
Y. Li

**Zhejiang University, Hangzhou, Zhejiang, China**  
Z. Lin , C. Lu , M. Xiao 

**Universidad de Los Andes, Bogota, Colombia**  
C. Avila , D.A. Barbosa Trujillo, A. Cabrera , C. Florez , J. Fraga , J.A. Reyes Vega

**Universidad de Antioquia, Medellin, Colombia**  
F. Ramirez , C. Rendón, M. Rodriguez , A.A. Ruales Barbosa , J.D. Ruiz Alvarez 

**University of Split, Faculty of Electrical Engineering, Mechanical Engineering and Naval Architecture, Split, Croatia**  
D. Giljanovic , N. Godinovic , D. Lelas , A. Sculac 

**University of Split, Faculty of Science, Split, Croatia**  
M. Kovac , A. Petkovic, T. Sculac 

**Institute Rudjer Boskovic, Zagreb, Croatia**  
P. Bargassa , V. Brigljevic , B.K. Chitroda , D. Ferencek , K. Jakovcic, A. Starodumov<sup>14</sup> , T. Susa 

**University of Cyprus, Nicosia, Cyprus**  
A. Attikis , K. Christoforou , A. Hadjiagapiou, C. Leonidou , J. Mousa , C. Nicolaou,

L. Paizanos, F. Ptochos [ID](#), P.A. Razis [ID](#), H. Rykaczewski, H. Saka [ID](#), A. Stepenov [ID](#)

**Charles University, Prague, Czech Republic**

M. Finger [ID](#), M. Finger Jr. [ID](#), A. Kveton [ID](#)

**Escuela Politecnica Nacional, Quito, Ecuador**

E. Ayala [ID](#)

**Universidad San Francisco de Quito, Quito, Ecuador**

E. Carrera Jarrin [ID](#)

**Academy of Scientific Research and Technology of the Arab Republic of Egypt, Egyptian Network of High Energy Physics, Cairo, Egypt**

B. El-mahdy, S. Khalil<sup>15</sup> [ID](#), E. Salama<sup>16,17</sup> [ID](#)

**Center for High Energy Physics (CHEP-FU), Fayoum University, El-Fayoum, Egypt**

M. Abdullah Al-Mashad [ID](#), M.A. Mahmoud [ID](#)

**National Institute of Chemical Physics and Biophysics, Tallinn, Estonia**

K. Ehataht [ID](#), M. Kadastik, T. Lange [ID](#), S. Nandan [ID](#), C. Nielsen [ID](#), J. Pata [ID](#), M. Raidal [ID](#), L. Tani [ID](#), C. Veelken [ID](#)

**Department of Physics, University of Helsinki, Helsinki, Finland**

H. Kirschenmann [ID](#), M. Voutilainen [ID](#)

**Helsinki Institute of Physics, Helsinki, Finland**

S. Bharthuar [ID](#), N. Bin Norjoharuddeen [ID](#), E. Brücke [ID](#), P. Inkaew [ID](#), K.T.S. Kallonen [ID](#), T. Lampén [ID](#), K. Lassila-Perini [ID](#), S. Lehti [ID](#), T. Lindén [ID](#), M. Myllymäki [ID](#), M.m. Rantanen [ID](#), H. Siikonen [ID](#), J. Tuominiemi [ID](#)

**Lappeenranta-Lahti University of Technology, Lappeenranta, Finland**

P. Luukka [ID](#), H. Petrow [ID](#)

**IRFU, CEA, Université Paris-Saclay, Gif-sur-Yvette, France**

M. Besancon [ID](#), F. Couderc [ID](#), M. Dejardin [ID](#), D. Denegri, J.L. Faure, F. Ferri [ID](#), S. Ganjour [ID](#), P. Gras [ID](#), G. Hamel de Monchenault [ID](#), M. Kumar [ID](#), V. Lohezic [ID](#), J. Malcles [ID](#), F. Orlando [ID](#), L. Portales [ID](#), A. Rosowsky [ID](#), M.Ö. Sahin [ID](#), A. Savoy-Navarro<sup>18</sup> [ID](#), P. Simkina [ID](#), M. Titov [ID](#), M. Tornago [ID](#)

**Laboratoire Leprince-Ringuet, CNRS/IN2P3, Ecole Polytechnique, Institut Polytechnique de Paris, Palaiseau, France**

F. Beaudette [ID](#), G. Boldrini [ID](#), P. Busson [ID](#), A. Cappati [ID](#), C. Charlote [ID](#), M. Chiusi [ID](#), T.D. Cuisset [ID](#), F. Damas [ID](#), O. Davignon [ID](#), A. De Wit [ID](#), I.T. Ehle [ID](#), B.A. Fontana Santos Alves [ID](#), S. Ghosh [ID](#), A. Gilbert [ID](#), R. Granier de Cassagnac [ID](#), A. Hakimi [ID](#), B. Harikrishnan [ID](#), L. Kalipoliti [ID](#), G. Liu [ID](#), M. Nguyen [ID](#), C. Ochando [ID](#), R. Salerno [ID](#), J.B. Sauvan [ID](#), Y. Sirois [ID](#), L. Urda Gómez [ID](#), E. Vernazza [ID](#), A. Zabi [ID](#), A. Zghiche [ID](#)

**Université de Strasbourg, CNRS, IPHC UMR 7178, Strasbourg, France**

J.-L. Agram<sup>19</sup> [ID](#), J. Andrea [ID](#), D. Apparu [ID](#), D. Bloch [ID](#), J.-M. Brom [ID](#), E.C. Chabert [ID](#), C. Collard [ID](#), S. Falke [ID](#), U. Goerlach [ID](#), R. Haeberle [ID](#), A.-C. Le Bihan [ID](#), M. Meena [ID](#), O. Ponchet [ID](#), G. Saha [ID](#), M.A. Sessini [ID](#), P. Van Hove [ID](#), P. Vaucelle [ID](#)

**Centre de Calcul de l'Institut National de Physique Nucléaire et de Physique des Particules, CNRS/IN2P3, Villeurbanne, France**

A. Di Florio [ID](#)

**Institut de Physique des 2 Infinis de Lyon (IP2I ), Villeurbanne, France**

D. Amram, S. Beauceron , B. Blançon , G. Boudoul , N. Chanon , D. Contardo , P. Depasse , C. Dozen<sup>20</sup> , H. El Mamouni, J. Fay , S. Gascon , M. Gouzevitch , C. Greenberg, G. Grenier , B. Ille , E. Jourd'huy, I.B. Laktineh, M. Lethuillier , L. Mirabito, S. Perries, A. Purohit , M. Vander Donckt , P. Verdier , J. Xiao 

**Georgian Technical University, Tbilisi, Georgia**

I. Lomidze , T. Toriashvili<sup>21</sup> , Z. Tsamalaidze<sup>14</sup> 

**RWTH Aachen University, I. Physikalisches Institut, Aachen, Germany**

V. Botta , S. Consuegra Rodríguez , L. Feld , K. Klein , M. Lipinski , D. Meuser , A. Pauls , D. Pérez Adán , N. Röwert , M. Teroerde 

**RWTH Aachen University, III. Physikalisches Institut A, Aachen, Germany**

S. Diekmann , A. Dodonova , N. Eich , D. Eliseev , F. Engelke , J. Erdmann , M. Erdmann , P. Fackeldey , B. Fischer , T. Hebbeker , K. Hoepfner , F. Ivone , A. Jung , M.y. Lee , F. Mausolf , M. Merschmeyer , A. Meyer , S. Mukherjee , D. Noll , F. Nowotny, A. Pozdnyakov , Y. Rath, W. Redjeb , F. Rehm, H. Reithler , V. Sarkisovi , A. Schmidt , C. Seth, A. Sharma , J.L. Spah , A. Stein , F. Torres Da Silva De Araujo<sup>22</sup> , S. Wiedenbeck , S. Zaleski

**RWTH Aachen University, III. Physikalisches Institut B, Aachen, Germany**

C. Dziwok , G. Flügge , T. Kress , A. Nowack , O. Pooth , A. Stahl , T. Ziemons , A. Zottz 

**Deutsches Elektronen-Synchrotron, Hamburg, Germany**

H. Aarup Petersen , M. Aldaya Martin , J. Alimena , S. Amoroso, Y. An , J. Bach , S. Baxter , M. Bayatmakou , H. Becerril Gonzalez , O. Behnke , A. Belvedere , F. Blekman<sup>23</sup> , K. Borras<sup>24</sup> , A. Campbell , A. Cardini , C. Cheng, F. Colombina , G. Eckerlin, D. Eckstein , L.I. Estevez Banos , E. Gallo<sup>23</sup> , A. Geiser , V. Guglielmi , M. Guthoff , A. Hinzmann , L. Jeppe , B. Kaech , M. Kasemann , C. Kleinwort , R. Kogler , M. Komm , D. Krücker , W. Lange, D. Leyva Pernia , K. Lipka<sup>25</sup> , W. Lohmann<sup>26</sup> , F. Lorkowski , R. Mankel , I.-A. Melzer-Pellmann , M. Mendizabal Morentin , A.B. Meyer , G. Milella , K. Moral Figueroa , A. Mussgiller , L.P. Nair , J. Niedziela , A. Nürnberg , Y. Otarid, J. Park , E. Ranken , A. Raspereza , D. Rastorguev , J. Rübenach, L. Rygaard, A. Saggio , M. Scham<sup>27,24</sup> , S. Schnake<sup>24</sup> , P. Schütze , C. Schwanenberger<sup>23</sup> , D. Selivanova , K. Sharko , M. Shchedrolosiev , D. Stafford, F. Vazzoler , A. Ventura Barroso , R. Walsh , D. Wang , Q. Wang , K. Wichmann, L. Wiens<sup>24</sup> , C. Wissing , Y. Yang , A. Zimermann Castro Santos 

**University of Hamburg, Hamburg, Germany**

A. Albrecht , S. Albrecht , M. Antonello , S. Bein , S. Bollweg, M. Bonanomi , P. Connor , K. El Morabit , Y. Fischer , E. Garutti , A. Grohsjean , J. Haller , D. Hundhausen, H.R. Jabusch , G. Kasieczka , P. Keicher, R. Klanner , W. Korcari , T. Kramer , C.c. Kuo, V. Kutzner , F. Labe , J. Lange , A. Lobanov , C. Matthies , L. Moureux , M. Mrowietz, A. Nigamova , Y. Nissan, A. Paasch , K.J. Pena Rodriguez , T. Quadfasel , B. Raciti , M. Rieger , D. Savoiu , J. Schindler , P. Schleper , M. Schröder , J. Schwandt , M. Sommerhalder , H. Stadie , G. Steinbrück , A. Tews, B. Wiederspan, M. Wolf 

**Karlsruhe Institut fuer Technologie, Karlsruhe, Germany**

S. Brommer , E. Butz , T. Chwalek , A. Dierlamm , A. Droll, U. Elicabuk, N. Faltermann , M. Giffels , A. Gottmann , F. Hartmann<sup>28</sup> , R. Hofsaess , M. Horzela 

U. Husemann [ID](#), J. Kieseler [ID](#), M. Klute [ID](#), R. Koppenhöfer [ID](#), O. Lavyork, J.M. Lawhorn [ID](#), M. Link, A. Lintuluoto [ID](#), S. Maier [ID](#), S. Mitra [ID](#), M. Mormile [ID](#), Th. Müller [ID](#), M. Neukum, M. Oh [ID](#), E. Pfeffer [ID](#), M. Presilla [ID](#), G. Quast [ID](#), K. Rabbertz [ID](#), B. Regnery [ID](#), N. Shadskiy [ID](#), I. Shvetsov [ID](#), H.J. Simonis [ID](#), L. Sowa, L. Stockmeier, K. Tauqeer, M. Toms [ID](#), N. Trevisani [ID](#), R.F. Von Cube [ID](#), M. Wassmer [ID](#), S. Wieland [ID](#), F. Wittig, R. Wolf [ID](#), X. Zuo [ID](#)

**Institute of Nuclear and Particle Physics (INPP), NCSR Demokritos, Aghia Paraskevi, Greece**

G. Anagnostou, G. Daskalakis [ID](#), A. Kyriakis, A. Papadopoulos<sup>28</sup>, A. Stakia [ID](#)

**National and Kapodistrian University of Athens, Athens, Greece**

P. Kontaxakis [ID](#), G. Melachroinos, Z. Painesis [ID](#), I. Papavergou [ID](#), I. Paraskevas [ID](#), N. Saoulidou [ID](#), K. Theofilatos [ID](#), E. Tziaferi [ID](#), K. Vellidis [ID](#), I. Zisopoulos [ID](#)

**National Technical University of Athens, Athens, Greece**

G. Bakas [ID](#), T. Chatzistavrou, G. Karapostoli [ID](#), K. Kousouris [ID](#), I. Papakrivopoulos [ID](#), E. Siamarkou, G. Tsipolitis [ID](#), A. Zacharopoulou

**University of Ioánnina, Ioánnina, Greece**

I. Bestintzanos, I. Evangelou [ID](#), C. Foudas, C. Kamtsikis, P. Katsoulis, P. Kokkas [ID](#), P.G. Kosmoglou Kioseoglou [ID](#), N. Manthos [ID](#), I. Papadopoulos [ID](#), J. Strologas [ID](#)

**HUN-REN Wigner Research Centre for Physics, Budapest, Hungary**

C. Hajdu [ID](#), D. Horvath<sup>29,30</sup> [ID](#), K. Márton, A.J. Rádl<sup>31</sup> [ID](#), F. Sikler [ID](#), V. Veszpremi [ID](#)

**MTA-ELTE Lendület CMS Particle and Nuclear Physics Group, Eötvös Loránd University, Budapest, Hungary**

M. Csand [ID](#), K. Farkas [ID](#), A. Fehrkuti<sup>32</sup> [ID](#), M.M.A. Gadallah<sup>33</sup> [ID](#), . Kadlecik [ID](#), P. Major [ID](#), G. Pasztor [ID](#), G.I. Veres [ID](#)

**Faculty of Informatics, University of Debrecen, Debrecen, Hungary**

L. Olah [ID](#), B. Ujvari [ID](#)

**HUN-REN ATOMKI - Institute of Nuclear Research, Debrecen, Hungary**

G. Bencze, S. Czellar, J. Molnar, Z. Szillasi

**Karoly Robert Campus, MATE Institute of Technology, Gyongyos, Hungary**

T. Csorgo<sup>32</sup> [ID](#), T. Novak [ID](#)

**Panjab University, Chandigarh, India**

S. Bansal [ID](#), S.B. Beri, V. Bhatnagar [ID](#), G. Chaudhary [ID](#), S. Chauhan [ID](#), N. Dhingra<sup>34</sup> [ID](#), A. Kaur [ID](#), A. Kaur [ID](#), H. Kaur [ID](#), M. Kaur [ID](#), S. Kumar [ID](#), T. Sheokand, J.B. Singh [ID](#), A. Singla [ID](#)

**University of Delhi, Delhi, India**

A. Ahmed [ID](#), A. Bhardwaj [ID](#), A. Chhetri [ID](#), B.C. Choudhary [ID](#), A. Kumar [ID](#), A. Kumar [ID](#), M. Naimuddin [ID](#), K. Ranjan [ID](#), M.K. Saini, S. Saumya [ID](#)

**Saha Institute of Nuclear Physics, HBNI, Kolkata, India**

S. Baradia [ID](#), S. Barman<sup>35</sup> [ID](#), S. Bhattacharya [ID](#), S. Das Gupta, S. Dutta [ID](#), S. Dutta, S. Sarkar

**Indian Institute of Technology Madras, Madras, India**

M.M. Ameen [ID](#), P.K. Behera [ID](#), S.C. Behera [ID](#), S. Chatterjee [ID](#), G. Dash [ID](#), P. Jana [ID](#), P. Kalbhor [ID](#), S. Kamble [ID](#), J.R. Komaragiri<sup>36</sup> [ID](#), D. Kumar<sup>36</sup> [ID](#), T. Mishra [ID](#), B. Parida<sup>37</sup> [ID](#), P.R. Pujahari [ID](#), N.R. Saha [ID](#), A. Sharma [ID](#), A.K. Sikdar [ID](#), R.K. Singh, P. Verma, S. Verma [ID](#), A. Vijay

**Tata Institute of Fundamental Research-A, Mumbai, India**S. Dugad, G.B. Mohanty , M. Shelake, P. Suryadevara**Tata Institute of Fundamental Research-B, Mumbai, India**A. Bala , S. Banerjee , R.M. Chatterjee, M. Guchait , Sh. Jain , A. Jaiswal, S. Kumar , G. Majumder , K. Mazumdar , S. Parolia , A. Thachayath **National Institute of Science Education and Research, An OCC of Homi Bhabha National Institute, Bhubaneswar, Odisha, India**S. Bahinipati<sup>38</sup> , C. Kar , D. Maity<sup>39</sup> , P. Mal , V.K. Muraleedharan Nair Bindhu<sup>39</sup> , K. Naskar<sup>39</sup> , A. Nayak<sup>39</sup> , S. Nayak, K. Pal, P. Sadangi, S.K. Swain , S. Varghese<sup>39</sup> , D. Vats<sup>39</sup> **Indian Institute of Science Education and Research (IISER), Pune, India**S. Acharya<sup>40</sup> , A. Alpana , S. Dube , B. Gomber<sup>40</sup> , P. Hazarika , B. Kansal , A. Laha , B. Sahu<sup>40</sup> , S. Sharma , K.Y. Vaish **Isfahan University of Technology, Isfahan, Iran**H. Bakhshiansohi<sup>41</sup> , A. Jafari<sup>42</sup> , M. Zeinali<sup>43</sup> **Institute for Research in Fundamental Sciences (IPM), Tehran, Iran**S. Bashiri, S. Chenarani<sup>44</sup> , S.M. Etesami , Y. Hosseini , M. Khakzad , E. Khazaie , M. Mohammadi Najafabadi , S. Tizchang<sup>45</sup> **University College Dublin, Dublin, Ireland**M. Felcini , M. Grunewald **INFN Sezione di Bari<sup>a</sup>, Università di Bari<sup>b</sup>, Politecnico di Bari<sup>c</sup>, Bari, Italy**M. Abbrescia<sup>a,b</sup> , A. Colaleo<sup>a,b</sup> , D. Creanza<sup>a,c</sup> , B. D'Anzi<sup>a,b</sup> , N. De Filippis<sup>a,c</sup> , M. De Palma<sup>a,b</sup> , W. Elmetenawee<sup>a,b,46</sup> , N. Ferrara<sup>a,b</sup> , L. Fiore<sup>a</sup> , G. Iaselli<sup>a,c</sup> , L. Longo<sup>a</sup> , M. Louka<sup>a,b</sup> , G. Maggi<sup>a,c</sup> , M. Maggi<sup>a</sup> , I. Margjeka<sup>a</sup> , V. Mastrapasqua<sup>a,b</sup> , S. My<sup>a,b</sup> , S. Nuzzo<sup>a,b</sup> , A. Pellecchia<sup>a,b</sup> , A. Pompili<sup>a,b</sup> , G. Pugliese<sup>a,c</sup> , R. Radogna<sup>a,b</sup> , D. Ramos<sup>a</sup> , A. Ranieri<sup>a</sup> , L. Silvestris<sup>a</sup> , F.M. Simone<sup>a,c</sup> , Ü. Sözbilir<sup>a</sup> , A. Stamerra<sup>a,b</sup> , D. Troiano<sup>a,b</sup> , R. Venditti<sup>a,b</sup> , P. Verwilligen<sup>a</sup> , A. Zaza<sup>a,b</sup> **INFN Sezione di Bologna<sup>a</sup>, Università di Bologna<sup>b</sup>, Bologna, Italy**G. Abbiendi<sup>a</sup> , C. Battilana<sup>a,b</sup> , D. Bonacorsi<sup>a,b</sup> , P. Capiluppi<sup>a,b</sup> , A. Castro<sup>+a,b</sup> , F.R. Cavallo<sup>a</sup> , M. Cuffiani<sup>a,b</sup> , G.M. Dallavalle<sup>a</sup> , T. Diotalevi<sup>a,b</sup> , F. Fabbri<sup>a</sup> , A. Fanfani<sup>a,b</sup> , D. Fasanella<sup>a</sup> , P. Giacomelli<sup>a</sup> , L. Giommi<sup>a,b</sup> , C. Grandi<sup>a</sup> , L. Guiducci<sup>a,b</sup> , S. Lo Meo<sup>a,47</sup> , M. Lorusso<sup>a,b</sup> , L. Lunerti<sup>a</sup> , S. Marcellini<sup>a</sup> , G. Masetti<sup>a</sup> , F.L. Navarria<sup>a,b</sup> , G. Paggi<sup>a,b</sup> , A. Perrotta<sup>a</sup> , F. Primavera<sup>a,b</sup> , A.M. Rossi<sup>a,b</sup> , S. Rossi Tisbeni<sup>a,b</sup> , T. Rovelli<sup>a,b</sup> , G.P. Siroli<sup>a,b</sup> **INFN Sezione di Catania<sup>a</sup>, Università di Catania<sup>b</sup>, Catania, Italy**S. Costa<sup>a,b,48</sup> , A. Di Mattia<sup>a</sup> , A. Lapertosa<sup>a</sup> , R. Potenza<sup>a,b</sup> , A. Tricomi<sup>a,b,48</sup> , C. Tuve<sup>a,b</sup> **INFN Sezione di Firenze<sup>a</sup>, Università di Firenze<sup>b</sup>, Firenze, Italy**P. Assiouras<sup>a</sup> , G. Barbagli<sup>a</sup> , G. Bardelli<sup>a,b</sup> , B. Camaiani<sup>a,b</sup> , A. Cassese<sup>a</sup> , R. Ceccarelli<sup>a</sup> , V. Ciulli<sup>a,b</sup> , C. Civinini<sup>a</sup> , R. D'Alessandro<sup>a,b</sup> , E. Focardi<sup>a,b</sup> , T. Kello<sup>a</sup>, G. Latino<sup>a,b</sup> , P. Lenzi<sup>a,b</sup> , M. Lizzo<sup>a</sup> , M. Meschini<sup>a</sup> , S. Paoletti<sup>a</sup> , A. Papanastassiou<sup>a,b</sup> , G. Sguazzoni<sup>a</sup> , L. Viliani<sup>a</sup> **INFN Laboratori Nazionali di Frascati, Frascati, Italy**

L. Benussi , S. Bianco , S. Meola<sup>49</sup> , D. Piccolo 

**INFN Sezione di Genova<sup>a</sup>, Università di Genova<sup>b</sup>, Genova, Italy**

M. Alves Gallo Pereira<sup>a</sup> , F. Ferro<sup>a</sup> , E. Robutti<sup>a</sup> , S. Tosi<sup>a,b</sup> 

**INFN Sezione di Milano-Bicocca<sup>a</sup>, Università di Milano-Bicocca<sup>b</sup>, Milano, Italy**

A. Benaglia<sup>a</sup> , F. Brivio<sup>a</sup> , F. Cetorelli<sup>a,b</sup> , F. De Guio<sup>a,b</sup> , M.E. Dinardo<sup>a,b</sup> , P. Dini<sup>a</sup> , S. Gennai<sup>a</sup> , R. Gerosa<sup>a,b</sup> , A. Ghezzi<sup>a,b</sup> , P. Govoni<sup>a,b</sup> , L. Guzzi<sup>a</sup> , M.T. Lucchini<sup>a,b</sup> , M. Malberti<sup>a</sup> , S. Malvezzi<sup>a</sup> , A. Massironi<sup>a</sup> , D. Menasce<sup>a</sup> , L. Moroni<sup>a</sup> , M. Paganoni<sup>a,b</sup> , S. Palluotto<sup>a,b</sup> , D. Pedrini<sup>a</sup> , A. Perego<sup>a,b</sup> , B.S. Pinolini<sup>a</sup>, G. Pizzati<sup>a,b</sup> , S. Ragazzi<sup>a,b</sup> , T. Tabarelli de Fatis<sup>a,b</sup> 

**INFN Sezione di Napoli<sup>a</sup>, Università di Napoli 'Federico II'<sup>b</sup>, Napoli, Italy; Università della Basilicata<sup>c</sup>, Potenza, Italy; Scuola Superiore Meridionale (SSM)<sup>d</sup>, Napoli, Italy**

S. Buontempo<sup>a</sup> , A. Cagnotta<sup>a,b</sup> , F. Carnevali<sup>a,b</sup> , N. Cavallo<sup>a,c</sup> , F. Fabozzi<sup>a,c</sup> , A.O.M. Iorio<sup>a,b</sup> , L. Lista<sup>a,b,50</sup> , P. Paolucci<sup>a,28</sup> , B. Rossi<sup>a</sup> 

**INFN Sezione di Padova<sup>a</sup>, Università di Padova<sup>b</sup>, Padova, Italy; Università di Trento<sup>c</sup>, Trento, Italy**

R. Ardino<sup>a</sup> , P. Azzi<sup>a</sup> , N. Bacchetta<sup>a,51</sup> , A. Bergnoli<sup>a</sup> , D. Bisello<sup>a,b</sup> , P. Bortignon<sup>a</sup> , G. Bortolato<sup>a,b</sup> , A. Bragagnolo<sup>a,b</sup> , A.C.M. Bulla<sup>a</sup> , R. Carlin<sup>a,b</sup> , T. Dorigo<sup>a</sup> , F. Gasparini<sup>a,b</sup> , U. Gasparini<sup>a,b</sup> , S. Giorgetti<sup>a</sup>, E. Lusiani<sup>a</sup> , M. Margoni<sup>a,b</sup> , A.T. Meneguzzo<sup>a,b</sup> , M. Migliorini<sup>a,b</sup> , J. Pazzini<sup>a,b</sup> , P. Ronchese<sup>a,b</sup> , R. Rossin<sup>a,b</sup> , F. Simonetto<sup>a,b</sup> , M. Tosi<sup>a,b</sup> , A. Triossi<sup>a,b</sup> , S. Ventura<sup>a</sup> , M. Zanetti<sup>a,b</sup> , P. Zotto<sup>a,b</sup> , A. Zucchetta<sup>a,b</sup> , G. Zumerle<sup>a,b</sup> 

**INFN Sezione di Pavia<sup>a</sup>, Università di Pavia<sup>b</sup>, Pavia, Italy**

A. Braghieri<sup>a</sup> , S. Calzaferri<sup>a</sup> , D. Fiorina<sup>a</sup> , P. Montagna<sup>a,b</sup> , V. Re<sup>a</sup> , C. Riccardi<sup>a,b</sup> , P. Salvini<sup>a</sup> , I. Vai<sup>a,b</sup> , P. Vitulo<sup>a,b</sup> 

**INFN Sezione di Perugia<sup>a</sup>, Università di Perugia<sup>b</sup>, Perugia, Italy**

S. Ajmal<sup>a,b</sup> , M.E. Ascoli<sup>a,b</sup> , G.M. Bilei<sup>a</sup> , C. Carrivale<sup>a,b</sup> , D. Ciangottini<sup>a,b</sup> , L. Fanò<sup>a,b</sup> , M. Magherini<sup>a,b</sup> , V. Mariani<sup>a,b</sup> , M. Merichelli<sup>a</sup> , F. Moscatelli<sup>a,52</sup> , A. Rossi<sup>a,b</sup> , A. Santocchia<sup>a,b</sup> , D. Spiga<sup>a</sup> , T. Tedeschi<sup>a,b</sup> 

**INFN Sezione di Pisa<sup>a</sup>, Università di Pisa<sup>b</sup>, Scuola Normale Superiore di Pisa<sup>c</sup>, Pisa, Italy; Università di Siena<sup>d</sup>, Siena, Italy**

C. Aimè<sup>a</sup> , C.A. Alexe<sup>a,c</sup> , P. Asenov<sup>a,b</sup> , P. Azzurri<sup>a</sup> , G. Bagliesi<sup>a</sup> , R. Bhattacharya<sup>a</sup> , L. Bianchini<sup>a,b</sup> , T. Boccali<sup>a</sup> , D. Bruschini<sup>a,c</sup> , R. Castaldi<sup>a</sup> , M.A. Ciocci<sup>a,b</sup> , M. Cipriani<sup>a,b</sup> , V. D'Amante<sup>a,d</sup> , R. Dell'Orso<sup>a</sup> , S. Donato<sup>a</sup> , A. Giassi<sup>a</sup> , F. Ligabue<sup>a,c</sup> , A.C. Marini<sup>a</sup> , D. Matos Figueiredo<sup>a</sup> , A. Messineo<sup>a,b</sup> , S. Mishra<sup>a</sup> , M. Musich<sup>a,b</sup> , F. Palla<sup>a</sup> , A. Rizzi<sup>a,b</sup> , G. Rolandi<sup>a,c</sup> , S. Roy Chowdhury<sup>a</sup> , T. Sarkar<sup>a</sup> , P. Spagnolo<sup>a</sup> , R. Tenchini<sup>a</sup> , G. Tonelli<sup>a,b</sup> , F. Vaselli<sup>a,c</sup> , A. Venturi<sup>a</sup> , P.G. Verdini<sup>a</sup> 

**INFN Sezione di Roma<sup>a</sup>, Sapienza Università di Roma<sup>b</sup>, Roma, Italy**

P. Barria<sup>a</sup> , C. Basile<sup>a,b</sup> , F. Cavallari<sup>a</sup> , L. Cunqueiro Mendez<sup>a,b</sup> , D. Del Re<sup>a,b</sup> , E. Di Marco<sup>a,b</sup> , M. Diemoz<sup>a</sup> , F. Errico<sup>a,b</sup> , R. Gargiulo<sup>a,b</sup> , E. Longo<sup>a,b</sup> , L. Martikainen<sup>a,b</sup> , J. Mijuskovic<sup>a,b</sup> , G. Organiti<sup>a,b</sup> , F. Pandolfi<sup>a</sup> , R. Paramatti<sup>a,b</sup> , C. Quaranta<sup>a,b</sup> , S. Rahatlou<sup>a,b</sup> , C. Rovelli<sup>a</sup> , F. Santanastasio<sup>a,b</sup> , L. Soffi<sup>a</sup> , V. Vladimirov<sup>a,b</sup> 

**INFN Sezione di Torino<sup>a</sup>, Università di Torino<sup>b</sup>, Torino, Italy; Università del Piemonte Orientale<sup>c</sup>, Novara, Italy**

N. Amapane<sup>a,b</sup> , R. Arcidiacono<sup>a,c</sup> , S. Argiro<sup>a,b</sup> , M. Arneodo<sup>a,c</sup> , N. Bartosik<sup>a</sup> , R. Bellan<sup>a,b</sup> , A. Bellora<sup>a,b</sup> , C. Biino<sup>a</sup> , C. Borca<sup>a,b</sup> , N. Cartiglia<sup>a</sup> , M. Costa<sup>a,b</sup> , R. Covarelli<sup>a,b</sup> , N. Demaria<sup>a</sup> , L. Finco<sup>a</sup> , M. Grippo<sup>a,b</sup> , B. Kiani<sup>a,b</sup> , F. Legger<sup>a</sup> , F. Luongo<sup>a,b</sup> , C. Mariotti<sup>a</sup> , L. Markovic<sup>a,b</sup> , S. Maselli<sup>a</sup> , A. Mecca<sup>a,b</sup> , L. Menzio<sup>a,b</sup> , P. Meridiani<sup>a</sup> , E. Migliore<sup>a,b</sup> , M. Monteno<sup>a</sup> , R. Mulargia<sup>a</sup> , M.M. Obertino<sup>a,b</sup> , G. Ortona<sup>a</sup> , L. Pacher<sup>a,b</sup> , N. Pastrone<sup>a</sup> , M. Pelliccioni<sup>a</sup> , M. Ruspa<sup>a,c</sup> , F. Siviero<sup>a,b</sup> , V. Sola<sup>a,b</sup> , A. Solano<sup>a,b</sup> , A. Staiano<sup>a</sup> , C. Tarricone<sup>a,b</sup> , D. Trocino<sup>a</sup> , G. Umoret<sup>a,b</sup> , R. White<sup>a,b</sup> 

**INFN Sezione di Trieste<sup>a</sup>, Università di Trieste<sup>b</sup>, Trieste, Italy**

J. Babbar<sup>a,b</sup> , S. Belforte<sup>a</sup> , V. Candelise<sup>a,b</sup> , M. Casarsa<sup>a</sup> , F. Cossutti<sup>a</sup> , K. De Leo<sup>a</sup> , G. Della Ricca<sup>a,b</sup> 

**Kyungpook National University, Daegu, Korea**

S. Dogra , J. Hong , B. Kim , J. Kim, D. Lee, H. Lee, S.W. Lee , C.S. Moon , Y.D. Oh , M.S. Ryu , S. Sekmen , B. Tae, Y.C. Yang 

**Department of Mathematics and Physics - GWNU, Gangneung, Korea**

M.S. Kim 

**Chonnam National University, Institute for Universe and Elementary Particles, Kwangju, Korea**

G. Bak , P. Gwak , H. Kim , D.H. Moon 

**Hanyang University, Seoul, Korea**

E. Asilar , J. Choi<sup>53</sup> , D. Kim , T.J. Kim , J.A. Merlin, Y. Ryou

**Korea University, Seoul, Korea**

S. Choi , S. Han, B. Hong , K. Lee, K.S. Lee , S. Lee , J. Yoo 

**Kyung Hee University, Department of Physics, Seoul, Korea**

J. Goh , S. Yang 

**Sejong University, Seoul, Korea**

H. S. Kim , Y. Kim, S. Lee

**Seoul National University, Seoul, Korea**

J. Almond, J.H. Bhyun, J. Choi , J. Choi, W. Jun , J. Kim , Y.W. Kim, S. Ko , H. Kwon , H. Lee , J. Lee , J. Lee , B.H. Oh , S.B. Oh , H. Seo , U.K. Yang, I. Yoon 

**University of Seoul, Seoul, Korea**

W. Jang , D.Y. Kang, Y. Kang , S. Kim , B. Ko, J.S.H. Lee , Y. Lee , I.C. Park , Y. Roh, I.J. Watson 

**Yonsei University, Department of Physics, Seoul, Korea**

S. Ha , K. Hwang, H.D. Yoo 

**Sungkyunkwan University, Suwon, Korea**

M. Choi , M.R. Kim , H. Lee, Y. Lee , I. Yu 

**College of Engineering and Technology, American University of the Middle East (AUM), Dasman, Kuwait**

T. Beyrouty, Y. Gharbia

**Kuwait University - College of Science - Department of Physics, Safat, Kuwait**

F. Alazemi 

**Riga Technical University, Riga, Latvia**

K. Dreimanis , A. Gaile , C. Munoz Diaz, D. Osite , G. Pikurs, A. Potrebko , M. Seidel , D. Sidiropoulos Kontos

**University of Latvia (LU), Riga, Latvia**

N.R. Strautnieks 

**Vilnius University, Vilnius, Lithuania**

M. Ambrozas , A. Juodagalvis , A. Rinkevicius , G. Tamulaitis 

**National Centre for Particle Physics, Universiti Malaya, Kuala Lumpur, Malaysia**

I. Yusuff<sup>54</sup> , Z. Zolkapli

**Universidad de Sonora (UNISON), Hermosillo, Mexico**

J.F. Benitez , A. Castaneda Hernandez , H.A. Encinas Acosta, L.G. Gallegos Maríñez, M. León Coello , J.A. Murillo Quijada , A. Sehrawat , L. Valencia Palomo 

**Centro de Investigacion y de Estudios Avanzados del IPN, Mexico City, Mexico**

G. Ayala , H. Castilla-Valdez , H. Crotte Ledesma, E. De La Cruz-Burelo , I. Heredia-De La Cruz<sup>55</sup> , R. Lopez-Fernandez , J. Mejia Guisao , C.A. Mondragon Herrera, A. Sánchez Hernández 

**Universidad Iberoamericana, Mexico City, Mexico**

C. Oropeza Barrera , D.L. Ramirez Guadarrama, M. Ramírez García 

**Benemerita Universidad Autonoma de Puebla, Puebla, Mexico**

I. Bautista , I. Pedraza , H.A. Salazar Ibarguen , C. Uribe Estrada 

**University of Montenegro, Podgorica, Montenegro**

I. Bubanja , N. Raicevic 

**University of Canterbury, Christchurch, New Zealand**

P.H. Butler 

**National Centre for Physics, Quaid-I-Azam University, Islamabad, Pakistan**

A. Ahmad , M.I. Asghar, A. Awais , M.I.M. Awan, H.R. Hoorani , W.A. Khan 

**National Centre for Nuclear Research, Swierk, Poland**

H. Bialkowska , M. Bluj , M. Górski , M. Kazana , M. Szleper , P. Zalewski 

**Institute of Experimental Physics, Faculty of Physics, University of Warsaw, Warsaw, Poland**

K. Bunkowski , K. Doroba , A. Kalinowski , M. Konecki , J. Krolikowski , A. Muhammad 

**Warsaw University of Technology, Warsaw, Poland**

P. Fokow , K. Pozniak , W. Zabolotny 

**Laboratório de Instrumentação e Física Experimental de Partículas, Lisboa, Portugal**

M. Araujo , D. Bastos , C. Beirão Da Cruz E Silva , A. Boletti , T. Camporesi , G. Da Molin , P. Faccioli , M. Gallinaro , J. Hollar , N. Leonardo , G.B. Marozzo, A. Petrilli , M. Pisano , J. Seixas , J. Varela , J.W. Wulff

**Faculty of Physics, University of Belgrade, Belgrade, Serbia**

P. Adzic , P. Milenovic 

**VINCA Institute of Nuclear Sciences, University of Belgrade, Belgrade, Serbia**

D. Devetak, M. Dordevic , J. Milosevic , L. Nadderd , V. Rekovic

**Centro de Investigaciones Energéticas Medioambientales y Tecnológicas (CIEMAT), Madrid, Spain**

J. Alcaraz Maestre , Cristina F. Bedoya , J.A. Brochero Cifuentes , Oliver M. Carretero , M. Cepeda , M. Cerrada , N. Colino , B. De La Cruz , A. Delgado Peris , A. Escalante Del Valle , D. Fernández Del Val , J.P. Fernández Ramos , J. Flix , M.C. Fouz , O. Gonzalez Lopez , S. Goy Lopez , J.M. Hernandez , M.I. Josa , J. Llorente Merino , E. Martin Viscasillas , D. Moran , C. M. Morcillo Perez , Á. Navarro Tobar , C. Perez Dengra , A. Pérez-Calero Yzquierdo , J. Puerta Pelayo , I. Redondo , S. Sánchez Navas , J. Sastre , J. Vazquez Escobar 

**Universidad Autónoma de Madrid, Madrid, Spain**

J.F. de Trocóniz 

**Universidad de Oviedo, Instituto Universitario de Ciencias y Tecnologías Espaciales de Asturias (ICTEA), Oviedo, Spain**

B. Alvarez Gonzalez , J. Cuevas , J. Fernandez Menendez , S. Folgueras , I. Gonzalez Caballero , P. Leguina , E. Palencia Cortezon , J. Prado Pico, C. Ramón Álvarez , V. Rodríguez Bouza , A. Soto Rodríguez , A. Trapote , C. Vico Villalba , P. Vischia 

**Instituto de Física de Cantabria (IFCA), CSIC-Universidad de Cantabria, Santander, Spain**

S. Bhowmik , S. Blanco Fernández , I.J. Cabrillo , A. Calderon , J. Duarte Campderros , M. Fernandez , G. Gomez , C. Lasosa García , R. Lopez Ruiz , C. Martinez Rivero , P. Martinez Ruiz del Arbol , F. Matorras , P. Matorras Cuevas , E. Navarrete Ramos , J. Piedra Gomez , L. Scodellaro , I. Vila , J.M. Vizan Garcia 

**University of Colombo, Colombo, Sri Lanka**

B. Kailasapathy<sup>56</sup> , D.D.C. Wickramarathna 

**University of Ruhuna, Department of Physics, Matara, Sri Lanka**

W.G.D. Dharmaratna<sup>57</sup> , K. Liyanage , N. Perera 

**CERN, European Organization for Nuclear Research, Geneva, Switzerland**

D. Abbaneo , C. Amendola , E. Auffray , G. Auzinger , D. Barney , A. Bermúdez Martínez , M. Bianco , A.A. Bin Anuar , A. Bocci , L. Borgonovi , C. Botta , E. Brondolin , C. Caillol , G. Cerminara , N. Chernyavskaya , D. d'Enterria , A. Dabrowski , A. David , A. De Roeck , M.M. Defranchis , M. Dobson , G. Franzoni , W. Funk , D. Gigi, K. Gill , F. Glege , J. Hegeman , J.K. Heikkilä , B. Huber, V. Innocente , T. James , P. Janot , O. Kaluzinska , O. Karacheban<sup>26</sup> , S. Laurila , P. Lecoq , E. Leutgeb , C. Lourenço , L. Malgeri , M. Mannelli , M. Matthewman, A. Mehta , F. Meijers , S. Mersi , E. Meschi , V. Milosevic , F. Monti , F. Moortgat , M. Mulders , I. Neutelings , S. Orfanelli , F. Pantaleo , G. Petruciani , A. Pfeiffer , M. Pierini , H. Qu , D. Rabady , B. Ribeiro Lopes , F. Riti , M. Rovere , H. Sakulin , S. Sanchez Cruz , S. Scarfi , C. Schwick, M. Selvaggi , A. Sharma , K. Shchelina , P. Silva , P. Sphicas<sup>58</sup> , A.G. Stahl Leiton , A. Steen , S. Summers , D. Treille , P. Tropea , D. Walter , J. Wanczyk<sup>59</sup> , J. Wang, K.A. Wozniak<sup>60</sup> , S. Wuchterl , P. Zehetner , P. Zejdl , W.D. Zeuner

**PSI Center for Neutron and Muon Sciences, Villigen, Switzerland**

T. Bevilacqua<sup>61</sup> , L. Caminada<sup>61</sup> , A. Ebrahimi , W. Erdmann , R. Horisberger , Q. Ingram , H.C. Kaestli , D. Kotlinski , C. Lange , M. Missiroli<sup>61</sup> , L. Noehte<sup>61</sup> , T. Rohe , A. Samalan

**ETH Zurich - Institute for Particle Physics and Astrophysics (IPA), Zurich, Switzerland**

T.K. Arrestad , M. Backhaus , G. Bonomelli, A. Calandri , C. Cazzaniga , K. Datta , P. De Bryas Dexmiers D'archiac<sup>59</sup> , A. De Cosa , G. Dissertori , M. Dittmar, M. Donegà , F. Eble , M. Galli , K. Gedia , F. Glessgen , C. Grab , N. Härringer , T.G. Harte, D. Hits , W. Lustermann , A.-M. Lyon , R.A. Manzoni , M. Marchegiani , L. Marchese , C. Martin Perez , A. Mascellani<sup>59</sup> , F. Nessi-Tedaldi , F. Pauss , V. Perovic , S. Pigazzini , B. Ristic , R. Seidita , J. Steggemann<sup>59</sup> , A. Tarabini , D. Valsecchi , R. Wallny 

**Universität Zürich, Zurich, Switzerland**

C. Amsler<sup>62</sup> , P. Bärtschi , M.F. Canelli , K. Cormier , M. Huwiler , W. Jin , A. Jofrehei , B. Kilminster , S. Leontsinis , S.P. Liechti , A. Macchiolo , P. Meiring , F. Meng , J. Motta , A. Reimers , P. Robmann, M. Senger , E. Shokr, F. Stäger , R. Tramontano 

**National Central University, Chung-Li, Taiwan**

C. Adloff<sup>63</sup>, D. Bhowmik, C.M. Kuo, W. Lin, P.K. Rout , P.C. Tiwari<sup>36</sup> 

**National Taiwan University (NTU), Taipei, Taiwan**

L. Ceard, K.F. Chen , Z.g. Chen, A. De Iorio , W.-S. Hou , T.h. Hsu, Y.w. Kao, S. Karmakar , G. Kole , Y.y. Li , R.-S. Lu , E. Paganis , X.f. Su , J. Thomas-Wilsker , L.s. Tsai, D. Tsionou, H.y. Wu, E. Yazgan 

**High Energy Physics Research Unit, Department of Physics, Faculty of Science, Chulalongkorn University, Bangkok, Thailand**

C. Asawatangtrakuldee , N. Srimanobhas , V. Wachirapusanand 

**Çukurova University, Physics Department, Science and Art Faculty, Adana, Turkey**

D. Agyel , F. Boran , F. Dolek , I. Dumanoglu<sup>64</sup> , E. Eskut , Y. Guler<sup>65</sup> , E. Gurpinar Guler<sup>65</sup> , C. Isik , O. Kara, A. Kayis Topaksu , U. Kiminsu , Y. Komurcu , G. Onengut , K. Ozdemir<sup>66</sup> , A. Polatoz , B. Tali<sup>67</sup> , U.G. Tok , S. Turkcapar , E. Uslan , I.S. Zorbakir 

**Middle East Technical University, Physics Department, Ankara, Turkey**

G. Sokmen, M. Yalvac<sup>68</sup> 

**Bogazici University, Istanbul, Turkey**

B. Akgun , I.O. Atakisi , E. Gülmез , M. Kaya<sup>69</sup> , O. Kaya<sup>70</sup> , S. Tekten<sup>71</sup> 

**Istanbul Technical University, Istanbul, Turkey**

A. Cakir , K. Cankocak<sup>64,72</sup> , G.G. Dincer<sup>64</sup> , S. Sen<sup>73</sup> 

**Istanbul University, Istanbul, Turkey**

O. Aydilek<sup>74</sup> , B. Hacisahinoglu , I. Hos<sup>75</sup> , H. Sert , C. Simsek , C. Zorbilmez 

**Yildiz Technical University, Istanbul, Turkey**

S. Cerci , B. Isildak<sup>76</sup> , D. Sunar Cerci , T. Yetkin 

**Institute for Scintillation Materials of National Academy of Science of Ukraine, Kharkiv, Ukraine**

A. Boyaryntsev , B. Grynyov 

**National Science Centre, Kharkiv Institute of Physics and Technology, Kharkiv, Ukraine**

L. Levchuk 

**University of Bristol, Bristol, United Kingdom**

D. Anthony [ID](#), J.J. Brooke [ID](#), A. Bundock [ID](#), F. Bury [ID](#), E. Clement [ID](#), D. Cussans [ID](#), H. Flacher [ID](#), M. Glowacki, J. Goldstein [ID](#), H.F. Heath [ID](#), M.-L. Holmberg [ID](#), L. Kreczko [ID](#), S. Paramesvaran [ID](#), L. Robertshaw, V.J. Smith [ID](#), K. Walkingshaw Pass

#### **Rutherford Appleton Laboratory, Didcot, United Kingdom**

A.H. Ball, K.W. Bell [ID](#), A. Belyaev<sup>77</sup> [ID](#), C. Brew [ID](#), R.M. Brown [ID](#), D.J.A. Cockerill [ID](#), C. Cooke [ID](#), A. Elliot [ID](#), K.V. Ellis, K. Harder [ID](#), S. Harper [ID](#), J. Linacre [ID](#), K. Manolopoulos, D.M. Newbold [ID](#), E. Olaiya, D. Petyt [ID](#), T. Reis [ID](#), A.R. Sahasransu [ID](#), G. Salvi [ID](#), T. Schuh, C.H. Shepherd-Themistocleous [ID](#), I.R. Tomalin [ID](#), K.C. Whalen [ID](#), T. Williams [ID](#)

#### **Imperial College, London, United Kingdom**

I. Andreou [ID](#), R. Bainbridge [ID](#), P. Bloch [ID](#), C.E. Brown [ID](#), O. Buchmuller, C.A. Carrillo Montoya [ID](#), G.S. Chahal<sup>78</sup> [ID](#), D. Colling [ID](#), J.S. Dancu, I. Das [ID](#), P. Dauncey [ID](#), G. Davies [ID](#), M. Della Negra [ID](#), S. Fayer, G. Fedi [ID](#), G. Hall [ID](#), A. Howard, G. Iles [ID](#), C.R. Knight [ID](#), P. Krueper, J. Langford [ID](#), K.H. Law [ID](#), J. León Holgado [ID](#), L. Lyons [ID](#), A.-M. Magnan [ID](#), B. Maier [ID](#), S. Mallios, M. Mieskolainen [ID](#), J. Nash<sup>79</sup> [ID](#), M. Pesaresi [ID](#), P.B. Pradeep, B.C. Radburn-Smith [ID](#), A. Richards, A. Rose [ID](#), K. Savva [ID](#), C. Seez [ID](#), R. Shukla [ID](#), A. Tapper [ID](#), K. Uchida [ID](#), G.P. Uttley [ID](#), T. Virdee<sup>28</sup> [ID](#), M. Vojinovic [ID](#), N. Wardle [ID](#), D. Winterbottom [ID](#)

#### **Brunel University, Uxbridge, United Kingdom**

J.E. Cole [ID](#), A. Khan, P. Kyberd [ID](#), I.D. Reid [ID](#)

#### **Baylor University, Waco, Texas, USA**

S. Abdullin [ID](#), A. Brinkerhoff [ID](#), E. Collins [ID](#), M.R. Darwish [ID](#), J. Dittmann [ID](#), K. Hatakeyama [ID](#), J. Hiltbrand [ID](#), B. McMaster [ID](#), J. Samudio [ID](#), S. Sawant [ID](#), C. Sutantawibul [ID](#), J. Wilson [ID](#)

#### **Catholic University of America, Washington, DC, USA**

R. Bartek [ID](#), A. Dominguez [ID](#), A.E. Simsek [ID](#), S.S. Yu [ID](#)

#### **The University of Alabama, Tuscaloosa, Alabama, USA**

B. Bam [ID](#), A. Buchot Perraguin [ID](#), R. Chudasama [ID](#), S.I. Cooper [ID](#), C. Crovella [ID](#), S.V. Gleyzer [ID](#), E. Pearson, C.U. Perez [ID](#), P. Rumerio<sup>80</sup> [ID](#), E. Usai [ID](#), R. Yi [ID](#)

#### **Boston University, Boston, Massachusetts, USA**

A. Akpinar [ID](#), C. Cosby [ID](#), G. De Castro, Z. Demiragli [ID](#), C. Erice [ID](#), C. Fangmeier [ID](#), C. Fernandez Madrazo [ID](#), E. Fontanesi [ID](#), D. Gastler [ID](#), F. Golf [ID](#), S. Jeon [ID](#), J. O'cain, I. Reed [ID](#), J. Rohlf [ID](#), K. Salyer [ID](#), D. Sperka [ID](#), D. Spitzbart [ID](#), I. Suarez [ID](#), A. Tsatsos [ID](#), A.G. Zecchinelli [ID](#)

#### **Brown University, Providence, Rhode Island, USA**

G. Benelli [ID](#), D. Cutts [ID](#), L. Gouskos [ID](#), M. Hadley [ID](#), U. Heintz [ID](#), J.M. Hogan<sup>81</sup> [ID](#), T. Kwon [ID](#), G. Landsberg [ID](#), K.T. Lau [ID](#), D. Li [ID](#), J. Luo [ID](#), S. Mondal [ID](#), T. Russell, S. Sagir<sup>82</sup> [ID](#), X. Shen, F. Simpson [ID](#), M. Stamenkovic [ID](#), N. Venkatasubramanian, X. Yan [ID](#)

#### **University of California, Davis, Davis, California, USA**

S. Abbott [ID](#), B. Barton [ID](#), C. Brainerd [ID](#), R. Breedon [ID](#), H. Cai [ID](#), M. Calderon De La Barca Sanchez [ID](#), M. Chertok [ID](#), M. Citron [ID](#), J. Conway [ID](#), P.T. Cox [ID](#), R. Erbacher [ID](#), F. Jensen [ID](#), O. Kukral [ID](#), G. Mocellin [ID](#), M. Mulhearn [ID](#), S. Ostrom [ID](#), W. Wei [ID](#), S. Yoo [ID](#), F. Zhang [ID](#)

#### **University of California, Los Angeles, California, USA**

K. Adamidis, M. Bachtis [ID](#), D. Campos, R. Cousins [ID](#), A. Datta [ID](#), G. Flores Avila [ID](#),

---

J. Hauser [ID](#), M. Ignatenko [ID](#), M.A. Iqbal [ID](#), T. Lam [ID](#), Y.f. Lo, E. Manca [ID](#), A. Nunez Del Prado, D. Saltzberg [ID](#), V. Valuev [ID](#)

**University of California, Riverside, Riverside, California, USA**

R. Clare [ID](#), J.W. Gary [ID](#), G. Hanson [ID](#)

**University of California, San Diego, La Jolla, California, USA**

A. Aportela, A. Arora [ID](#), J.G. Branson [ID](#), S. Cittolin [ID](#), S. Cooperstein [ID](#), D. Diaz [ID](#), J. Duarte [ID](#), L. Giannini [ID](#), Y. Gu, J. Guiang [ID](#), R. Kansal [ID](#), V. Krutelyov [ID](#), R. Lee [ID](#), J. Letts [ID](#), M. Masciovecchio [ID](#), F. Mokhtar [ID](#), S. Mukherjee [ID](#), M. Pieri [ID](#), M. Quinnan [ID](#), B.V. Sathia Narayanan [ID](#), V. Sharma [ID](#), M. Tadel [ID](#), E. Vourliotis [ID](#), F. Würthwein [ID](#), Y. Xiang [ID](#), A. Yagil [ID](#)

**University of California, Santa Barbara - Department of Physics, Santa Barbara, California, USA**

A. Barzdukas [ID](#), L. Brennan [ID](#), C. Campagnari [ID](#), K. Downham [ID](#), C. Grieco [ID](#), J. Incandela [ID](#), J. Kim [ID](#), A.J. Li [ID](#), P. Masterson [ID](#), H. Mei [ID](#), J. Richman [ID](#), S.N. Santpur [ID](#), U. Sarica [ID](#), R. Schmitz [ID](#), F. Setti [ID](#), J. Sheplock [ID](#), D. Stuart [ID](#), T.Á. Vámi [ID](#), S. Wang [ID](#), D. Zhang

**California Institute of Technology, Pasadena, California, USA**

S. Bhattacharya [ID](#), A. Bornheim [ID](#), O. Cerri, A. Latorre, J. Mao [ID](#), H.B. Newman [ID](#), G. Reales Gutiérrez, M. Spiropulu [ID](#), J.R. Vlimant [ID](#), C. Wang [ID](#), S. Xie [ID](#), R.Y. Zhu [ID](#)

**Carnegie Mellon University, Pittsburgh, Pennsylvania, USA**

J. Alison [ID](#), S. An [ID](#), P. Bryant [ID](#), M. Cremonesi, V. Dutta [ID](#), T. Ferguson [ID](#), T.A. Gómez Espinosa [ID](#), A. Harilal [ID](#), A. Kallil Tharayil, C. Liu [ID](#), T. Mudholkar [ID](#), S. Murthy [ID](#), P. Palit [ID](#), K. Park, M. Paulini [ID](#), A. Roberts [ID](#), A. Sanchez [ID](#), W. Terrill [ID](#)

**University of Colorado Boulder, Boulder, Colorado, USA**

J.P. Cumalat [ID](#), W.T. Ford [ID](#), A. Hart [ID](#), A. Hassani [ID](#), G. Karathanasis [ID](#), N. Manganelli [ID](#), J. Pearkes [ID](#), C. Savard [ID](#), N. Schonbeck [ID](#), K. Stenson [ID](#), K.A. Ulmer [ID](#), S.R. Wagner [ID](#), N. Zipper [ID](#), D. Zuolo [ID](#)

**Cornell University, Ithaca, New York, USA**

J. Alexander [ID](#), S. Bright-Thonney [ID](#), X. Chen [ID](#), D.J. Cranshaw [ID](#), J. Fan [ID](#), X. Fan [ID](#), S. Hogan [ID](#), P. Kotamnives, J. Monroy [ID](#), M. Oshiro [ID](#), J.R. Patterson [ID](#), M. Reid [ID](#), A. Ryd [ID](#), J. Thom [ID](#), P. Wittich [ID](#), R. Zou [ID](#)

**Fermi National Accelerator Laboratory, Batavia, Illinois, USA**

M. Albrow [ID](#), M. Alyari [ID](#), O. Amram [ID](#), G. Apollinari [ID](#), A. Apresyan [ID](#), L.A.T. Bauerdick [ID](#), D. Berry [ID](#), J. Berryhill [ID](#), P.C. Bhat [ID](#), K. Burkett [ID](#), J.N. Butler [ID](#), A. Canepa [ID](#), G.B. Cerati [ID](#), H.W.K. Cheung [ID](#), F. Chlebana [ID](#), G. Cummings [ID](#), J. Dickinson [ID](#), I. Dutta [ID](#), V.D. Elvira [ID](#), Y. Feng [ID](#), J. Freeman [ID](#), A. Gandrakota [ID](#), Z. Gecse [ID](#), L. Gray [ID](#), D. Green, A. Grummer [ID](#), S. Grünendahl [ID](#), D. Guerrero [ID](#), O. Gutsche [ID](#), R.M. Harris [ID](#), R. Heller [ID](#), T.C. Herwig [ID](#), J. Hirschauer [ID](#), B. Jayatilaka [ID](#), S. Jindariani [ID](#), M. Johnson [ID](#), U. Joshi [ID](#), T. Klijnsma [ID](#), B. Klima [ID](#), K.H.M. Kwok [ID](#), S. Lammel [ID](#), C. Lee [ID](#), D. Lincoln [ID](#), R. Lipton [ID](#), T. Liu [ID](#), C. Madrid [ID](#), K. Maeshima [ID](#), C. Mantilla [ID](#), D. Mason [ID](#), P. McBride [ID](#), P. Merkel [ID](#), S. Mrenna [ID](#), S. Nahn [ID](#), J. Ngadiuba [ID](#), D. Noonan [ID](#), S. Norberg, V. Papadimitriou [ID](#), N. Pastika [ID](#), K. Pedro [ID](#), C. Pena<sup>83</sup> [ID](#), F. Ravera [ID](#), A. Reinsvold Hall<sup>84</sup> [ID](#), L. Ristori [ID](#), M. Safdari [ID](#), E. Sexton-Kennedy [ID](#), N. Smith [ID](#), A. Soha [ID](#), L. Spiegel [ID](#), S. Stoynev [ID](#), J. Strait [ID](#), L. Taylor [ID](#), S. Tkaczyk [ID](#), N.V. Tran [ID](#), L. Uplegger [ID](#), E.W. Vaandering [ID](#), I. Zoi [ID](#)

**University of Florida, Gainesville, Florida, USA**

C. Aruta [ID](#), P. Avery [ID](#), D. Bourilkov [ID](#), P. Chang [ID](#), V. Cherepanov [ID](#), R.D. Field, C. Huh [ID](#),

E. Koenig [ID](#), M. Kolosova [ID](#), J. Konigsberg [ID](#), A. Korytov [ID](#), K. Matchev [ID](#), N. Menendez [ID](#), G. Mitselmakher [ID](#), K. Mohrman [ID](#), A. Muthirakalayil Madhu [ID](#), N. Rawal [ID](#), S. Rosenzweig [ID](#), Y. Takahashi [ID](#), J. Wang [ID](#)

**Florida State University, Tallahassee, Florida, USA**

T. Adams [ID](#), A. Al Kadhim [ID](#), A. Askew [ID](#), S. Bower [ID](#), R. Hashmi [ID](#), R.S. Kim [ID](#), S. Kim [ID](#), T. Kolberg [ID](#), G. Martinez, H. Prosper [ID](#), P.R. Prova, M. Wulansatiti [ID](#), R. Yohay [ID](#), J. Zhang

**Florida Institute of Technology, Melbourne, Florida, USA**

B. Alsufyani, M.M. Baarmand [ID](#), S. Butalla [ID](#), S. Das [ID](#), T. Elkafrawy<sup>17</sup> [ID](#), M. Hohlmann [ID](#), E. Yanes

**University of Illinois Chicago, Chicago, Illinois, USA**

M.R. Adams [ID](#), A. Baty [ID](#), C. Bennett, R. Cavanaugh [ID](#), R. Escobar Franco [ID](#), O. Evdokimov [ID](#), C.E. Gerber [ID](#), M. Hawksworth, A. Hingrajiya, D.J. Hofman [ID](#), J.h. Lee [ID](#), D. S. Lemos [ID](#), A.H. Merrit [ID](#), C. Mills [ID](#), S. Nanda [ID](#), G. Oh [ID](#), B. Ozek [ID](#), D. Pilipovic [ID](#), R. Pradhan [ID](#), E. Prifti, T. Roy [ID](#), S. Rudrabhatla [ID](#), N. Singh, M.B. Tonjes [ID](#), N. Varelas [ID](#), M.A. Wadud [ID](#), Z. Ye [ID](#), J. Yoo [ID](#)

**The University of Iowa, Iowa City, Iowa, USA**

M. Alhusseini [ID](#), D. Blend, K. Dilsiz<sup>85</sup> [ID](#), L. Emediato [ID](#), G. Karaman [ID](#), O.K. Köseyan [ID](#), J.-P. Merlo, A. Mestvirishvili<sup>86</sup> [ID](#), O. Neogi, H. Ogul<sup>87</sup> [ID](#), Y. Onel [ID](#), A. Penzo [ID](#), C. Snyder, E. Tiras<sup>88</sup> [ID](#)

**Johns Hopkins University, Baltimore, Maryland, USA**

B. Blumenfeld [ID](#), L. Corcodilos [ID](#), J. Davis [ID](#), A.V. Gritsan [ID](#), L. Kang [ID](#), S. Kyriacou [ID](#), P. Maksimovic [ID](#), M. Roguljic [ID](#), J. Roskes [ID](#), S. Sekhar [ID](#), M. Swartz [ID](#)

**The University of Kansas, Lawrence, Kansas, USA**

A. Abreu [ID](#), L.F. Alcerro Alcerro [ID](#), J. Anguiano [ID](#), S. Arteaga Escatel [ID](#), P. Baringer [ID](#), A. Bean [ID](#), Z. Flowers [ID](#), D. Grove [ID](#), J. King [ID](#), G. Krintiras [ID](#), M. Lazarovits [ID](#), C. Le Mahieu [ID](#), J. Marquez [ID](#), M. Murray [ID](#), M. Nickel [ID](#), M. Pitt [ID](#), S. Popescu<sup>89</sup> [ID](#), C. Rogan [ID](#), R. Salvatico [ID](#), S. Sanders [ID](#), C. Smith [ID](#), G. Wilson [ID](#)

**Kansas State University, Manhattan, Kansas, USA**

B. Allmond [ID](#), R. Guju Gurunadha [ID](#), A. Ivanov [ID](#), K. Kaadze [ID](#), Y. Maravin [ID](#), J. Natoli [ID](#), D. Roy [ID](#), G. Sorrentino [ID](#)

**University of Maryland, College Park, Maryland, USA**

A. Baden [ID](#), A. Belloni [ID](#), J. Bistany-riebman, Y.M. Chen [ID](#), S.C. Eno [ID](#), N.J. Hadley [ID](#), S. Jabeen [ID](#), R.G. Kellogg [ID](#), T. Koeth [ID](#), B. Kronheim, Y. Lai [ID](#), S. Lascio [ID](#), A.C. Mignerey [ID](#), S. Nabili [ID](#), C. Palmer [ID](#), C. Papageorgakis [ID](#), M.M. Paranjpe, E. Popova<sup>90</sup> [ID](#), A. Shevelev [ID](#), L. Wang [ID](#)

**Massachusetts Institute of Technology, Cambridge, Massachusetts, USA**

J. Bendavid [ID](#), I.A. Cali [ID](#), P.c. Chou [ID](#), M. D'Alfonso [ID](#), J. Eysermans [ID](#), C. Freer [ID](#), G. Gomez-Ceballos [ID](#), M. Goncharov, G. Grossi, P. Harris, D. Hoang, D. Kovalevskyi [ID](#), J. Krupa [ID](#), L. Lavezzi [ID](#), Y.-J. Lee [ID](#), K. Long [ID](#), C. McGinn, A. Novak [ID](#), M.I. Park [ID](#), C. Paus [ID](#), C. Reissel [ID](#), C. Roland [ID](#), G. Roland [ID](#), S. Rothman [ID](#), G.S.F. Stephans [ID](#), Z. Wang [ID](#), B. Wyslouch [ID](#), T. J. Yang [ID](#)

**University of Minnesota, Minneapolis, Minnesota, USA**

B. Crossman [ID](#), B.M. Joshi [ID](#), C. Kapsiak [ID](#), M. Krohn [ID](#), D. Mahon [ID](#), J. Mans [ID](#), B. Marzocchi [ID](#), M. Revering [ID](#), R. Rusack [ID](#), R. Saradhy [ID](#), N. Strobbe [ID](#)

**University of Nebraska-Lincoln, Lincoln, Nebraska, USA**

K. Bloom [ID](#), D.R. Claes [ID](#), G. Haza [ID](#), J. Hossain [ID](#), C. Joo [ID](#), I. Kravchenko [ID](#), J.E. Siado [ID](#), W. Tabb [ID](#), A. Vagnerini [ID](#), A. Wightman [ID](#), F. Yan [ID](#), D. Yu [ID](#)

**State University of New York at Buffalo, Buffalo, New York, USA**

H. Bandyopadhyay [ID](#), L. Hay [ID](#), H.w. Hsia, I. Iashvili [ID](#), A. Kalogeropoulos [ID](#), A. Kharchilava [ID](#), M. Morris [ID](#), D. Nguyen [ID](#), S. Rappoccio [ID](#), H. Rejeb Sfar, A. Williams [ID](#), P. Young [ID](#)

**Northeastern University, Boston, Massachusetts, USA**

G. Alverson [ID](#), E. Barberis [ID](#), J. Bonilla [ID](#), B. Bylsma, M. Campana [ID](#), J. Dervan, Y. Haddad [ID](#), Y. Han [ID](#), I. Israr [ID](#), A. Krishna [ID](#), J. Li [ID](#), M. Lu [ID](#), G. Madigan [ID](#), R. McCarthy [ID](#), D.M. Morse [ID](#), V. Nguyen [ID](#), T. Orimoto [ID](#), A. Parker [ID](#), L. Skinnari [ID](#), D. Wood [ID](#)

**Northwestern University, Evanston, Illinois, USA**

J. Bueghly, S. Dittmer [ID](#), K.A. Hahn [ID](#), Y. Liu [ID](#), M. Mcginnis [ID](#), Y. Miao [ID](#), D.G. Monk [ID](#), M.H. Schmitt [ID](#), A. Taliercio [ID](#), M. Velasco

**University of Notre Dame, Notre Dame, Indiana, USA**

G. Agarwal [ID](#), R. Band [ID](#), R. Bucci, S. Castells [ID](#), A. Das [ID](#), R. Goldouzian [ID](#), M. Hildreth [ID](#), K.W. Ho [ID](#), K. Hurtado Anampa [ID](#), T. Ivanov [ID](#), C. Jessop [ID](#), K. Lannon [ID](#), J. Lawrence [ID](#), N. Loukas [ID](#), L. Lutton [ID](#), J. Mariano, N. Marinelli, I. Mcalister, T. McCauley [ID](#), C. McGrady [ID](#), C. Moore [ID](#), Y. Musienko<sup>14</sup> [ID](#), H. Nelson [ID](#), M. Osherson [ID](#), A. Piccinelli [ID](#), R. Ruchti [ID](#), A. Townsend [ID](#), Y. Wan, M. Wayne [ID](#), H. Yockey, M. Zarucki [ID](#), L. Zygala [ID](#)

**The Ohio State University, Columbus, Ohio, USA**

A. Basnet [ID](#), M. Carrigan [ID](#), L.S. Durkin [ID](#), C. Hill [ID](#), M. Joyce [ID](#), M. Nunez Ornelas [ID](#), K. Wei, D.A. Wenzl, B.L. Winer [ID](#), B. R. Yates [ID](#)

**Princeton University, Princeton, New Jersey, USA**

H. Bouchamaoui [ID](#), K. Coldham, P. Das [ID](#), G. Dezoort [ID](#), P. Elmer [ID](#), A. Frankenthal [ID](#), B. Greenberg [ID](#), N. Haubrich [ID](#), K. Kennedy, G. Kopp [ID](#), S. Kwan [ID](#), D. Lange [ID](#), A. Loeliger [ID](#), D. Marlow [ID](#), I. Ojalvo [ID](#), J. Olsen [ID](#), D. Stickland [ID](#), C. Tully [ID](#), L.H. Vage

**University of Puerto Rico, Mayaguez, Puerto Rico, USA**

S. Malik [ID](#), R. Sharma

**Purdue University, West Lafayette, Indiana, USA**

A.S. Bakshi [ID](#), S. Chandra [ID](#), R. Chawla [ID](#), A. Gu [ID](#), L. Gutay, M. Jones [ID](#), A.W. Jung [ID](#), A.M. Koshy, M. Liu [ID](#), G. Negro [ID](#), N. Neumeister [ID](#), G. Paspalaki [ID](#), S. Piperov [ID](#), V. Scheurer, J.F. Schulte [ID](#), M. Stojanovic [ID](#), J. Thieman [ID](#), A. K. Virdi [ID](#), F. Wang [ID](#), A. Wildridge [ID](#), W. Xie [ID](#), Y. Yao [ID](#)

**Purdue University Northwest, Hammond, Indiana, USA**

J. Dolen [ID](#), N. Parashar [ID](#), A. Pathak [ID](#)

**Rice University, Houston, Texas, USA**

D. Acosta [ID](#), T. Carnahan [ID](#), K.M. Ecklund [ID](#), P.J. Fernández Manteca [ID](#), S. Freed, P. Gardner, F.J.M. Geurts [ID](#), I. Krommydas [ID](#), W. Li [ID](#), J. Lin [ID](#), O. Miguel Colin [ID](#), B.P. Padley [ID](#), R. Redjimi, J. Rotter [ID](#), E. Yigitbasi [ID](#), Y. Zhang [ID](#)

**University of Rochester, Rochester, New York, USA**

A. Bodek [ID](#), P. de Barbaro [ID](#), R. Demina [ID](#), J.L. Dulemba [ID](#), A. Garcia-Bellido [ID](#), O. Hindrichs [ID](#), A. Khukhunaishvili [ID](#), N. Parmar, P. Parygin<sup>90</sup> [ID](#), R. Taus [ID](#)

**Rutgers, The State University of New Jersey, Piscataway, New Jersey, USA**

B. Chiarito, J.P. Chou [ID](#), S.V. Clark [ID](#), D. Gadkari [ID](#), Y. Gershtein [ID](#), E. Halkiadakis [ID](#), M. Heindl [ID](#), C. Houghton [ID](#), D. Jaroslawski [ID](#), S. Konstantinou [ID](#), I. Laflotte [ID](#), A. Lath [ID](#), R. Montalvo, K. Nash, J. Reichert [ID](#), H. Routray [ID](#), P. Saha [ID](#), S. Salur [ID](#), S. Schnetzer, S. Somalwar [ID](#), R. Stone [ID](#), S.A. Thayil [ID](#), S. Thomas, J. Vora [ID](#), H. Wang [ID](#)

**University of Tennessee, Knoxville, Tennessee, USA**

D. Ally [ID](#), A.G. Delannoy [ID](#), S. Fiorendi [ID](#), S. Higginbotham [ID](#), T. Holmes [ID](#), A.R. Kanuganti [ID](#), N. Karunaratna [ID](#), L. Lee [ID](#), E. Nibigira [ID](#), S. Spanier [ID](#)

**Texas A&M University, College Station, Texas, USA**

D. Aebi [ID](#), M. Ahmad [ID](#), T. Akhter [ID](#), K. Androssov<sup>59</sup> [ID](#), O. Bouhali<sup>91</sup> [ID](#), R. Eusebi [ID](#), J. Gilmore [ID](#), T. Huang [ID](#), T. Kamon<sup>92</sup> [ID](#), H. Kim [ID](#), S. Luo [ID](#), R. Mueller [ID](#), D. Overton [ID](#), D. Rathjens [ID](#), A. Safonov [ID](#)

**Texas Tech University, Lubbock, Texas, USA**

N. Akchurin [ID](#), J. Damgov [ID](#), N. Gogate [ID](#), V. Hegde [ID](#), A. Hussain [ID](#), Y. Kazhykarim, K. Lamichhane [ID](#), S.W. Lee [ID](#), A. Mankel [ID](#), T. Peltola [ID](#), I. Volobouev [ID](#)

**Vanderbilt University, Nashville, Tennessee, USA**

E. Appelt [ID](#), Y. Chen [ID](#), S. Greene, A. Gurrola [ID](#), W. Johns [ID](#), R. Kunawalkam Elayavalli [ID](#), A. Melo [ID](#), F. Romeo [ID](#), P. Sheldon [ID](#), S. Tuo [ID](#), J. Velkovska [ID](#), J. Viinikainen [ID](#)

**University of Virginia, Charlottesville, Virginia, USA**

B. Cardwell [ID](#), H. Chung, B. Cox [ID](#), J. Hakala [ID](#), R. Hirosky [ID](#), A. Ledovskoy [ID](#), C. Neu [ID](#)

**Wayne State University, Detroit, Michigan, USA**

S. Bhattacharya [ID](#), P.E. Karchin [ID](#)

**University of Wisconsin - Madison, Madison, Wisconsin, USA**

A. Aravind, S. Banerjee [ID](#), K. Black [ID](#), T. Bose [ID](#), E. Chavez [ID](#), S. Dasu [ID](#), P. Everaerts [ID](#), C. Galloni, H. He [ID](#), M. Herndon [ID](#), A. Herve [ID](#), C.K. Koraka [ID](#), A. Lanaro, R. Loveless [ID](#), J. Madhusudanan Sreekala [ID](#), A. Mallampalli [ID](#), A. Mohammadi [ID](#), S. Mondal, G. Parida [ID](#), L. Pétré [ID](#), D. Pinna, A. Savin, V. Shang [ID](#), V. Sharma [ID](#), W.H. Smith [ID](#), D. Teague, H.F. Tsoi [ID](#), W. Vetens [ID](#), A. Warden [ID](#)

**Authors affiliated with an institute or an international laboratory covered by a cooperation agreement with CERN**

S. Afanasiev [ID](#), V. Alexakhin [ID](#), D. Budkouski [ID](#), I. Golutvin<sup>†</sup> [ID](#), I. Gorbunov [ID](#), V. Karjavine [ID](#), V. Korenkov [ID](#), A. Lanev [ID](#), A. Malakhov [ID](#), V. Matveev<sup>93</sup> [ID](#), V. Palichik [ID](#), V. Perelygin [ID](#), M. Savina [ID](#), V. Shalaev [ID](#), S. Shmatov [ID](#), S. Shulha [ID](#), V. Smirnov [ID](#), O. Teryaev [ID](#), N. Voytishin [ID](#), B.S. Yuldashev<sup>94</sup>, A. Zarubin [ID](#), I. Zhizhin [ID](#), G. Gavrilov [ID](#), V. Golovtcov [ID](#), Y. Ivanov [ID](#), V. Kim<sup>93</sup> [ID](#), P. Levchenko<sup>95</sup> [ID](#), V. Murzin [ID](#), V. Oreshkin [ID](#), D. Sosnov [ID](#), V. Sulimov [ID](#), L. Uvarov [ID](#), A. Vorobyev<sup>†</sup>, Yu. Andreev [ID](#), A. Dermenev [ID](#), S. Gninenko [ID](#), N. Golubev [ID](#), A. Karneyeu [ID](#), D. Kirpichnikov [ID](#), M. Kirsanov [ID](#), N. Krasnikov [ID](#), I. Tlisova [ID](#), A. Toropin [ID](#), T. Aushev [ID](#), K. Ivanov [ID](#), V. Gavrilov [ID](#), N. Lychkovskaya [ID](#), A. Nikitenko<sup>96,97</sup> [ID](#), V. Popov [ID](#), A. Zhokin [ID](#), M. Chadeeva<sup>93</sup> [ID](#), R. Chistov<sup>93</sup> [ID](#), S. Polikarpov<sup>93</sup> [ID](#), V. Andreev [ID](#), M. Azarkin [ID](#), M. Kirakosyan, A. Terkulov [ID](#), E. Boos [ID](#), V. Bunichev [ID](#), A. Demiyanov [ID](#), L. Dudko [ID](#), A. Gribushin [ID](#), L. Khein, V. Klyukhin [ID](#), O. Kodolova<sup>97</sup> [ID](#), O. Lukina [ID](#), S. Obraztsov [ID](#), V. Savrin [ID](#), A. Snigirev [ID](#), V. Blinov<sup>93</sup>, T. Dimova<sup>93</sup> [ID](#), A. Kozyrev<sup>93</sup> [ID](#), O. Radchenko<sup>93</sup> [ID](#), Y. Skovpen<sup>93</sup> [ID](#), V. Kachanov [ID](#), D. Konstantinov [ID](#), S. Slabospitskii [ID](#), A. Uzunian [ID](#), A. Babaev [ID](#)

<sup>†</sup>: Deceased

<sup>1</sup>Also at Yerevan State University, Yerevan, Armenia

<sup>2</sup>Also at TU Wien, Vienna, Austria

<sup>3</sup>Also at Ghent University, Ghent, Belgium

<sup>4</sup>Also at Universidade do Estado do Rio de Janeiro, Rio de Janeiro, Brazil

<sup>5</sup>Also at Universidade Estadual de Campinas, Campinas, Brazil

<sup>6</sup>Also at Federal University of Rio Grande do Sul, Porto Alegre, Brazil

<sup>7</sup>Also at University of Chinese Academy of Sciences, Beijing, China

<sup>8</sup>Also at China Center of Advanced Science and Technology, Beijing, China

<sup>9</sup>Also at University of Chinese Academy of Sciences, Beijing, China

<sup>10</sup>Also at China Spallation Neutron Source, Guangdong, China

<sup>11</sup>Now at Henan Normal University, Xinxiang, China

<sup>12</sup>Also at University of Shanghai for Science and Technology, Shanghai, China

<sup>13</sup>Now at The University of Iowa, Iowa City, Iowa, USA

<sup>14</sup>Also at an institute or an international laboratory covered by a cooperation agreement with CERN

<sup>15</sup>Also at Zewail City of Science and Technology, Zewail, Egypt

<sup>16</sup>Also at British University in Egypt, Cairo, Egypt

<sup>17</sup>Now at Ain Shams University, Cairo, Egypt

<sup>18</sup>Also at Purdue University, West Lafayette, Indiana, USA

<sup>19</sup>Also at Université de Haute Alsace, Mulhouse, France

<sup>20</sup>Also at İstinye University, Istanbul, Turkey

<sup>21</sup>Also at Tbilisi State University, Tbilisi, Georgia

<sup>22</sup>Also at The University of the State of Amazonas, Manaus, Brazil

<sup>23</sup>Also at University of Hamburg, Hamburg, Germany

<sup>24</sup>Also at RWTH Aachen University, III. Physikalisches Institut A, Aachen, Germany

<sup>25</sup>Also at Bergische University Wuppertal (BUW), Wuppertal, Germany

<sup>26</sup>Also at Brandenburg University of Technology, Cottbus, Germany

<sup>27</sup>Also at Forschungszentrum Jülich, Juelich, Germany

<sup>28</sup>Also at CERN, European Organization for Nuclear Research, Geneva, Switzerland

<sup>29</sup>Also at HUN-REN ATOMKI - Institute of Nuclear Research, Debrecen, Hungary

<sup>30</sup>Now at Universitatea Babes-Bolyai - Facultatea de Fizica, Cluj-Napoca, Romania

<sup>31</sup>Also at MTA-ELTE Lendület CMS Particle and Nuclear Physics Group, Eötvös Loránd University, Budapest, Hungary

<sup>32</sup>Also at HUN-REN Wigner Research Centre for Physics, Budapest, Hungary

<sup>33</sup>Also at Physics Department, Faculty of Science, Assiut University, Assiut, Egypt

<sup>34</sup>Also at Punjab Agricultural University, Ludhiana, India

<sup>35</sup>Also at University of Visva-Bharati, Santiniketan, India

<sup>36</sup>Also at Indian Institute of Science (IISc), Bangalore, India

<sup>37</sup>Also at Amity University Uttar Pradesh, Noida, India

<sup>38</sup>Also at IIT Bhubaneswar, Bhubaneswar, India

<sup>39</sup>Also at Institute of Physics, Bhubaneswar, India

<sup>40</sup>Also at University of Hyderabad, Hyderabad, India

<sup>41</sup>Also at Deutsches Elektronen-Synchrotron, Hamburg, Germany

<sup>42</sup>Also at Isfahan University of Technology, Isfahan, Iran

<sup>43</sup>Also at Sharif University of Technology, Tehran, Iran

<sup>44</sup>Also at Department of Physics, University of Science and Technology of Mazandaran, Behshahr, Iran

<sup>45</sup>Also at Department of Physics, Faculty of Science, Arak University, ARAK, Iran

<sup>46</sup>Also at Helwan University, Cairo, Egypt

- <sup>47</sup>Also at Italian National Agency for New Technologies, Energy and Sustainable Economic Development, Bologna, Italy
- <sup>48</sup>Also at Centro Siciliano di Fisica Nucleare e di Struttura Della Materia, Catania, Italy
- <sup>49</sup>Also at Università degli Studi Guglielmo Marconi, Roma, Italy
- <sup>50</sup>Also at Scuola Superiore Meridionale, Università di Napoli 'Federico II', Napoli, Italy
- <sup>51</sup>Also at Fermi National Accelerator Laboratory, Batavia, Illinois, USA
- <sup>52</sup>Also at Consiglio Nazionale delle Ricerche - Istituto Officina dei Materiali, Perugia, Italy
- <sup>53</sup>Also at Institut de Physique des 2 Infinis de Lyon (IP2I ), Villeurbanne, France
- <sup>54</sup>Also at Department of Applied Physics, Faculty of Science and Technology, Universiti Kebangsaan Malaysia, Bangi, Malaysia
- <sup>55</sup>Also at Consejo Nacional de Ciencia y Tecnología, Mexico City, Mexico
- <sup>56</sup>Also at Trincomalee Campus, Eastern University, Sri Lanka, Nilaveli, Sri Lanka
- <sup>57</sup>Also at Saegis Campus, Nugegoda, Sri Lanka
- <sup>58</sup>Also at National and Kapodistrian University of Athens, Athens, Greece
- <sup>59</sup>Also at Ecole Polytechnique Fédérale Lausanne, Lausanne, Switzerland
- <sup>60</sup>Also at University of Vienna, Vienna, Austria
- <sup>61</sup>Also at Universität Zürich, Zurich, Switzerland
- <sup>62</sup>Also at Stefan Meyer Institute for Subatomic Physics, Vienna, Austria
- <sup>63</sup>Also at Laboratoire d'Annecy-le-Vieux de Physique des Particules, IN2P3-CNRS, Annecy-le-Vieux, France
- <sup>64</sup>Also at Near East University, Research Center of Experimental Health Science, Mersin, Turkey
- <sup>65</sup>Also at Konya Technical University, Konya, Turkey
- <sup>66</sup>Also at Izmir Bakircay University, Izmir, Turkey
- <sup>67</sup>Also at Adiyaman University, Adiyaman, Turkey
- <sup>68</sup>Also at Bozok Universitetesi Rektörlüğü, Yozgat, Turkey
- <sup>69</sup>Also at Marmara University, Istanbul, Turkey
- <sup>70</sup>Also at Milli Savunma University, Istanbul, Turkey
- <sup>71</sup>Also at Kafkas University, Kars, Turkey
- <sup>72</sup>Now at Istanbul Okan University, Istanbul, Turkey
- <sup>73</sup>Also at Hacettepe University, Ankara, Turkey
- <sup>74</sup>Also at Erzincan Binali Yıldırım University, Erzincan, Turkey
- <sup>75</sup>Also at Istanbul University - Cerrahpasa, Faculty of Engineering, Istanbul, Turkey
- <sup>76</sup>Also at Yildiz Technical University, Istanbul, Turkey
- <sup>77</sup>Also at School of Physics and Astronomy, University of Southampton, Southampton, United Kingdom
- <sup>78</sup>Also at IPPP Durham University, Durham, United Kingdom
- <sup>79</sup>Also at Monash University, Faculty of Science, Clayton, Australia
- <sup>80</sup>Also at Università di Torino, Torino, Italy
- <sup>81</sup>Also at Bethel University, St. Paul, Minnesota, USA
- <sup>82</sup>Also at Karamanoğlu Mehmetbey University, Karaman, Turkey
- <sup>83</sup>Also at California Institute of Technology, Pasadena, California, USA
- <sup>84</sup>Also at United States Naval Academy, Annapolis, Maryland, USA
- <sup>85</sup>Also at Bingöl University, Bingöl, Turkey
- <sup>86</sup>Also at Georgian Technical University, Tbilisi, Georgia
- <sup>87</sup>Also at Sinop University, Sinop, Turkey
- <sup>88</sup>Also at Erciyes University, Kayseri, Turkey
- <sup>89</sup>Also at Horia Hulubei National Institute of Physics and Nuclear Engineering (IFIN-HH), Bucharest, Romania

<sup>90</sup>Now at another institute or international laboratory covered by a cooperation agreement with CERN

<sup>91</sup>Also at Texas A&M University at Qatar, Doha, Qatar

<sup>92</sup>Also at Kyungpook National University, Daegu, Korea

<sup>93</sup>Also at another institute or international laboratory covered by a cooperation agreement with CERN

<sup>94</sup>Also at Institute of Nuclear Physics of the Uzbekistan Academy of Sciences, Tashkent, Uzbekistan

<sup>95</sup>Also at Northeastern University, Boston, Massachusetts, USA

<sup>96</sup>Also at Imperial College, London, United Kingdom

<sup>97</sup>Now at Yerevan Physics Institute, Yerevan, Armenia

<sup>98</sup>Also at Universiteit Antwerpen, Antwerpen, Belgium

## B The TOTEM Collaboration

G. Antchev <sup>a</sup>, P. Aspell<sup>8</sup>, I. Atanassov <sup>a</sup>, V. Avati<sup>7,8</sup>, J. Baechler<sup>8</sup>, C. Baldenegro Barrera <sup>11</sup>, V. Berardi <sup>4a,4b</sup>, M. Berretti <sup>2a</sup>, V. Borshch <sup>12</sup>, E. Bossini <sup>6a</sup>, U. Bottigli <sup>6b</sup>, M. Bozzo <sup>5a,5b</sup>, H. Burkhardt<sup>8</sup>, F.S. Cafagna <sup>4a</sup>, M.G. Catanesi <sup>4a</sup>, M. Deile <sup>8</sup>, F. De Leonardis <sup>4a,4c</sup>, M. Doubek <sup>1c</sup>, D. Druzhkin <sup>3a,8</sup>, K. Eggert<sup>10</sup>, V. Eremin<sup>c</sup>, A. Fiergolski<sup>8</sup>, F. Garcia <sup>2a</sup>, V. Georgiev<sup>1a</sup>, S. Giani<sup>8</sup>, L. Grzanka <sup>7</sup>, J. Hammerbauer<sup>1a</sup>, T. Isidori <sup>11</sup>, V. Ivanchenko <sup>12</sup>, M. Janda <sup>1c</sup>, A. Karev<sup>8</sup>, J. Kašpar <sup>1b,8</sup>, B. Kaynak <sup>9</sup>, J. Kopal <sup>8</sup>, V. Kundrát <sup>1b</sup>, S. Lami <sup>6a</sup>, R. Linhart<sup>1a</sup>, C. Lindsey<sup>11</sup>, M.V. Lokajíček <sup>t,1b</sup>, L. Losurdo <sup>6b</sup>, F. Lucas Rodríguez<sup>8</sup>, M. Macrì <sup>5a</sup>, M. Malawski <sup>7</sup>, N. Minafra <sup>11</sup>, S. Minutoli <sup>5a</sup>, K. Misan <sup>7</sup>, T. Naaranoja <sup>2a,2b</sup>, F. Nemes <sup>3a,3b,8</sup>, H. Niewiadomski<sup>10</sup>, E. Oliveri <sup>8</sup>, F. Oljemark <sup>2a,2b</sup>, M. Oriunno<sup>b</sup>, K. Österberg <sup>2a,2b</sup>, S. Ozkorucuklu <sup>9</sup>, P. Palazzi <sup>8</sup>, V. Passaro <sup>4a,4c</sup>, Z. Peroutka<sup>1a</sup>, O. Potok <sup>9</sup>, J. Procházka <sup>1b,t</sup>, M. Quinto <sup>4a,4b</sup>, E. Radermacher<sup>8</sup>, E. Radicioni <sup>4a</sup>, F. Ravotti <sup>8</sup>, C. Royon <sup>11</sup>, G. Ruggiero<sup>8</sup>, H. Saarikko <sup>2a,2b</sup>, V.D. Samoylenko<sup>c</sup>, A. Scribano <sup>6a,11</sup>, J. Široky<sup>1a</sup>, J. Smajek<sup>8</sup>, W. Snoeys <sup>8</sup>, R. Stefanovitch <sup>3a,8</sup>, C. Taylor <sup>10</sup>, E. Tcherniaev <sup>12</sup>, N. Turini <sup>6b</sup>, O. Urban<sup>1a</sup>, V. Vacek <sup>1c</sup>, O. Vavroch<sup>1a</sup>, J. Welti <sup>2a,2b</sup>, J. Williams <sup>11</sup>, J. Zich<sup>1a</sup>

<sup>t</sup>Deceased

<sup>1a</sup>University of West Bohemia, Pilsen, Czech Republic

<sup>1b</sup>Institute of Physics of the Academy of Sciences of the Czech Republic, Prague, Czech Republic

<sup>1c</sup>Czech Technical University, Prague, Czech Republic

<sup>2a</sup>Helsinki Institute of Physics, University of Helsinki, Helsinki, Finland

<sup>2b</sup>Department of Physics, University of Helsinki, Helsinki, Finland

<sup>3a</sup>Wigner Research Centre for Physics, RMKI, Budapest, Hungary

<sup>3b</sup>MATE Institute of Technology KRC, Gyöngyös, Hungary

<sup>4a</sup>INFN Sezione di Bari, Bari, Italy

<sup>4b</sup>Dipartimento Interateneo di Fisica di Bari, University of Bari, Bari, Italy

<sup>4c</sup>Dipartimento di Ingegneria Elettrica e dell'Informazione — Politecnico di Bari, Bari, Italy

<sup>5a</sup>INFN Sezione di Genova, Genova, Italy

<sup>5b</sup>Università degli Studi di Genova, Genova, Italy

<sup>6a</sup>INFN Sezione di Pisa, Pisa, Italy

<sup>6b</sup>Università degli Studi di Siena and Gruppo Collegato INFN di Siena, Siena, Italy

<sup>7</sup>Akademia Górniczo-Hutnicza (AGH) University of Kraków, Faculty of Computer Science,

Kraków, Poland

<sup>8</sup>CERN, Geneva, Switzerland

<sup>9</sup>Istanbul University, Istanbul, Turkey

<sup>10</sup>Case Western Reserve University, Department of Physics, Cleveland, Ohio, USA

<sup>11</sup>The University of Kansas, Lawrence, Kansas, USA

<sup>12</sup>Authors affiliated with an institute or an international laboratory covered by a cooperation agreement with CERN

---

<sup>a</sup> INRNE-BAS, Institute for Nuclear Research and Nuclear Energy, Bulgarian Academy of Sciences, Sofia, Bulgaria

<sup>b</sup> SLAC, Stanford University, California, USA

<sup>c</sup> Authors affiliated with an institute or an international laboratory covered by a cooperation agreement with CERN